
[All ETDs from UAB](#)

[UAB Theses & Dissertations](#)

2015

Modulation Of The Unfolded Protein Response To Delay Apoptosis In An Autosomal Dominant Retinitis Pigmentosa Animal Model

Yogesh Bhootada
University of Alabama at Birmingham

Follow this and additional works at: <https://digitalcommons.library.uab.edu/etd-collection>

Recommended Citation

Bhootada, Yogesh, "Modulation Of The Unfolded Protein Response To Delay Apoptosis In An Autosomal Dominant Retinitis Pigmentosa Animal Model" (2015). *All ETDs from UAB*. 1165.
<https://digitalcommons.library.uab.edu/etd-collection/1165>

This content has been accepted for inclusion by an authorized administrator of the UAB Digital Commons, and is provided as a free open access item. All inquiries regarding this item or the UAB Digital Commons should be directed to the [UAB Libraries Office of Scholarly Communication](#).

"MODULATION OF THE UNFOLDED PROTEIN RESPONSE TO DELAY
APOPTOSIS IN AN AUTOSOMAL DOMINANT RETINITIS PIGMENTOSA
ANIMAL MODEL."

by

YOGESH BHOOTADA

Dr. MARINA S. GORBATYUK, ADVISOR
Dr. ALECIA GROSS, COMMITTEE CHAIR
Dr. SHU-ZHEN WANG
Dr. STEVEN PITTLER
Dr. ZSUZSANNA BEBOK

A DISSERTATION

Submitted to the graduate faculty of The University of Alabama at Birmingham,
In partial fulfillment of the requirements for the degree of
Doctor of Philosophy

BIRMINGHAM, ALABAMA

2015

Copyright by
Yogesh Bhootada
2015

MODULATION OF THE UNFOLDED PROTEIN RESPONSE TO DELAY
APOPTOSIS IN AN AUTOSOMAL DOMINANT RETINITIS PIGMENTOSA
ANIMAL MODEL

YOGESH BHOOTADA

SCHOOL OF OPTOMETRY-VISION SCIENCES

ABSTRACT

Retinitis pigmentosa (RP) is a group of retinal degenerative diseases characterized by the loss of rod photoreceptor cells that can be followed by cone degeneration eventually culminating in total photoreceptor cell loss. This disease affects approximately 1.5 million people worldwide and can be transmitted in an autosomal dominant (ADRP) manner accounting for nearly 30% of all RP cases. Dominant rhodopsin mutations have been divided into class I and class II based on the folding of rhodopsin protein, thermal stability, and chromophore regeneration. A threonine-17-methionine (T17M) mutation in rhodopsin is a class II mutation, characterized by a thermal instability/folding defect and minimal regeneration with the chromophore. Misfolded opsin interferes with the trafficking of wild-type rhodopsin, causing accumulation in the endoplasmic reticulum (ER) and stimulation of a signal transduction cascade known as the Unfolded Protein Response (UPR). If not deactivated, this pathway triggers photoreceptor death, presumably through triggering apoptosis.

T17M mutant rhodopsin mice have become a valuable animal model for the study of ADRP. In these mice we have demonstrated that PERK (RNA-activates protein kinase-like ER kinase) signaling, is upregulated leading to an increase in phosphorylated (p) translational eukaryotic initiation factor 2 α (eIF2 α), ATF4 (Activating transcription factor 4) and CHOP (C/EBP Homologous Protein) mRNA, starting at postnatal day (P) 18. Manipulating ATF4 and CHOP expression in a mouse model of retinal degeneration with

UPR activation, we demonstrated for the first time that ATF4 overexpression accelerates retinal degeneration through CHOP and caspase induced cell death. In contrast, genetic ablation of one allele of ATF4 and CHOP altogether mitigates retinal degeneration and provides long term rescue.

Several studies have suggested that Caspase-12 acts as an initiator caspase during ER stress-induced apoptosis, activating an effector caspase-3 or -7 which then cleaves key substrates required for normal cellular functions, thus leading to apoptosis. Here, we validated caspase-12 as a therapeutic target, ablation of which significantly protects T17M photoreceptors from progressing degeneration. Although the inhibition of apoptotic activity alone was not sufficient to rescue T17M photoreceptors, in combination with other non-apoptotic targets, caspase-12 could be used to treat inherited retinopathy.

Keywords: Retinitis Pigmentosa, Unfolded Protein Response, ATF4, CHOP, Caspase-12

Dedication

I dedicate this thesis to god for bestowing his kind blessings onto me at every stage of my life. I also dedicate this work to my parents, wife and brother who have been a constant support to me throughout my life's journey.

Acknowledgment

By simply acknowledging in writing would undervalue the support and help I have received in successfully completing this thesis. Nonetheless, first and foremost, I would like to start with expressing my sincere and deepest gratitude to my advisor Dr. Marina Gorbatyuk, for her constant guidance, encouragement and endless support in completing this thesis project and throughout my academic endeavor. I would also like to extend this appreciation to my committee members, Dr. Alecia Gross, Dr. Shu-Zhen Wang, Dr. Steven Pittler and Dr. Zsuzsanna Bebok for their valuable suggestions, expert comments, creative ideas and criticisms. Without their motivation, this thesis would have been an unfinished work.

I would like to thank Dr. Vincenzo Guarcello for imparting the necessary knowledge, training me various laboratory instrumentation and constant guidance throughout my graduate study. My sincere thanks also extend to Vision Science Graduate Program Director, Coordinator and other faculty members at the vision sciences program, University of Alabama at Birmingham for providing every means for my success. I would like to convey my appreciation to my fellow graduate students and members of Dr. Gorbatyuk's lab who made my stay and study joyous and memorable.

Finally, words would not sum up the blessings and love that my parents showered on me. Words fail to express the eternal debt I owe them. I will always be grateful to my elder brother who supported me and always looking out for me. I thank my wife and the love of my life for support and motivation, and for always accrediting my capabilities. A blend of gratitude, pleasure and great satisfaction, is what I feel to convey my gratitude to all my relatives, friends and colleagues who have directly or indirectly contributed to my thesis.

TABLE OF CONTENTS

	Page	
ABSTRACT.....	iii	
DEDICATION.....	v	
ACKNOWLEDGMENTS.....	vi	
LIST OF FIGURES.....	x	
LIST OF ABBREVIATIONS.....	xii	
CHAPTER		
I.INTRODUCTION.....	1	
II. LIMITED ATF4 EXPRESSION IN DEGENRATING RETINAS WITH ONGOING ER STRESS PROMOTES PHOTORECEPTOR SURVIVAL IN A MOUSE MODEL OF AUTOSOMAL RETINITIS PIGMENTOSA.....		24
ABSTRACT.....	25	
INTRODUCTION.....	26	
MATERIAL AND METHODS.....	28	
RESULTS.....	33	
Overexpression of ATF4 in the T17M retina accelerates retinal degeneration.....	33	
T17M mice deficient in ATF4 exhibit a delay of the onset of retinal degeneration as measured by functional vision test.....	37	
T17M ATF4 ^{+/-} mice experience delayed onset of retinal degeneration, as measured by imaging and histological analyses.....	39	
The T17M ATF4 ^{+/-} mouse retinas demonstrate diminished ER stress.....	41	
The T17M ATF4 ^{+/-} mice demonstrate increases in NRF2 and diminished oxidative stress.....	46	

Retinal degeneration in T17M mice is associated with an impaired autophagy signaling.	48
Delay of the onset of retinal degeneration in T17M ATF4 mice is associated with improved RHO biosynthesis.	50
DISCUSSION.....	52
Molecular mechanism of T17M photoreceptor degeneration.....	53
Molecular mechanism of T17M ATF4 ^{+/-} photoreceptor degeneration.....	55
Rhodopsin expression machinery in ADRP retinas.....	57
CONCLUSION.....	59
III. Controlling PERK-ATF4-CHOP branch of the UPR is the key to reverse retinal degeneration of T17M Retina	67
ABSTRACT.....	68
INTRODUCTION	69
MATERIAL AND METHODS.....	70
RESULTS	72
Coupled downregulation of ATF4 and CHOP preserves ADRP mice from vision loss.....	72
Coupled downregulation of ATF4 and CHOP in ADRP mice prevents photoreceptor cell death.....	74
ISRIB reduces ATF4 and CHOP levels rescues photopic ERG function in one month old T17M Mice.	75
DISCUSSION.....	78
IV. Targeting caspase-12 to preserve vision in mice with inherited retinal degeneration.	81
ABSTRACT.....	82
INTRODUCTION	83

MATERIAL AND METHODS	85
RESULTS	89
The T17M mouse retinas demonstrate an increase in the expression and activity of Csp-12.....	89
Csp-12 ablation significantly delays loss of function for T17M photoreceptors.....	90
Csp-12 ablation significantly delays death of T17M photoreceptors and preserves retinal integrity.....	92
Csp-12 ablation in T17M mice significantly modifies expression of Ca ²⁺ sensor genes and reduces apoptosis.	95
DISCUSSION.....	99
DISCUSSION AND CONCLUSION	105
LIST OF REFERENCES	109
APPENDIX.....	111

LIST OF FIGURES

<i>Figure</i>		<i>Page</i>
	Introduction	
1	The Unfolded Protein Response	15
	Limited ATF4 Expression in Degenerating Retinas with Ongoing ER Stress Promotes Photoreceptor Survival in a Mouse Model of Autosomal Dominant Retinitis Pigmentosa.	
1.	Overexpression of ATF4 accelerates and induces retinal degeneration in T17M mice and C57BL/6 mice, respectively.	36
2.	Knockdown of ATF4 prevents functional loss in T17M retina as measured by scotopic and photopic ERG.	38
3.	ATF4 knockdown protects T17M mice from loss of retinal integrity and photoreceptors.....	41
4.	ATF4 knockdown in the ADRP retinas reduces overall ER stress.....	45
5.	ATF4 knockdown launches the antioxidant cellular defense mechanism in T17M and protects the ADRP retina against oxidative stress	48
6.	ATF4 deficiency in T17M retinas results in upregulation of autophagosome associated genes.	49
7.	ATF4 knockdown in T17M photoreceptors has a positive influence on the RHO expression machinery.....	51
8.	Proposed mechanism of retinal degeneration in T17M and T17M ATF4 ^{+/-} mice.....	53
9.	Expression of T17M RHO in ADRP rod photoreceptors results in photoreceptor cell death and leads to severe retinal degeneration.....	60
10.	Knockdown of ATF4 prevents loss of function and photoreceptor cell death in one-, two-, and three-month-old T17M retinas.....	60
11.	Representative images of Western blots.....	61

Controlling PERK-ATF4-CHOP branch of the UPR is the key to reverse retinal degeneration of T17M Retina.

1. ATF4 and CHOP deficiency prevents functional loss of T17M retina as measure by scotopic and photopic ERG.....73
2. ATF4 and CHOP knockdown protects T17M mice from photoreceptor loss.75
3. ISRIB reduces ATF4 and CHOP expression rescues photopic ERG function in one month old T17M Mice.....77

Targeting caspase-12 to preserve vision in mice with inherited retinal degeneration

1. Expression and activation of Csp-12 in the T17M retina during ADRP progression.....90
2. Lack of Csp-12 protects T17M retinas from degeneration as measured by scotopic ERG responses.....91
3. The preservation of retinal structure and prevention of photoreceptor cell death in T17M Csp-12^{-/-} retinas.....94
4. Ca²⁺ sensor protein expression in T17M Csp-12^{-/-} retinas.....98
5. Csp-12 ablation in T17M retinas results in decreased levels of apoptosis. Four animals in each group were used in the experiment.....99

CONCLUSION

1. Targeting PERK branch of the UPR could be therapeutic target to prevent Retinal Degeneration.....108

LIST OF ABBREVIATIONS

1. AAV-Adeno-Associated Virus
2. ADRP- Autosomal Dominant Retinitis Pigmentosa
3. ATF4-Activating Transcription Factor 4
4. ATF6- Activating Transcription Factor 6
5. ER – Endoplasmic Reticulum
6. ERG- Electroretinography
7. GCL-Ganglion Cell Layer
8. H&E- Haemotoxylin and Eosin
9. INL-Inner Nuclear Layer
10. IS- Inner Segment
11. OCT- Optical Coherence Tomography
12. ONL- Outer Nuclear Layer
13. OS- Outer Segment
14. PERK-Protein kinase RNA (PKR)-like ER kinase
15. RP- Retinitis Pigmentosa
16. RHO- Rhodopsin
17. RPE- Retinal Pigment Epithelium
18. UPR- Unfolded Protein Response
19. WT- Wild Type/C57BL/6

CHAPTER 1

GENERAL INTRODUCTION

Retina

The retina is a thin layer of tissue that lines the inner surface of the eye. The function of the retina is to convert light energy into neural signals and send these signals on to the brain for visual recognition. The retina processes light through a layer of photoreceptor cells. These are light-sensitive cells responsible for detecting qualities such as color and light-intensity. The retina processes the information gathered by the photoreceptor cells and sends this information to the brain via the optic nerve. The retina is the neurosensory element of the eye. It is a layered structure and its cellular components are defined in a way to meet the functional requirements of the different regions of the retina (1).

Retinal Pigment Epithelium: Each human eye contains approximately 3.5 million RPE cells (2, 3) which are held together by junctional complexes to form a single layer of hexagonal cells. The tight junctions between these RPE cells separate the choroid blood flow from the outer segments of photoreceptors, thus creating the part of the outer blood-retina barrier (4, 5). This barrier helps to control the extracellular environment and maintain the function of the outer retina. RPE has several functions such as epithelial transport (6), visual cycle (7), phagocytosis of outer segment of photoreceptors (8) essential for visual function that support normal photoreceptor function.

Photoreceptor Layer: The photoreceptor layer consists of two types of photoreceptor cells: rods and cones. Rod photoreceptor cells are responsible for dim light vision and have only one type of photo pigment rhodopsin (9). Cone photoreceptors are responsible for day light and color vision with high acuity. Cone cells have three types of photo pigment: short, middle and long wavelength opsin (10). Rod and cone cells are tightly stacked together into a single stockade layer of photoreceptors (11). Photoreceptor cells are the only cells in the retina which are directly sensitive to light and, thus, the site of visual transduction. All other layers of the retina collectively assist to process and transmit these nerve signals.

Outer Nuclear Layer: The outer nuclear layer contains the nuclei of the rod and cone photoreceptor cells. The human retina comprises about 4-5 million cones and 77–107 million rods (12).

Outer Plexiform Layer: Photoreceptor cells of the outer nuclear layer form networks with the bipolar and horizontal cells of the inner nuclear layers in the OPL. This is the first and important synapse in the retina. The terminals of the photoreceptor cells, the rod spherules and cone pedicles, form the synapses with the photoreceptor, bipolar, and horizontal cells (13). Photoreceptor signals are connected in such a way that they give rise to two important pathways an ON and Off-center pathways and a center surround organization in the retina (14, 15). These signals are then transmitted to the next layer of the IPL for processing by bipolar cells (12).

Inner Nuclear Layer: This layer consists of the nuclei of five different types of cells: the bipolar, the horizontal, the amacrine, the interplexiform, and the Müller cells. The horizontal cells are located on the outer side of the inner nuclear layer facing the OPL,

whereas the amacrine cells are placed in the inner part of the INL. The nuclei of the bipolar, interplexiform, and Müller cells take up intermediary positions (13).

Inner Plexiform Layer: The IPL is the second retinal processing layer with interlaced dendrites of ganglion cells and cells of the inner nuclear layer. The processing of the photoreceptor input through detailed interactions between the bipolar, amacrine, and ganglion cells occurs in six lamina of the IPL (12).

Ganglion Cell Layer: GCL contains approximately 1.2 million ganglion cells and displaced amacrine cells. The axon of ganglion cells (nerve fiber layer) merges into the optic nerve and transmits all the information to the brain (16).

Visual Transduction in Retina

Rhodopsin of rod photoreceptors cells consists of the protein opsin and a chromophore 11 *cis*-retinal. Photon absorption by rhodopsin (R) leads to photo isomerization (R*) and conversion of 11 *cis*-retinal to all-*trans* retinal (17). This causes a conformational change in rhodopsin and transduces an enzyme cascade leading to closure of the cation channels of the photoreceptor membrane. The light-activated opsin R* binds to transducin, a G protein that is found on the cytosolic surface of the disc membrane (9). The alpha subunit of the G protein (T_{α}) replaces a molecule of GDP with a molecule of GTP and becomes activated (T_{α} -GTP). Transducin activates cGMP phosphodiesterase (PDE*), an enzyme that reduces the concentration of cyclic GMP by hydrolyzing its conversion into 5'-GMP (5'-guanosine monophosphate) (1). cGMP is the second messenger, and reduced intracellular concentrations of cGMP cause the closure of the cGMP-gated cation channels in the outer segment of photoreceptor cell membrane, resulting in the hyperpolarization of the photoreceptors. In the dark condition, steady “dark current”

flows into the open channels, carried mainly by Na^{2+} ions, and depolarizes the photoreceptor cell. The depolarized photoreceptor releases a neurotransmitter (glutamate) from its synaptic terminals on to secondary retinal cells in the dark. Upon light stimulation of the photopigment, the above enzyme cascade ensues, leading to closure of the cation channels of the photoreceptor membrane, stopping the dark current, and causing the photoreceptor cell membrane to hyperpolarize and terminate glutamate release (12).

During subsequent light activation of rhodopsin and enzyme cascade, timely deactivation of photoreceptor is essential, because the deactivation determines the speed and the sensitivity of the cellular response to light. Deactivation is a rate limiting step in phototransduction (18). The photoresponse recovery from light occurs in two parts, inactivation of each of the activated components R^* , T_{α^*} , PDE^* and efficient regeneration of rhodopsin (R) and rapid restoration of the cGMP concentration. R^* inactivation occurs through phosphorylation of rhodopsin protein by the rhodopsin kinase (19), followed by arrestin binding to phosphorylated R^* (20). Regulator of G-protein signaling (RGS9) inactivates transducin via hydrolysis of bound GTP to GDP ($\text{T}_{\alpha^*}\text{-GTP}$ to $\text{T}_{\alpha^*}\text{-GDP}$) through an intrinsic GTPase activity (21). The inactivation of transducin results in the dissociation of $\text{T}_{\alpha^*}\text{-GTP}$ from PDE^* and terminates the PDE^* -mediated cGMP hydrolysis (22). Guanylate cyclase activating proteins I and II (GCAP) (23) detects a decrease in Ca^{2+} level due to light exposure. This stimulates guanylyl cyclase activation which restores cGMP concentration to the dark state and re-opening of cGMP-gated channels (24).

Visual Transduction Proteins

Rhodopsin protein belongs to G-protein coupled receptor family (GPCR) (25). It is composed of the protein opsin (~40 kD in size) covalently linked to 11-cis-retinal through Lys²⁹⁶ amino acid via a protonated Schiff base (26). The crystal structure of rhodopsin at 2.8 Å in ground state (27), revealed seven-transmembrane α -helices with hydrophobic binding pocket for 11-cis-retinal. Seven transmembrane α helices of protein opsin have N-terminus exposed to intradiscal space and C-terminus exposed to cytoplasm (28). Rod disc membranes contains over 90% of rhodopsin protein, which are densely packed in disc membrane with an average density of about 25,000 molecules/ μm^2 (29).

Upon light activation, rhodopsin (R) rapidly photoisomerized to the intermediates of rhodopsin in an order of bathorhodopsin, lumirhodopsin, metarhodopsin I (Meta I), and metarhodopsin II (Meta II) within 1 millisecond (30). Meta II is the active conformation (R*) of rhodopsin, which in turn decays to Meta III inactive conformation (31).

Inactivation of rhodopsin (R*) occurs in two steps. It starts with rhodopsin kinase phosphorylation of R*, which lowers the activity of activated rhodopsin (32). And ends, with binding of accessory protein arrestin (48 kD) to phosphorylated R*. C-terminus of rhodopsin protein has several potential serine/threonine phosphorylation sites (33). Rhodopsin kinase protein (63kD), exclusively found in rods and cones, belongs to serine/threonine protein kinase family called G-protein couple receptor kinases (GRKs) (34) and is required for R* phosphorylation.

The activity of rhodopsin kinase (GRK1) on phosphorylation of R* is regulated by calcium binding protein recoverin (23 kD) (35-37). In the dark, when intracellular Ca^{2+} concentration is high recoverin- Ca^{2+} binds to rhodopsin kinase and inhibits R* phosphorylation. But, during the light response a fall in Ca^{2+} concentration results in

dissociation of recoverin from Ca^{2+} , consequently inhibition of recoverin is reduced on GRK1 (36).

Arrestin protein belongs to family of inhibitory proteins participating in signal transduction (38) which binds to phosphorylated R^* and limits its catalytic activity to activate transducin. It has two splice variants in rod cells: a full-length p48 and c-terminal truncated form p44 (39). The splice variant p44 has been shown to be more efficient in turning off R^* than full length p48 (32). The lifetime of R^* is ~80 millisecond (40, 41).

G-protein transducin is a heterotrimeric protein composed of α , β , and γ subunits (42). Activated rhodopsin R^* catalytically stimulates transducin by exchange of GTP for GDP on α subunit ($\text{T}\alpha^*$). $\text{T}\alpha^*$ dissociates from R^* as well as its native partners and activates membrane-bound PDE6 to carry the signal forward. Guanyl nucleotide binding and GTP hydrolysis sites are present on α subunit of transducin (43). Binding of $\text{T}\alpha$ to GTP releases R^* which remains active and can bind to another transducin molecule. Single R^* has a rate of transducin activation $\sim 120 \text{ s}^{-1}$, this rate is approximately double in mammalian rods due to a difference in body temperature (44). The amount of transducin is about 10% of total pigment. Different isoforms of transducin have been reported in rods ($\text{G}\alpha_1\text{G}\beta_1\text{v}_1$) and cones ($\text{G}\alpha_2\text{G}\beta_3\text{v}_8$) (45, 46).

PDE6 is a tetrameric protein with two catalytic subunits α , β and two identical inhibitory subunit γ_2 (47). The activation of PDE6 requires two $\text{T}\alpha^*$ -GTP molecule. PDE6 density is about 1-2% of rhodopsin. Two inhibitory subunits γ_2 mask the catalytic subunits in the dark, due to light activation $\text{T}\alpha$ -GTP sterically displaces the inhibitory subunits and relieving inhibition. Activated PDE6 hydrolyzes cGMP to 5'-GMP, reduces cGMP cytosolic concentration and results in shut down of cGMP-gated channel in the plasma membrane of rod outer segment(1).

Transducin is inactivated when its bound GTP ($T\alpha$ -GTP) is hydrolyzed to GDP. The slow intrinsic GTPase activity is present in α subunit of transducin. But, this intrinsic activity is greatly accelerated by GTPase activating protein (GAP) complex. Primary GTPase accelerator in photoreceptor is composed of RGS9-1, the long form of G β 5 subunit and a membrane-anchor protein R9AP (48-50). PDE γ exert its inhibitory action after hydrolysis of $T\alpha$ -GTP to $T\alpha$ -GDP and enhance GAP activity on transducin (48).

The final step in phototransduction is shut down of cGMP-gated channel located on the plasma membrane, which results in hyperpolarization of photoreceptors. The cGMP-gated channel belongs to cyclic nucleotide-gated (CNG) channel family, which is member of the superfamily of voltage-gated cation channel (51). Rod channel has a 3CNGA1:1CNGB1 subunit (52, 53), whereas cone channel exhibits a 2CNGA3:2CNGB3 stoichiometry (54). In the dark condition CNG channel allows inward flow of Na^+ which is a predominant external cation. This inward current is balanced by an outward flow of K^+ across the inner segment membrane. This current is also called “dark current” (55).

PDE-mediated hydrolysis and guanylate-cyclase (GC)-mediated synthesis determine the free cytosolic cGMP concentration. After phototransduction PDE6 mediated hydrolysis should be terminated and cGMP level has to be restored to the level of dark state. In mouse photoreceptors two forms of GCs are present GC1 (GC-E) and GC2 (GC-F) (56, 57). GC-1 is present in both rods and cones, and GC-2 is present in rods only (58). GC-1 and GC-2 deletion makes photoreceptor nonfunctional and unstable (59).

Guanylate-cyclase-activating proteins (GCAPs) regulate GC activity. GCAPs are calmodulin-like Ca^{2+} -binding proteins. In the dark condition high concentration of Ca^{2+} facilitates formation of Ca^{2+} -GCAPs, which inhibits GCs. In light condition, Ca^{2+}

concentration falls releasing GCAPs and activates cGMP synthesis mediated by GCs. This calcium dependent negative feedback mechanism is important in restoring cGMP concentration. Two form of GCAPs protein (I&II) are present in mammalian rod and cone photoreceptor, whereas cone photoreceptor also exclusively expresses another form GCAP-III (60).

Visual Cycle

After photon absorption by rhodopsin, its chromophore 11-cis-retinal isomerizes into all-trans-retinal and rhodopsin becomes meta-rhodopsin. After inactivation of meta-rhodopsin by phosphorylation and additional reaction steps, opsin has to be regenerated with 11-cis-retinal so that it can be activated again by a photon. Therefore, all-trans-retinal has to be re-isomerized to 11-cis-retinal for successful rhodopsin regeneration and maintain visual function. Photoreceptor lacks the enzyme re-isomerase required for re-isomerization steps, thus all-trans-retinal is transported to RPE for conversion into 11-cis-retinal. This process is called visual cycle (7, 30, 61).

All-trans-retinal is transported from intradiscal space to the cytosolic space of the rod outer segment by an ATP –binding cassette protein (ABCA4). The transportation occurs by a reaction between all-trans-retinal with phosphatidylethanolamine (PE) to an N-retinylidene-PE complex. All-trans- retinal is dissociates from PE and converted to all-trans-retinol by a membrane bound all-trans-retinol dehydrogenase and delivered to RPE by the carrier protein, IRBP (interstitial retinal binding protein). In the RPE retinol is transferred to CRBP (cellular retinol binding protein), which deliver retinol to a enzyme complex of LRAT ((lecithin:retinol transferase), RPE65 (RPE protein with 65 kDa) , RDH5 (11-cis-retinol dehydrogenase) and CRALBP (cellular retinylaldehyde-binding

protein). By the three step enzymatic reaction: esterification of retinol by adding an acyl-group (LRAT), re-isomerisation to 11-cis using the energy from ester-hydrolysis (RPE65) and oxidation to 11-cis retinal (RDH5), all-trans-retinol converts to 11-cis-retinal. CRALBP binds to the final product 11-cis-retinal which releases it to IRBP and transported back to photoreceptor (61).

Retinitis Pigmentosa

Retinitis Pigmentosa (RP) is a heterogeneous group of inherited retinal disorder that leads to the progressive loss of retinal function. RP affects over 1 million individuals with a worldwide prevalence rate of 1 in 4000 (62). More than 45 genes have been identified and over 100 genes implicated so far which are responsible for retinitis pigmentosa. RP patients typically lose night vision in adolescence, peripheral vision in young adults, and then gradually central vision in later life because of progressive loss of rod and cone photoreceptors. Inheritance pattern for RP includes autosomal dominant (30-40% of cases), autosomal-recessive (50-60%), or X-linked (5-15) trait (63). Usually RP disease confined to retinal degeneration, however about 20-30% patients shows non-ocular disease symptoms and fall under more than 30 different syndromes. Usher's syndrome is the most frequent syndromic form (64), in which vision loss is associated with hearing impairment. Another major example of syndromic RP is Bardet-Biedl syndrome, in which along with retinal degeneration patients suffers from obesity, cognitive impairment, hypogonadism, and renal disease (65).

Symptoms

Retinitis pigmentosa patients usually fall into classic pattern of nyctalopia in early stages. However, defects at this stage are rare or minimal in day light and patients have normal habit life. To establish a diagnosis is difficult at this stage especially, if there is no familial history. Fundus examination may seem normal because of no pigment deposition and optic disc appear normal. The electroretinogram (ERG) testing is key at this stage, because only it can detects decrease in maximum ERG amplitude under scotopic condition. During mid stage, night blindness is prominent with difficulties to drive, and to walk in dark. Patient's develops photophobia and dyschromatopsia symptoms. Clinical signs become more visible with pigment deposition, cataract formation, narrowing of blood vessels along with atrophy of the retina. In the later stages of disease, patients develop intense photophobia, no visual acuity, and widespread pigment deposits (66).

Rhodopsin Mutations

Rhodopsin, the major visual pigment of the rod photoreceptor cell, consists of a covalent complex between the 348-amino-acid integral membrane glycoprotein opsin and 11-cis retinal (27). Rhodopsin protein is synthesized and glycosylated inside endoplasmic reticulum. After proper folding of rhodopsin protein, molecular chaperones pass it to Golgi membranes for its transport to the outer segment of rod photoreceptors (67). As described earlier, rhodopsin protein has seven transmembrane helices embedded in plasma membrane with extracellular domain and intradiscal domain. N-terminal glycosylation inside endoplasmic reticulum is important for conformational maturation of protein and binding of chromophore 11-cis-retina, while C-terminal is responsible for rhodopsin sorting and trafficking to the outer segment. Over 100 mutations in the

rhodopsin gene have been described (68), and several studies at cellular and transgenic animal levels demonstrated protein misfolding, poor regeneration with chromophore or trafficking (69). Mutations in the transmembrane, intradiscal or cytoplasmic domains results in misfolded/misrouted protein and rod photoreceptor cell death. However, the mechanisms of cell death are still under investigation (70).

Mutations in rhodopsin gene (*RHO*, OMIM 180380, accession ID U49742) are the most common cause of autosomal dominant retinitis pigmentosa (ADRP), in which progressive loss of rod cells followed by loss of cone cells leads to night blindness, tunnel vision, and often complete blindness (71). Although, a number of treatments for rhodopsin RP have been proposed and tested in animal models and clinical studies (62), the disease remains untreatable. The failure to develop a significant therapy may actually be due to an incomplete understanding of the mechanisms by which rhodopsin variants cause RP. One hypothesis considers (68) defective rhodopsin –mediated RP as a protein-misfolding disease (also called protein conformational disease) in which the misfolding or misassembly of a mutant protein alters its cellular fate and induces cell death.

The T17M mutation within the Rhodopsin (*RHO*) gene, which substitutes a threonine with a methionine at position 17, affects the assembly of the opsin protein with 11-cis-retinal and presumably impairs protein stability, folding and trafficking. This leads to a severe form of retinal degeneration known as ADRP (68). It has been proposed that ADRP photoreceptors, in general (72) and T17M, in particular (73), die through apoptosis. Recently, our lab has demonstrated that endoplasmic reticulum (ER) stress is involved in the mechanism of S334ter, P23H and T17M Rho photoreceptor death (74-76).

The ability of cells to respond to perturbations in ER function, or ‘ER stress’, is critical for cell survival, but chronic or unresolved ER stress can lead to apoptosis. Factors that perturb ER function and contribute to the development of ER stress include increases in protein synthesis or protein misfolding rates that exceed the capacity of protein chaperones (client load), alterations in calcium stores in the ER lumen, oxidative stress and disturbances to the redox balance in the ER lumen (77). In multicellular eukaryotes, ER stress is sensed by three upstream signaling proteins that, when activated, begin a cascade of corrective actions (77). The activity of these three pathways collectively constitutes an ER-specific unfolded protein response (UPR). Non resolving ER-stress induced apoptosis is becoming increasingly recognized as an important pathogenic factor in a number of widespread and devastating diseases, including neurodegenerative, diabetes, atherosclerosis and renal diseases (78). The mechanisms of photoreceptor loss in RP are unclear, with several pathophysiologic mechanisms implicated (68). An understanding of this signaling pathway is important in the diagnosis and treatment of a variety of diseases.

The UPR tries to reestablish equilibrium through the following strategies: 1) suppression of protein translation to prevent the generation of more unfolded proteins, 2) facilitation of the refolding of unfolded proteins by the induction of ER molecular chaperones, and 3) activation of the ER-associated degradation to remove unfolded proteins that have accumulated in the ER by the ubiquitin-proteasome pathway. If these strategies fail, cells go to ER stress-induced apoptosis. The three major transducers of the UPR are PERK (PKR-like endoplasmic reticulum kinase), IRE1 (inositol- requiring 1) and ATF6 (activating transcription factor 6) (Fig.1) (79). These three transducers sense the presence of the unfolded proteins in the ER lumen and transduce signals to the cytosol or nucleus.

Activation of PERK leads to the phosphorylation of the α -subunit of the eukaryotic initiation factor 2 (eIF2 α), which inhibits the assembly of the 80S ribosome and inhibits protein synthesis. In contrast to most proteins, ATF4 (activating transcription factor 4) escapes translational attenuation by eIF2 α phosphorylation because ATF4 has upstream open reading frames (ORFs) in its 5'-untranslated region. These upstream ORFs, which prevent translation of the true ATF4 under normal conditions, are bypassed only when eIF2 α is phosphorylated, and therefore ATF4 translation occurs (80). In addition to ER stress related function, ATF4 is crucial to many other physiological activities including hematopoiesis, lens and skeletal development, learning and memory formation, hypoxia resistance, tumor growth, autophagy, and amino acid deprivation. Being elevated in many pathological conditions, ATF4 is an attractive therapeutic target (80-82). The role of ATF4 in promoting neurodegenerative disorders, however, is ambiguous and therefore, is still under further investigation. It is known that ATF4 may exert either protective or deleterious effects on cell survival, depending on the paradigm and the benefit from ATF4 overexpression or deficit is a source of continuous debate in the literature (15). ATF4 is expressed constitutively only at low concentrations but becomes rapidly induced under particular cell-stress conditions. The significance of the up regulation is not yet clear (83, 84). In chapter 2, we describe the role of ATF4 in the progression of autosomal dominant inherited retinopathy. Manipulating ATF4 expression in a mouse model of retinal degeneration with UPR activation, we demonstrated for the first time that ATF4 overexpression accelerates retinal degeneration. In contrast, genetic ablation of one allele of ATF4 mitigates retinal degeneration and significantly protects ADRP photoreceptors from rapid deterioration.

Another hallmark of activated UPR is CHOP protein (85). Studies using *Chop* null mice have established the role of CHOP in ER stress induced apoptosis in a number of disease models including renal dysfunction, diabetes, ethanol induced hepatocyte injury, Parkinson's disease, experimental colitis, atherosclerosis, cardiac pressure overload (86-88). "However, the molecular mechanisms are not completely understood". It has been shown that CHOP is involved in macrophage apoptosis induced by combinations of ER stressors and pattern recognition receptor ligands; deletion of CHOP blocks apoptosis without leading to default necrosis (89, 90). Previous studies have also demonstrated that disruption of the CHOP gene protects the islet cells of *Ins2WT/C96Y* mice from apoptosis, thus delaying the onset of ER stress-mediated diabetes (86). Recent findings also indicate that ER stress-mediated CHOP activation plays a central role in causing Alzheimer Disease (AD) pathology by leading to cholesterol oxidization to produce the metabolite 27-hydroxycholesterol (27-OHC) (88). In addition, in the hearts of CHOP-deficient mice, phosphorylation of eIF2 α , which may reduce protein translation, is enhanced compared to that of wild-type mice (91). The same study also proposed the novel concept that CHOP, which may modify protein translation and mediate ER-initiated apoptotic cell death, contributes to the development of cardiac hypertrophy and failure, leading to myocyte apoptosis. In chapter 3, we show that pharmacological modulation of ATF4-CHOP inhibition can be achieved to produce neuroprotection. We found that treatment with the Integrated Stress Response Inhibitor (ISRIB) drug, which successfully reduced ATF4 and CHOP expression, restored cone physiological response in T17M mice which usually shows diminished light-adapted (photopic) ERG amplitude at P30.

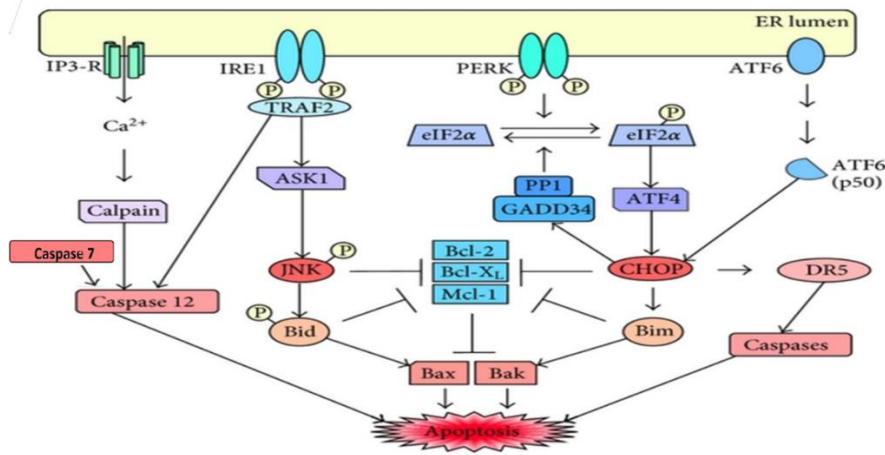


Figure1: Accumulation of misfolded protein leads to the UPR and the activation of the ER stress signaling pathway that is transmitted through three different branches: IRE1, ATF6 and PERK and controls cell survival or death.

It is known that downstream of the UPR, activation of caspases occurs, which promotes apoptosis if the UPR is persistent (78). Caspase-12 is ubiquitously expressed in mouse tissues. It is expressed at high levels in muscle, liver and kidney, and at moderate levels in brain. It belongs to the inflammatory caspases subgroup including caspase-1, -4, -5 and -11 (92). Murine caspase-12 expression is induced by IFN γ and NF- κ B (93); AP-1 binding sites are present in its promoter region (94). Interestingly, caspase-12 has been linked to neuronal degeneration in neurotoxicity caused by amyloid- β protein (95), by prion protein (96) and by mutant superoxide dismutase in animal models of ALS (97). It has been shown that caspase-12 is localized to the ER and activated by ER stress, including disruption of ER calcium homeostasis and accumulation of excess proteins in the ER (95). In unstressed cells, pro-caspase-12 forms a stable complex with TRAF2. The stimuli that induce ER stress and the recruitment of TRAF2 to IRE1 lead to its disassociation from pro-caspase-12, thus, promoting the latter's oligomerization and positioning it for either auto activation or activation by calpain-2 (98) or caspase-7 (99). It has also shown that the cleaved active form of caspase-12 participates in promoting apoptosis by translocation to the nucleus (100). The observation that caspase-12

processing occurs during ER stress apoptosis led to the suggestion that caspase-12 may be the initiator caspase during this process and a potential therapeutic target.

It has been shown that caspase-12 plays an important role in the mechanism of retinal degeneration. For example, photoreceptor apoptosis in the *rd1* mice is accompanied by up-regulation of the protein levels of BiP, caspase-12, phospho-eIF2a and phospho-PERK in a time-dependent manner (101). This up-regulation coincides with or precedes photoreceptor apoptosis. The authors proposed that these ER stress modulators may be strong candidates as therapeutic agents in the treatment of retinal degenerative diseases. The same group demonstrated up-regulation of BiP, caspase-12, phospho-eIF2a and phospho-PERK in a mouse model of retinal photic injury, confirming an idea that the ER stress plays an important role in light-induced photoreceptor apoptosis and that ER stress modulators could be therapeutic candidates in the treatment of retinal degenerative diseases (102). In the fourth and final Chapter we have validated Caspase-12 as a potential therapeutic target, which in combination with non-apoptotic molecular targets might be efficiently used to arrest retinal degeneration in ADRP patients.

Reference

1. Kolb H (1995) Simple Anatomy of the Retina. *Webvision: The Organization of the Retina and Visual System*, eds Kolb H, Fernandez E, & Nelson RSalt Lake City (UT)).
2. Panda-Jonas S, Jonas JB, & Jakobczyk-Zmija M (1996) Retinal pigment epithelial cell count, distribution, and correlations in normal human eyes. *Am J Ophthalmol* 121(2):181-189.
3. Boulton M & Dayhaw-Barker P (2001) The role of the retinal pigment epithelium: topographical variation and ageing changes. *Eye (Lond)* 15(Pt 3):384-389.
4. Cunha-Vaz JG (2004) The blood-retinal barriers system. Basic concepts and clinical evaluation. *Exp Eye Res* 78(3):715-721.
5. Strauss O (2005) The retinal pigment epithelium in visual function. *Physiol Rev* 85(3):845-881.
6. Steinberg RH (1985) Interactions between the retinal pigment epithelium and the neural retina. *Doc Ophthalmol* 60(4):327-346.
7. Baylor D (1996) How photons start vision. *Proc Natl Acad Sci U S A* 93(2):560-565.
8. LaVail MM (1983) Outer segment disc shedding and phagocytosis in the outer retina. *Trans Ophthalmol Soc U K* 103 (Pt 4):397-404.
9. Alberts B, et al. (*Molecular biology of the cell* Sixth edition. Ed pp xxxiv, 1342, 1334, 1353, 1341 pages.
10. Albert DM, Azar DT, & Miller JW (2008) Albert & Jakobiec's principles and practice of ophthalmology. (Saunders/Elsevier,, Philadelphia), p 1 online resource (4 v.).
11. Curcio CA, Sloan KR, Jr., Packer O, Hendrickson AE, & Kalina RE (1987) Distribution of cones in human and monkey retina: individual variability and radial asymmetry. *Science* 236(4801):579-582.
12. Adler FH, Alm A, Kaufman PL, & Levin LA (2011) *Adler's physiology of the eye* (Saunders/Elsevier, London ; New York) 11th Ed pp xii, 795 p.
13. Ogden TE (1983) Nerve fiber layer of the macaque retina: retinotopic organization. *Invest Ophthalmol Vis Sci* 24(1):85-98.
14. Kolb H (1977) The organization of the outer plexiform layer in the retina of the cat: electron microscopic observations. *J Neurocytol* 6(2):131-153.
15. Hopkins JM & Boycott BB (1995) Synapses between cones and diffuse bipolar cells of a primate retina. *J Neurocytol* 24(9):680-694.
16. Provis JM (2001) Development of the primate retinal vasculature. *Prog Retin Eye Res* 20(6):799-821.
17. Yoshizawa T & Wald G (1963) Pre-lumirhodopsin and the bleaching of visual pigments. *Nature* 197:1279-1286.

18. Arshavsky VY, Lamb TD, & Pugh EN, Jr. (2002) G proteins and phototransduction. *Annu Rev Physiol* 64:153-187.
19. Shichi H & Somers RL (1978) Light-dependent phosphorylation of rhodopsin. Purification and properties of rhodopsin kinase. *J Biol Chem* 253(19):7040-7046.
20. Kuhn H & Wilden U (1987) Deactivation of photoactivated rhodopsin by rhodopsin-kinase and arrestin. *J Recept Res* 7(1-4):283-298.
21. Fain GL, Matthews HR, Cornwall MC, & Koutalos Y (2001) Adaptation in vertebrate photoreceptors. *Physiol Rev* 81(1):117-151.
22. Stryer L (1991) Visual excitation and recovery. *J Biol Chem* 266(17):10711-10714.
23. Dizhoor AM, Lowe DG, Olshevskaya EV, Laura RP, & Hurley JB (1994) The human photoreceptor membrane guanylyl cyclase, RetGC, is present in outer segments and is regulated by calcium and a soluble activator. *Neuron* 12(6):1345-1352.
24. Jindrova H (1998) Vertebrate phototransduction: activation, recovery, and adaptation. *Physiol Res* 47(3):155-168.
25. Henderson R & Schertler GF (1990) The structure of bacteriorhodopsin and its relevance to the visual opsins and other seven-helix G-protein coupled receptors. *Philos Trans R Soc Lond B Biol Sci* 326(1236):379-389.
26. Dryja TP, *et al.* (1990) A point mutation of the rhodopsin gene in one form of retinitis pigmentosa. *Nature* 343(6256):364-366.
27. Palczewski K, *et al.* (2000) Crystal structure of rhodopsin: A G protein-coupled receptor. *Science* 289(5480):739-745.
28. Hargrave PA, *et al.* (1983) The structure of bovine rhodopsin. *Biophys Struct Mech* 9(4):235-244.
29. Pugh EN, Jr. & Lamb TD (1993) Amplification and kinetics of the activation steps in phototransduction. *Biochim Biophys Acta* 1141(2-3):111-149.
30. Okada T & Palczewski K (2001) Crystal structure of rhodopsin: implications for vision and beyond. *Curr Opin Struct Biol* 11(4):420-426.
31. Schoenlein RW, Peteanu LA, Mathies RA, & Shank CV (1991) The first step in vision: femtosecond isomerization of rhodopsin. *Science* 254(5030):412-415.
32. Langlois G, Chen CK, Palczewski K, Hurley JB, & Vuong TM (1996) Responses of the phototransduction cascade to dim light. *Proc Natl Acad Sci U S A* 93(10):4677-4682.
33. Ohguro H, Van Hooser JP, Milam AH, & Palczewski K (1995) Rhodopsin phosphorylation and dephosphorylation in vivo. *J Biol Chem* 270(24):14259-14262.
34. Lefkowitz RJ (1993) G protein-coupled receptor kinases. *Cell* 74(3):409-412.
35. Kawamura S (1992) Light-sensitivity modulating protein in frog rods. *Photochem Photobiol* 56(6):1173-1180.

36. Kawamura S (1993) Rhodopsin phosphorylation as a mechanism of cyclic GMP phosphodiesterase regulation by S-modulin. *Nature* 362(6423):855-857.
37. Klenchin VA, Calvert PD, & Bownds MD (1995) Inhibition of rhodopsin kinase by recoverin. Further evidence for a negative feedback system in phototransduction. *J Biol Chem* 270(27):16147-16152.
38. Palczewski K (1994) Structure and functions of arrestins. *Protein Sci* 3(9):1355-1361.
39. Smith WC, *et al.* (1994) A splice variant of arrestin. Molecular cloning and localization in bovine retina. *J Biol Chem* 269(22):15407-15410.
40. Krispel CM, *et al.* (2006) RGS expression rate-limits recovery of rod photoresponses. *Neuron* 51(4):409-416.
41. Lamb TD & Pugh EN, Jr. (2004) Dark adaptation and the retinoid cycle of vision. *Prog Retin Eye Res* 23(3):307-380.
42. Fung BK, Hurley JB, & Stryer L (1981) Flow of information in the light-triggered cyclic nucleotide cascade of vision. *Proc Natl Acad Sci U S A* 78(1):152-156.
43. Stryer L, Hurley JB, & Fung BK (1983) Transducin and the cyclic GMP phosphodiesterase of retinal rod outer segments. *Methods Enzymol* 96:617-627.
44. Heck M & Hofmann KP (2001) Maximal rate and nucleotide dependence of rhodopsin-catalyzed transducin activation: initial rate analysis based on a double displacement mechanism. *J Biol Chem* 276(13):10000-10009.
45. Fung BK, Lieberman BS, & Lee RH (1992) A third form of the G protein beta subunit. 2. Purification and biochemical properties. *J Biol Chem* 267(34):24782-24788.
46. Lerea CL, Somers DE, Hurley JB, Klock IB, & Bunt-Milam AH (1986) Identification of specific transducin alpha subunits in retinal rod and cone photoreceptors. *Science* 234(4772):77-80.
47. Baehr W, Devlin MJ, & Applebury ML (1979) Isolation and characterization of cGMP phosphodiesterase from bovine rod outer segments. *J Biol Chem* 254(22):11669-11677.
48. He W, Cowan CW, & Wensel TG (1998) RGS9, a GTPase accelerator for phototransduction. *Neuron* 20(1):95-102.
49. Makino ER, Handy JW, Li T, & Arshavsky VY (1999) The GTPase activating factor for transducin in rod photoreceptors is the complex between RGS9 and type 5 G protein beta subunit. *Proc Natl Acad Sci U S A* 96(5):1947-1952.
50. Hu G & Wensel TG (2002) R9AP, a membrane anchor for the photoreceptor GTPase accelerating protein, RGS9-1. *Proc Natl Acad Sci U S A* 99(15):9755-9760.
51. Kaupp UB & Seifert R (2002) Cyclic nucleotide-gated ion channels. *Physiol Rev* 82(3):769-824.
52. Weitz D, Ficek N, Kremmer E, Bauer PJ, & Kaupp UB (2002) Subunit stoichiometry of the CNG channel of rod photoreceptors. *Neuron* 36(5):881-889.

53. Zheng J, Trudeau MC, & Zagotta WN (2002) Rod cyclic nucleotide-gated channels have a stoichiometry of three CNGA1 subunits and one CNGB1 subunit. *Neuron* 36(5):891-896.
54. Peng C, Rich ED, & Varnum MD (2004) Subunit configuration of heteromeric cone cyclic nucleotide-gated channels. *Neuron* 42(3):401-410.
55. Hagins WA, Penn RD, & Yoshikami S (1970) Dark current and photocurrent in retinal rods. *Biophys J* 10(5):380-412.
56. Cooper N, *et al.* (1995) The bovine rod outer segment guanylate cyclase, ROS-GC, is present in both outer segment and synaptic layers of the retina. *J Mol Neurosci* 6(3):211-222.
57. Liu X, *et al.* (1994) Ultrastructural localization of retinal guanylate cyclase in human and monkey retinas. *Exp Eye Res* 59(6):761-768.
58. Lowe DG, *et al.* (1995) Cloning and expression of a second photoreceptor-specific membrane retina guanylyl cyclase (RetGC), RetGC-2. *Proc Natl Acad Sci U S A* 92(12):5535-5539.
59. Baehr W, *et al.* (2007) The function of guanylate cyclase 1 and guanylate cyclase 2 in rod and cone photoreceptors. *J Biol Chem* 282(12):8837-8847.
60. Imanishi Y, *et al.* (2002) Characterization of retinal guanylate cyclase-activating protein 3 (GCAP3) from zebrafish to man. *Eur J Neurosci* 15(1):63-78.
61. Baehr W, Wu SM, Bird AC, & Palczewski K (2003) The retinoid cycle and retina disease. *Vision Res* 43(28):2957-2958.
62. Hartong DT, Berson EL, & Dryja TP (2006) Retinitis pigmentosa. *Lancet* 368(9549):1795-1809.
63. Humphries P, Kenna P, & Farrar GJ (1992) On the molecular genetics of retinitis pigmentosa. *Science* 256(5058):804-808.
64. Boughman JA, Vernon M, & Shaver KA (1983) Usher syndrome: definition and estimate of prevalence from two high-risk populations. *J Chronic Dis* 36(8):595-603.
65. Beales PL, Elcioglu N, Woolf AS, Parker D, & Flintner FA (1999) New criteria for improved diagnosis of Bardet-Biedl syndrome: results of a population survey. *J Med Genet* 36(6):437-446.
66. Hamel C (2006) Retinitis pigmentosa. *Orphanet J Rare Dis* 1:40.
67. Doi T, Molday RS, & Khorana HG (1990) Role of the intradiscal domain in rhodopsin assembly and function. *Proc Natl Acad Sci U S A* 87(13):4991-4995.
68. Mendes HF, van der Spuy J, Chapple JP, & Cheetham ME (2005) Mechanisms of cell death in rhodopsin retinitis pigmentosa: implications for therapy. *Trends Mol Med* 11(4):177-185.
69. Kaushal S & Khorana HG (1994) Structure and function in rhodopsin. 7. Point mutations associated with autosomal dominant retinitis pigmentosa. *Biochemistry* 33(20):6121-6128.

70. Portera-Cailliau C, Sung CH, Nathans J, & Adler R (1994) Apoptotic photoreceptor cell death in mouse models of retinitis pigmentosa. *Proc Natl Acad Sci U S A* 91(3):974-978.
71. Bowne SJ, *et al.* (2011) A dominant mutation in RPE65 identified by whole-exome sequencing causes retinitis pigmentosa with choroidal involvement. *European journal of human genetics : EJHG* 19(10):1074-1081.
72. Chang GQ, Hao Y, & Wong F (1993) Apoptosis: final common pathway of photoreceptor death in rd, rds, and rhodopsin mutant mice. *Neuron* 11(4):595-605.
73. White DA, Fritz JJ, Hauswirth WW, Kaushal S, & Lewin AS (2007) Increased sensitivity to light-induced damage in a mouse model of autosomal dominant retinal disease. *Investigative ophthalmology & visual science* 48(5):1942-1951.
74. Shinde VM, Sizova OS, Lin JH, LaVail MM, & Gorbatyuk MS (2012) ER stress in retinal degeneration in S334ter Rho rats. *PloS one* 7(3):e33266.
75. Kunte MM, *et al.* (2012) ER stress is involved in T17M rhodopsin-induced retinal degeneration. *Investigative ophthalmology & visual science* 53(7):3792-3800.
76. Gorbatyuk MS, *et al.* (2010) Restoration of visual function in P23H rhodopsin transgenic rats by gene delivery of BiP/Grp78. *Proceedings of the National Academy of Sciences of the United States of America* 107(13):5961-5966.
77. Ron D & Walter P (2007) Signal integration in the endoplasmic reticulum unfolded protein response. *Nature reviews. Molecular cell biology* 8(7):519-529.
78. Tabas I & Ron D (2011) Integrating the mechanisms of apoptosis induced by endoplasmic reticulum stress. *Nature cell biology* 13(3):184-190.
79. Rutkowski DT & Kaufman RJ (2007) That which does not kill me makes me stronger: adapting to chronic ER stress. *Trends in biochemical sciences* 32(10):469-476.
80. Ameri K & Harris AL (2008) Activating transcription factor 4. *The international journal of biochemistry & cell biology* 40(1):14-21.
81. Malabanan KP & Khachigian LM (2010) Activation transcription factor-4 and the acute vascular response to injury. *Journal of molecular medicine* 88(6):545-552.
82. Fels DR & Koumenis C (2006) The PERK/eIF2alpha/ATF4 module of the UPR in hypoxia resistance and tumor growth. *Cancer biology & therapy* 5(7):723-728.
83. Lange PS, *et al.* (2008) ATF4 is an oxidative stress-inducible, prodeath transcription factor in neurons in vitro and in vivo. *The Journal of experimental medicine* 205(5):1227-1242.
84. Sun X, *et al.* (2013) ATF4 protects against neuronal death in cellular Parkinson's disease models by maintaining levels of parkin. *The Journal of neuroscience : the official journal of the Society for Neuroscience* 33(6):2398-2407.
85. Oyadomari S & Mori M (2004) Roles of CHOP/GADD153 in endoplasmic reticulum stress. *Cell death and differentiation* 11(4):381-389.
86. Oyadomari S, *et al.* (2001) Nitric oxide-induced apoptosis in pancreatic beta cells is mediated by the endoplasmic reticulum stress pathway. *Proceedings of the*

- National Academy of Sciences of the United States of America* 98(19):10845-10850.
87. Thorp E, *et al.* (2009) Reduced apoptosis and plaque necrosis in advanced atherosclerotic lesions of Apoe^{-/-} and Ldlr^{-/-} mice lacking CHOP. *Cell metabolism* 9(5):474-481.
 88. Prasanthi JR, Larson T, Schommer J, & Ghribi O (2011) Silencing GADD153/CHOP gene expression protects against Alzheimer's disease-like pathology induced by 27-hydroxycholesterol in rabbit hippocampus. *PLoS one* 6(10):e26420.
 89. Devries-Seimon T, *et al.* (2005) Cholesterol-induced macrophage apoptosis requires ER stress pathways and engagement of the type A scavenger receptor. *The Journal of cell biology* 171(1):61-73.
 90. Feng B, *et al.* (2003) The endoplasmic reticulum is the site of cholesterol-induced cytotoxicity in macrophages. *Nature cell biology* 5(9):781-792.
 91. Fu HY, *et al.* (2010) Ablation of C/EBP homologous protein attenuates endoplasmic reticulum-mediated apoptosis and cardiac dysfunction induced by pressure overload. *Circulation* 122(4):361-369.
 92. Lamkanfi M, Declercq W, Kalai M, Saelens X, & Vandenameele P (2002) Alice in caspase land. A phylogenetic analysis of caspases from worm to man. *Cell death and differentiation* 9(4):358-361.
 93. Kalai M, *et al.* (2003) Regulation of the expression and processing of caspase-12. *The Journal of cell biology* 162(3):457-467.
 94. Oubrahim H, Wang J, Stadtman ER, & Chock PB (2005) Molecular cloning and characterization of murine caspase-12 gene promoter. *Proceedings of the National Academy of Sciences of the United States of America* 102(7):2322-2327.
 95. Nakagawa T, *et al.* (2000) Caspase-12 mediates endoplasmic-reticulum-specific apoptosis and cytotoxicity by amyloid-beta. *Nature* 403(6765):98-103.
 96. Hetz C, Russelakis-Carneiro M, Maundrell K, Castilla J, & Soto C (2003) Caspase-12 and endoplasmic reticulum stress mediate neurotoxicity of pathological prion protein. *The EMBO journal* 22(20):5435-5445.
 97. Wootz H, Hansson I, Korhonen L, Napankangas U, & Lindholm D (2004) Caspase-12 cleavage and increased oxidative stress during motoneuron degeneration in transgenic mouse model of ALS. *Biochemical and biophysical research communications* 322(1):281-286.
 98. Nakagawa T & Yuan J (2000) Cross-talk between two cysteine protease families. Activation of caspase-12 by calpain in apoptosis. *The Journal of cell biology* 150(4):887-894.
 99. Rao RV, *et al.* (2001) Coupling endoplasmic reticulum stress to the cell death program. Mechanism of caspase activation. *The Journal of biological chemistry* 276(36):33869-33874.

100. Fujita E, *et al.* (2002) Caspase-12 processing and fragment translocation into nuclei of tunicamycin-treated cells. *Cell death and differentiation* 9(10):1108-1114.
101. Yang LP, Wu LM, Guo XJ, & Tso MO (2007) Activation of endoplasmic reticulum stress in degenerating photoreceptors of the rd1 mouse. *Investigative ophthalmology & visual science* 48(11):5191-5198.
102. Yang LP, Wu LM, Guo XJ, Li Y, & Tso MO (2008) Endoplasmic reticulum stress is activated in light-induced retinal degeneration. *Journal of neuroscience research* 86(4):910-919.

CHAPTER 2

LIMITED ATF4 EXPRESSION IN DEGENERATING RETINAS WITH ONGOING ER STRESS PROMOTES PHOTORECEPTOR SURVIVAL IN A MOUSE MODEL OF AUTOSOMAL DOMINANT RETINITIS PIGMENTOSA.

by

YOGESH BHOTADA, SERGEI ZOLOTUKHIN, OLEG GORBATYUK,
ZSUZSANNA BEBOK AND MARINA GORBATYUK.

Submitted to *Molecular Neurodegeneration*

Format adapted for dissertation

Limited ATF4 Expression in Degenerating Retinas with Ongoing ER Stress Promotes Photoreceptor Survival in a Mouse Model of Autosomal Dominant Retinitis Pigmentosa.

Abstract

Background: Expression of T17M rhodopsin in rod photoreceptors leads to severe retinal degeneration and is associated with activation of the Unfolded Protein Response (UPR) and elevation of the UPR marker, ATF4. A role for ATF4 in photoreceptor cellular pathology has not been explored previously. We used knockout mice and adeno-associated viral (AAV) delivery of ATF4 to the retina to validate a novel therapeutic approach based on the reduction of ATF4 over the course of retinal degeneration. We demonstrated a pro-death role for ATF4 overexpression during autosomal dominant retinitis pigmentosa (ADRP).

Results: In T17M rhodopsin mice, we observed an association between ATF4 overexpression, reduced p62 levels, and elevation of p53 levels. These expression changes, together with increased CHOP and caspase-3/7 activity, contributed to the mechanism of photoreceptor cell loss. Conversely, ATF4 knockdown retarded retinal degeneration in 1-month-old T17M Rhodopsin mice and promoted photoreceptor survival, as measured by scotopic and photopic ERGs and photoreceptor nuclei row counts. ATF4 knockdown also markedly delayed the onset of retinal degeneration in 3-month-old ADRP animals. This delay was accompanied by a dramatic decrease in UPR markers, the launching of anti-oxidant defenses, initiation of autophagy, and improvement of rhodopsin biosynthesis, which together aided in combating the cellular stress found in the T17M rhodopsin retina.

Conclusion: Our data indicate that ATF4 overexpression during retinal degeneration plays a cytotoxic role by triggering photoreceptor cell death, whereas ATF4 deficiency

tremendously delays the onset of retinal degeneration. Thus, future ADRP therapy might be aimed at controlling ATF4 expression in degenerating retinas.

Introduction

T17M Rhodopsin mice, carrying a mutant human rhodopsin (*RHO*) gene, have become a valuable animal model for studying autosomal dominant retinitis pigmentosa (ADRP). Severe retinal degeneration is detected by one month in these animals, as shown by a significant loss of scotopic a- and b-wave ERG amplitudes and in compromised retinal integrity [1-3] as a result of apoptotic photoreceptor cell death. The mechanism responsible for retinal degeneration in the ADRP retina includes the impaired assembly of the opsin protein with its chromophore, 11-cis-retinal, and due to its modified stability, folding and trafficking [4]. The accumulation of mutant misfolded rhodopsin in the endoplasmic reticulum (ER) can trigger a signal transduction cascade known as the Unfolded Protein Response (UPR); we have previously shown UPR activation in T17M *RHO* photoreceptors [3]. In these mice we have demonstrated that PERK (RNA-activated protein kinase-like ER kinase) signaling is upregulated, thus, leading to an increase in phosphorylated (p) translational eukaryotic initiation factor 2 α (eIF2 α) and Activating transcription factor 4 (ATF4 or cAMP responsive element binding protein, CREB) mRNA, starting at postnatal day (P) 18. The accumulation of p-eIF2 α has also been found in the retina of an ADRP rat model carrying the P23H *RHO* gene [5]. This mutation, like the T17M *RHO* mutant, represents a Class II mutation [6] and leads to dramatic retinal degeneration [5]. These findings suggest that activated PERK signaling could be a common hallmark of progressive ADRP.

One of the major mediators of PERK signaling is ATF4. On the molecular level, ATF4 is known to be a key ER stress-induced transcription factor that plays a pivotal role in both adaptation to stress and activation of apoptosis. Cellular ER stress activates the PERK pathway and induces phosphorylation of eIF2 α , an upstream activator of ATF4 that regulates the expression of the apoptosis-related CHOP transcription factor [7]. In addition, an extracellular stress signal is known to be promoted by ATF4-controlled expression of growth factors, cytokines, chemoattractants, and adhesion molecules [8].

Besides ER stress, ATF4 is crucial to many other physiological activities including hematopoiesis, lens and skeletal development, learning and memory formation, hypoxia resistance, tumor growth, autophagy, and amino acid deprivation [9]. Being elevated in many pathological conditions, ATF4 has become an attractive therapeutic target. Thus the current work on targeting ATF4 in cancer progression focuses on strategies aimed at inhibiting transcriptional activity or increasing ATF4 degradation [10]. The role of ATF4 in promoting neurodegenerative disorders, however, is ambiguous and therefore still under investigation. It is known that ATF4 may exert either protective or deleterious effects on cell survival, depending on the paradigm [11], and the benefit from ATF4 overexpression or deficit is a source of continuous debate in the literature. ATF4 is expressed constitutively only at low levels but becomes rapidly induced under particular cell-stress conditions [12]. Elevated expression of ATF4 results in its binding to the promoter regions of target genes that are involved in amino acid metabolism, redox control, and apoptosis [13,14].

In ocular degenerative diseases, the elevation of ATF4 as well as the activation of the UPR have been described in different retinal cell types, reviewed in [15]. The majority of these experiments have been conducted in cellular models of ocular disorders; *in vivo*

studies have also highlighted the involvement of ATF4 in the pathology of diabetes[16], oxygen induced retinopathy [17, 18], and retinitis pigmentosa [19, 3, 5].

Here, we investigated the role of ATF4 in the progression of autosomal dominant inherited retinopathy. Manipulating ATF4 expression in a mouse model of retinal degeneration with UPR activation, we demonstrated for the first time that ATF4 overexpression accelerates retinal degeneration. In contrast, genetic ablation of one allele of ATF4 mitigates retinal degeneration and significantly protects ADRP photoreceptors from rapid deterioration. The results of this study together with our previous work [7,319] highlight PERK-mediated UPR signaling as a cellular network that controls the rate of retinal degeneration and validate ATF4 as a future therapeutic target.

Material and Methods

Study approval

All experiments with mice followed the animal protocol approved by the Animal Care and Use Committee of the University of Alabama at Birmingham, conforming to the Association for Research in Vision and Ophthalmology guidelines.

Animals

Transgenic mice expressing human T17M RHO^{+/+}, C57BL/6J, RHO^{-/-} and ATF4^{+/-} knockout mice were used in this study to generate T17M RHO^{+/-} (T17M), T17M RHO^{+/-} ATF4^{+/-} (T17M ATF4^{+/-}). ATF4^{+/-} mice were purchased from Jackson (Bar Harbor, ME; <http://www.jax.org>) and have a normal appearance, organ morphology and eye development. T17M RHO mice were raised under a 12-h dim light/12-h dark cycle. The genotyping of ATF4^{+/-} mice was performed using forward primers: ATATTGCTGAAGAGCTTGGCGGC for Neo allele and

AGCAAAACAAGACAGCAGCCACTA for wild type allele and a common reverse primer GTTTCTACAGCTTCCTCCACTCTT for both alleles. The T17M genotyping was performed as previously described [1]. To visualize UPR activation and splicing of the Xbp1 transcriptional factor (IRE1 pathway) in the ADRP retina, ERAI (**ER** stress Activating Inducer) mice were used as previously described [3].

Sub-retinal injections were performed in pups at postnatal day 15 with 1 μ l of either AA2/5 virus (serotype 5) expressing the mouse ATF4 cDNA or GFP (10^{13} genome particle per ml for both viruses) driven by the CMV enhancer-chicken β -actin (CBA) promoter in their right eye and GFP in their left eye, as previously described [3]. Animals were monitored for 2 weeks. ERG and protein analysis of injected mice were performed to evaluate the results of ATF4 overexpression.

Electroretinography

Mice were dark-adapted overnight, then anesthetized with ketamine (100 mg/kg) and xylazine (10 mg/kg), and their pupils were dilated in dim red light with 2.5% phenylephrine hydrochloride ophthalmic solution (Akorn, Inc.). Scotopic ERGs were recorded using a wire contacting the corneal surface with 2.5% hypromellose ophthalmic demulcent solution (Akorn, Inc.). ERG was performed at different light intensities (0 db (2.5 cd*s/m²), 5 db (7.91 cd*s/m²), 10 db (25 cd*s/m²), and 15 db (79.1 cd*s/m²). Five scans were performed and averaged at different light intensities. Photopic, cone-mediated responses were performed following 10 min light adaptation on the background light intensity of 30 cd*s/m². Recordings were obtained at the light intensity of 25 cd*s/m². Fifteen waveforms from each animal were recorded and the values were averaged. The a-wave amplitudes were measured from the baseline to the peak in the cornea-negative direction, and the b-wave amplitudes were determined from the cornea-negative peak to

the major cornea-positive peak. The signal was amplified, digitized, and stored using the LKC UTAS-3000 Diagnostic System (Gaithersburg, MD).

Spectra Domain-Optical Coherent Tomography (SD-OCT)

SD-OCT was performed in P30, P60 and P90 animals using the Spectral Domain Ophthalmic Imaging System (SDOIS) (Bioptigen). The mice were anesthetized. Horizontal volume scans through the area dorso-temporal from the optic nerve (superior retina) and the area ventro-temporal from the optic nerve (inferior retina) were used to evaluate the thickness of the ONL. For measuring the thickness of the ONL, six calibrated calipers were placed in the superior and inferior hemispheres of retinas within 100, 200, 300 and 400 μm of the optic nerve head. The thickness of the ONL was determined by averaging ten measurements.

Retinal Imaging

Mice were anesthetized with 100 mg/kg ketamine and 5 mg/kg xylazine intraperitoneally, and the pupils were dilated using 2.5% phenylephrine hydrochloride ophthalmic solution (Akorn, Inc.). The fundus was examined using the Micron IV camera (Phoenix Research Laboratories, Pleasanton, CA) with StreamPix 5 software in fluorescent modes. GFP fluorescence was detectable using green fluorescent barrier filters.

Histology and Immunohistochemistry

Mouse eyes were enucleated at 1 and 3 months of age and were fixed overnight in 4% paraformaldehyde freshly made in phosphate-buffered saline (PBS) as previously described [1]. Hematoxylin and eosin staining of 12-micron retinal cryosections as well as counting of retinal nuclei were performed as previously described [2]. Digital images of right and left retinas of individual mice were analyzed in the central superior and

inferior equally located from the optic nerve head. A masked investigator analyzed the images.

For immunohistochemistry retinal cryosections were rinsed in PBS and blocked in 2% normal goat serum, 0.3% Triton X-100 in 0.01% BSA in PBS for 1 hour at room temperature. The sections were then stained with primary anti-rhodopsin antibodies (1D4, University of British Columbia, Vancouver, Canada) which were diluted in PBS with 0.1% Triton X-100 and 1% BSA and incubated overnight at 4⁰C. The Cy2-labeled anti-IgG secondary antibody (Jackson ImmunoResearch Laboratories, West Grove, PA) diluted 1:500 in PBS was applied at room temperature for 1 hour. Sections were mounted with Vectashield Mounting Medium (Vector Lab) and cover slipped. Images were taken using a confocal microscope (Leica SP1 UV Confocal Laser Scanning Microscope).

For staining retinas for reactive oxygen species, 12-micron sections were incubated with a general oxidative stress indicator, CM-H2DCFDA, Invitrogen (10 μ M/L in PBS) in the dark for 1 hour. Sections were washed three times and were mounted and coverslip with Vectashield Mounting Medium. The 485nm fluorescence filter was used to take images. Images were converted to black and white to improve contrast.

Quantitative real-time RT-PCR

For RNA extraction, whole retinas were isolated from 1- month-old mice (C57BL/6J, ATF4^{+/-}, T17M and T17M ATF4^{+/-}) by surgical excision. Total RNA was extracted using the QIAGEN RNeasy Mini Kit. One μ g of purified RNA was reverse transcribed into cDNA using iScriptTM Reverse Transcription Supermix (BioRad). Integrity of the RNA samples as well as efficiency of cDNA reaction was verified prior to the qRT-PCR. TaqMan Gene Expression Assay kits (Applied Biosystems) were used to measure gene expression (mRho: Mm00520345m1; HRho: Hs00892431_m1; Gapdh: Mm99999915g1;

Bip: Mm00517690_g1; XBP1: Mm03464496_m1; GADD34: Mm00435119_m1; CHOP: Mm01135937_g1). TaqMan miRNA assay was performed using the TaqMan MicroRNA Reverse Transcription kit (Applied Biosystems) and a total of 500 ng RNA was reverse transcribed into cDNA with specific miRNA primers (hsa-miR-708: mmu-miR-708-5p). Small nucleolar RNA 202 (snoRNA202: AF357327) was used as a control. Quantitative real-time PCR was performed with the Step One Plus™ Real-Time PCR System (Applied Biosystems) based on the relative standard curve method. Reactions were performed at 50°C for 2 minutes and 95°C for 10 minutes, followed by 40 cycles at 95°C for 15 seconds and 60°C for 1 minute. Results were expressed as cycle threshold time (Ct) and were normalized to Ct times for the housekeeping gene GAPDH. The replicated RQ (Relative Quantity) values for each biological sample were averaged. Biological samples from each strain were used for qRT-PCR analyses.

Western Blot

For protein extraction, whole retinas were isolated from 1-month-old mice (C57BL/6J, ATF4^{+/-}, T17M and T17M ATF4^{+/-}) by surgical excision. Total protein was extracted via sonication in a protein extraction buffer containing 25 mM sucrose, 100 mM Tris-HCl, pH = 7.8, and a mixture of protease inhibitors (PMSF, TLCK, aprotinin, leupeptin, and pepstatin). Protein concentrations were determined using BioRad Protein Assays based on the Bradford method for protein quantitation. Proteins (30–40 µg) were separated in 4–20% Criterion Precast gels and 5% polyacrylamide gels (BioRad), transferred to a polyvinylidene difluoride (PVDF) membrane using the Trans-Blot Turbo Transfer System (BioRad) and incubated with primary antibodies overnight at 4°C under agitation. After washing, the membranes were incubated for 1.5 h with respective (anti-mouse, anti-rabbit or anti-goat immunoglobulin) Fluorescence or HRP conjugated secondary antibody

(LI-COR Odyssey). For HRP tagged antibody blots were developed with enhanced chemiluminescence (ECL) according to manufacturer's instructions (Amersham Bioscience). β -actin was used as a gel loading control and was detected using an anti- β -actin antibody (1:5000, Sigma-Aldrich, #A1978). The developed membrane was imaged using the LI-COR Odyssey Quantitative Fluorescence Imaging System.

Caspase 3/7 Activity Assay. The detection of caspase 3/7 activity was performed using the Caspase-Glo 3/7 Luciferase assay (#G8091; Promega, Madison, WI) kit in accordance with the manufacturer's recommendations. Luciferase signal was read by a luminescent plate reader (Infinite m200, Tecan Group Ltd., Meannedorf, Switzerland) and used to compare the activation of caspase 3/7 in C57BL/6J, ATF4^{+/-}, T17M and T17M ATF4^{+/-} retinal tissues.

Statistical analysis

Two-way ANOVA comparisons were used to calculate differences in the a- and b-wave ERG amplitudes and in the average ONL thickness of inferior and superior retinas in 1-, 2- and 3-month-old mice. A one-way ANOVA and *t*-test were used to calculate a fold change of mRNA expressions and a level of normalized proteins in P30 retinas. For all experiments, *P*-value higher than 0.05 was considered significant (**P*<0.05, ***P*<0.01, ****P*<0.001, and *****P*<0.0001). Data are represented using mean \pm SEM.

Results

We up- and downregulated *Atf4* gene expression either by genetic ablation of one copy or by overexpression by means of AAV2/5 –mediated ATF4 gene delivery.

Overexpression of ATF4 in the T17M retina accelerates retinal degeneration

We determined if ATF4 overexpression is cytoprotective in ADRP retinas by injecting P15 T17M and C57BL/6 pups with AAV2/5-ATF4 in the right and AAV2/5- GFP in the left eyes. This serotype has been shown to preferentially transduce photoreceptors in the retina [20, 21]. The viral-mediated GFP expression in the eye was confirmed by Micron IV funduscopy (Fig. S1). The physiological response of photoreceptors to ATF4 overexpression was measured by scotopic ERG at 2-weeks post-injection. This time point was chosen since only a short window of opportunity is available for functional and structural rescue in T17M mice, which experience photoreceptor cell death by P30 (Fig. S1). Our analysis of ERG recordings (Fig. 1A) revealed a significant reduction in ERG amplitudes in retinas with a 2.3-fold overexpression of ATF4 (Fig. 1B). The AAV2/5 - GFP-injected eyes showed a decline in ERG amplitudes similar to that found in control naïve animals with progressive ADRP. In addition to T17M, a slightly greater reduction was observed in the amplitudes of the scotopic ERG a- and b-waves in C57BL/6 mice injected with AAV2/5- ATF4 (Fig. 1A) suggesting that overexpression of ATF4 is harmful to both degenerating and normally functioning photoreceptors.

Accelerated loss of function is usually accompanied by a greater rate of cell death. Our examination of H&E-stained T17M retinal cryostat sections and counts of the number of photoreceptor rows (Fig. 1C and D) revealed a significant decline in the number of rows of photoreceptor nuclei in T17M ATF4-injected retinas, which further supported the functional test results indicating that ATF4 overexpression in T17M retinas accelerates retinal degeneration.

The induction of ATF4 generally results in increases in apoptosis-related CHOP mRNA [22]. Our analysis of CHOP production in the ATF4-overexpressed T17M retina showed that ATF4 vector transduction resulted in higher CHOP levels than were observed in

AAV2/5-GFP-injected retinas (Fig. 1B). Therefore, we analyzed the activation of the executioner caspases 3/7 in ATF4-injected retinas, since CHOP overexpression is known to trigger apoptosis. The increased level of CHOP in ATF4-overexpressing T17M retinas was correlated with increased levels of caspase-3/7 activity (Fig. 1E). The AAV2/5-ATF4 injection also elevated caspase-3/7 activity in wild type retinas.

Thus, our experiments revealed that, in general, sustained ATF4 overexpression in photoreceptors provokes severe retinal degeneration in both wild type and degenerating retinas through activation of programmed cell death.

Figure 1

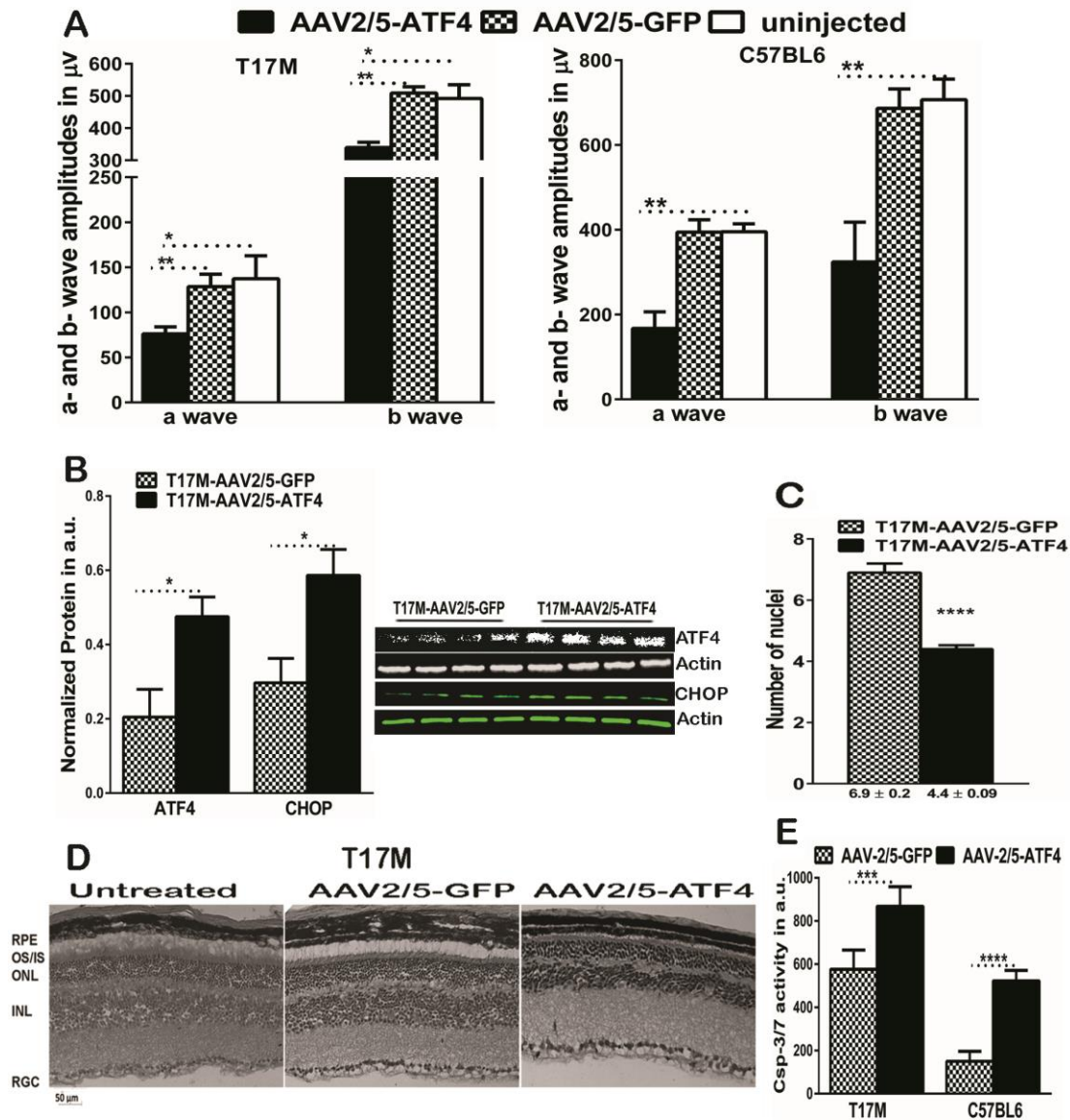


Figure 1 Overexpression of ATF4 accelerates and induces retinal degeneration in T17M mice and C57BL/6 mice, respectively.

(A) ERG amplitudes were registered as described in the methods and were analyzed by one-way ANOVA. Data analysis demonstrated that subretinal injections of AAV2/5-ATF4 led to a loss of photoreceptor function in the right ATF4-injected T17M retina compared to the left AAV2/5- GFP-injected eye (N=6, $P<0.05$ for both a and b-wave amplitudes). The C57BL/6 retina overexpressing ATF4 also experienced a decline in a- and b- wave ERG amplitudes (N=4, for both $P<0.01$) as compared to GFP-injected controls or uninjected animals (N=4). Results of the scotopic ERG amplitudes registered at 25 cd*s/m² are shown. (B) Overexpression of ATF4 in the injected (right) retinas was

measured by western blotting. A 2.3-fold (N=6, *t*-test *p*=0.017) increase in ATF4 was found in the right eye when compared to the left eye. This resulted in upregulation of CHOP protein (N=6, *t*-test *p*=0.046) in ATF4 overexpressing eyes. Representative images of western blots probed with antibody against ATF4, CHOP, and β -actin are shown on the side. **(C)** Overexpression of ATF4 and CHOP proteins in T17M retinas was associated with a loss of photoreceptor cells measured by counting the nuclei rows in H&E stained retinal sections (N=4, *t*-test *P*<0.001). **(D)** Representative images of the H&E stained T17M retina injected with AAV2/5-GFP and AAV2/5-ATF4. **(E)** Photoreceptor cell death in T17M and the wild type retinas overexpressing ATF4 was associated with highly activated caspase-3/7 (N=4, *t*-test *p*=0.011 and *P*<0.0001, respectively). The data are presented as mean \pm SEM.

T17M mice deficient in ATF4 exhibit a delay of the onset of retinal degeneration as measured by functional vision test. We tested the hypothesis that a reduction in ATF4 expression in ADRP mice experiencing severe UPR activation [3] would preserve visual function and prevent photoreceptor cell death in T17M retinas. We knocked down ATF4 levels in ADRP retinas by genetically modifying mice. ATF4^{-/-} mice develop severe microphthalmia with no recognizable lens, thus, were unsuitable for this experiment. However, ATF4^{+/-} *Rho*^{+/+} mice (henceforth referred to as ATF4^{+/-} mice) appear to develop normally and have normal vision. We created an ADRP animal model with reduced ATF4 expression by crossing T17M^{+/-} *Rho*^{+/+} ATF4^{+/-} mice with *Rho*^{-/-} mice to obtain T17M^{+/-} *Rho*^{+/-} ATF4^{+/-} mice (henceforth referred to as T17M ATF4^{+/-} or ADRP ATF4 deficient mice) and T17M^{+/-} *Rho*^{+/-} (henceforth referred to as T17M or ADRP) animals. These mice were compared to C57BL/6 (*Rho*^{+/+}) and ATF4^{+/-} mice.

Analysis of the scotopic ERG responses (Fig. 2A) demonstrated that T17M mice already experienced profound loss of a- and b-wave amplitudes at 1 month of age, the age-matched T17M ATF4^{+/-} animals demonstrated a functional protection of ADRP photoreceptors. No difference was observed between T17M ATF4^{+/-} and C57BL/6 animals at this age. However, by 2 months of age, when T17M mice exhibited significant

decreases in their ERG responses, T17M ATF4^{+/-} mice did begin to demonstrate a slight drop in a-wave amplitudes, with b-wave amplitudes remaining unchanged relative to C57BL/6 controls. At 3 months of age, the drop in ERG amplitudes for T17M ATF4^{+/-} mice became more noticeable. Despite the initial degeneration, the scotopic a- and b-wave ERG amplitudes were 2.15- and 1.3-fold greater, respectively, in T17M ATF4^{+/-} mice when compared to T17M animals (Fig. 2).

Importantly, light-adapted (photopic) ERG amplitude was already diminished in 1-month-old T17M mice (Fig. 2B). However, deficiency in ATF4 led to a remarkable recovery of both wave amplitudes. No difference was observed between 1-month-old T17M ATF4^{+/-} and C57BL/6 or ATF4^{+/-} groups, suggesting normal cone function in P30 ADRP retinas.

The functional test demonstrated that ATF4 deficiency in T17M significantly preserves vision in mice with retinal degeneration.

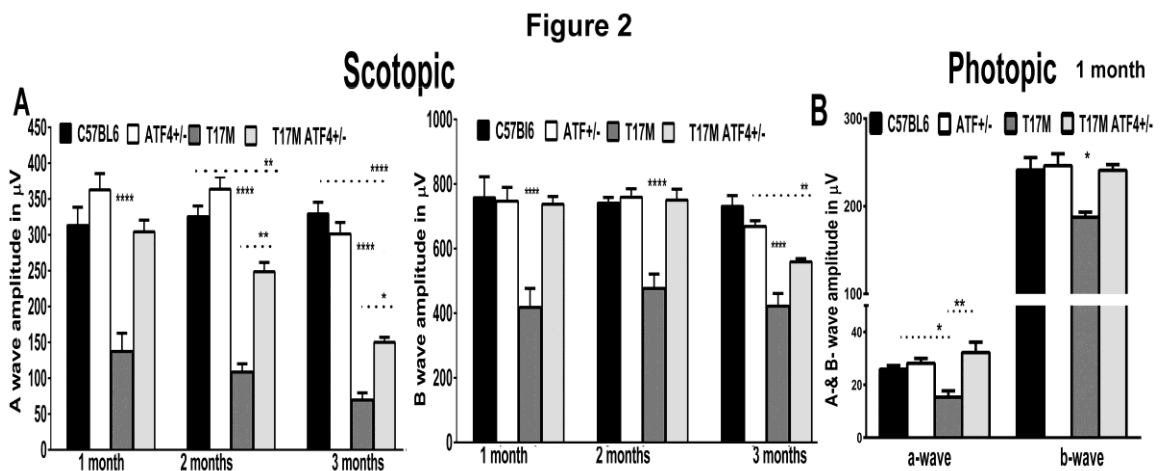


Figure 2 Knockdown of ATF4 prevents functional loss in T17M retina as measure by scotopic and photopic ERG.

(A and B) ERG amplitudes were registered as described in the methods. The data are presented as mean \pm SEM. See Figure S2 for details. (A) The two-way ANOVA analysis of the scotopic ERG results registered at 25 cd*s/m² demonstrated no difference in the a-

wave amplitudes of T17M ATF4^{+/-} mice (N=10) at 1 month when compared to C57BL/6 (N=6) or ATF4 (N=8) mice, whereas the T17M mice (N=5) showed an ERG a-wave reduction ($P<0.0001$ as compared to all groups). However, a decline in the a-wave amplitudes began at 2 months in the T17M ATF4^{+/-} retina, with a subsequent decline at 3 months of age, when compared to C57BL/6 retinas ($P<0.01$ and $P<0.0001$, respectively); but the the T17M ATF4^{+/-} amplitudes were higher than those of 2- and 3-month-old T17M mice, ($P<0.01$ and $P<0.05$, respectively). The b-wave of the scotopic ERG amplitude was better preserved in the T17M ATF4^{+/-} retinas. No difference between T17M ATF4^{+/-} and C57BL/6 or ATF4^{+/-} mice (n.s.) was detected during the first 2 months. By 3 months of age, the T17M ATF4^{+/-} started to exhibit a 24% decline in b-wave amplitudes as compared to C57BL/6 retinas ($P<0.01$). **(B)** The photopic ERGs registered at 25 cd*s/m², analyzed by one-way ANOVA, demonstrated dramatic declines in the a- and b-wave amplitudes in T17M retinas (N=4) by 1 month compared to C57BL/6 mice (N=6) ($P<0.05$ for both waves). Knockdown of ATF4 in ADRP retinas (N=4) significantly protected the T17M cone photoreceptors from functional loss and led to dramatic elevation of a-wave ($P<0.01$) and b-wave ($P<0.05$) amplitudes as compared to T17M retinas.

T17M ATF4^{+/-} mice experience delayed onset of retinal degeneration, as measured by imaging and histological analyses. We determined if ATF4 deficiency prevents loss of retinal integrity and photoreceptor cells in ADRP mice by analyzing results from SD-OCT imaging and by histological evaluation of cryostat sectioned retinas stained with H&E. The SD-OCT measurements confirmed marked preservation of ONL thickness in 1-month-old T17M ATF4^{+/-} mice. Representative spidergrams of the distribution of ONL thicknesses across the retina at 1, 2, and 3 months of age are shown in Fig. 3A. The T17M retinas demonstrated a significant reduction in ONL thickness over a period of 3 months, whereas ATF4-deficient ADRP retinas showed a pronounced delay in this reduction of ONL thickness. Thus, at 1 month, the average T17M ATF4^{+/-} ONL thickness in the superior and inferior hemispheres were both appreciably preserved when compared to T17M mice and were 83% of the ONL thickness found in C57BL/6 mice. The 2-month-old T17M ATF4^{+/-} mice also showed a significant increase in the average ONL thickness in both hemispheres when compared with T17M mice. This trend continued in

3-month-old T17M ATF4^{+/-} mice. Results from SD-OCT analysis of 3-month-old-retinas indicated that, despite a slight drop in the average inferior ONL thickness at 3 months, the average superior and inferior ONL thickness were both higher in T17M ATF4^{+/-} than in T17M animals (Fig. 3A).

The finding of a marked preservation of retinal structure in T17M retinas deficient in ATF4 suggested that these animals were able to circumvent photoreceptor cell death. Histological analysis and counts of the number of photoreceptor nuclei rows in the retinas (Fig. 3B and C) revealed a similar number of photoreceptor cells in T17M ATF4^{+/-} and C57BL/6 retinas at P30, whereas T17M mice experienced a dramatic loss of photoreceptor cells. However, by P90, the T17M ATF4^{+/-} retinas showed a 37% loss of photoreceptor cells when compared to C57BL/6, suggesting delayed retinal degeneration. This photoreceptor cell number was still notably higher than that of the degenerating P90 T17M retinas.

Therefore, imaging and histological analyses demonstrated significant preservation of retinal structure and decreased photoreceptor cell death in T17M mice deficient in ATF4.

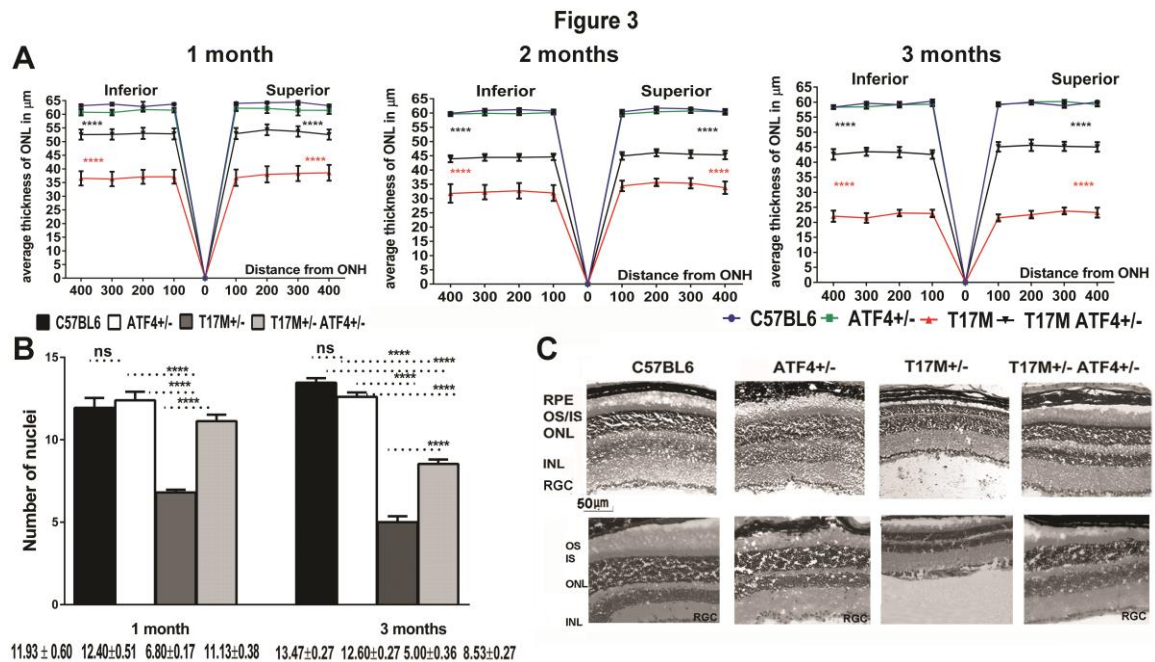


Figure 3 ATF4 knockdown protects T17M mice from loss of retinal integrity and photoreceptors.

(A) We found dramatic increases in the average ONL thicknesses of both hemispheres of 1, 2, and 3-month-old T17M ATF4^{+/-} retinas compared to T17M. Representative spidergrams of the distribution of ONL thicknesses across the retina at 1, 2, and 3 months of age are shown. The data were analyzed by two-way ANOVA. The T17M ATF4^{+/-} retinas (N=8) demonstrated an increase in the superior and inferior ONL thickness at 1, 2, and 3 months of age as compared to T17M mice (N=11). All regions from both ADRP retinas were significantly different from C57BL/6 (N=7) and ATF4 (N=7) mice ($P < 0.0001$ for both strains and all regions). The data are presented as mean \pm SEM. Representative SD-OCT images of one-month-old mice are shown in Fig. S2. (B) The ATF4 deficiency in T17M mice protected their retinas from photoreceptor cell loss, resulting in an increase in the number of photoreceptors relative to T17M as measured by two way ANOVA ($P < 0.0001$). The number of rows of photoreceptor nuclei between T17M ATF4^{+/-} (N=4) and C57BL/6 (N=4) retinas was similar at P30, whereas the T17M mice lost 43% of their photoreceptor cells ($P < 0.0001$ as compared to all groups). However, by 3 months, both the T17M ATF4^{+/-} and the T17M mice experienced a loss of photoreceptor cells as compared to C57BL/6 mice ($P < 0.0001$). The data are presented as mean \pm SEM. (C) Representative images of H&E stained retinal sections from all four groups. Images of one-month-old (upper) and 3-month-old (bottom) control and experimental retinas. Scale bar indicates 50 μm .

The T17M ATF4^{+/-} mouse retinas demonstrate diminished ER stress.

Overexpression of ATF4, the UPR mediator, elevates production of CHOP and activates caspase-3/7 in injected retinas; therefore, ATF4 knockdown would be predicted to

modulate UPR-associated hallmark expression as well as the status of executioner caspase activity in ADRP mice. Previous studies have shown activated UPR markers in T17M retinas [3, 1]. In contrast with prior work, which was conducted with mice expressing a transgene in addition to two endogenous rhodopsin copies, the current work used T17M RHO^{+/-} mice, which could have a faster rate of photoreceptor cell death and different dynamics of activated cellular signaling. Fig.4 show the results of qRT-PCR, Western Blot, and immunohistochemical analyses conducted in P15 and P30 retinas. These experiments showed elevated expression of *Bip* (1.3-fold) and *Chop* (1.65-fold) mRNAs, whereas *Hsp90* mRNA was downregulated (1.92-fold) in T17M retinas compared to wild type retinas, suggesting an active ER stress response. In T17M retinas deficient in ATF4, however, the *Hsp90* and *Chop* mRNA levels were restored to the level of wild type retinas. Both ADRP strain retinas showed activation of the IRE1 arm marker, *Xbp1* mRNA splicing at P15, suggesting that UPR activation occurred earlier than at P30 (Fig. 4B).

We demonstrated *XBPI* mRNA splicing using T17M ERAI^{+/-} and T17M ATF4^{+/-} ERAI^{+/-} mice (Fig. 4B), which were obtained by crossing T17M and T17M ATF4^{+/-} mice with ERAI (ER stress-Associated Inducer) transgenic mice carrying a human *XBPI* and a Venus (a variant of green fluorescent protein) fusion gene under control of a CAG promoter, as previously described [23]. The splicing of *XBPI* mRNA resulted in GFP expression that was detected in the ONL of both T17M and T17M ATF4^{+/-} retinas at P15, suggesting activation of IRE1 UPR signaling in both ADRP groups.

We also confirmed UPR activation by measuring the expression of UPR-induced cleavage of pATF6, pPERK, peIF2, ATF4, CHOP, and GADD34 proteins (Fig. 4C and S3). Western Blot analysis of UPR markers demonstrated that the pPERK level was

significantly upregulated in both T17M and T17M ATF4^{+/-} retinas as compared to C57BL/6 retinas. However, the pPERK upregulation was 2-fold lower in T17M mice deficient in ATF4 than in T17M mice. Analysis of other PERK signaling markers, ATF4 and CHOP, showed that they were up-regulated in T17M retinas and were significantly diminished in T17M ATF4^{+/-} retinas; ATF4 was up-regulated 1.8-fold in T17M retinas as compared to C57BL/6 retinas and almost 2-fold downregulated in T17M ATF4^{+/-} retinas as compared to T17M retinas. The ATF4 level in T17M ATF4^{+/-} retinas was correspondingly insignificant different and higher when compared to C57BL/6 and ATF4^{+/-} retinas. The difference between the ATF4^{+/-} and T17M ATF4^{+/-} groups was confirmed as statistically significant only by the Student *t*-test (P=0.002), which would suggest the occurrence of a limited ATF4 increase in ADRP retinas expressing one ATF4 copy.

We also found that levels of CHOP protein declined in T17M ATF4^{+/-} retinas, while its production was elevated 1.7-fold in T17M retinas when compared to C57BL/6 retinas. Upregulation of CHOP is known to control expression of GADD34, so we expected to observe GADD34 downregulation in these animals. However, despite the downregulation of CHOP protein in ADRP retinas deficient in ATF4, the T17M ATF4^{+/-} mice were the only group to show increased GADD34 protein production. An almost 3-fold elevation in GADD34 protein was observed in these mice when compared to ATF4^{+/-} or T17M.

GADD34 is known to provide regulatory feedback that can reverse translational attenuation; therefore, our finding that GADD34 upregulation coincided with a dramatic inhibition of p-eIF2 α in T17M ATF4^{+/-} retinas was not surprising. We verified that this inhibition was not due to reduced eIF2 α expression by Western blotting. This showed no differences in eIF2 α levels among all four groups (Fig. S3). This suggests that the

phosphorylation of eIF2a is indeed inhibited in T17M ATF4^{+/-} and that this perhaps occurs via sustained over-expression of GADD34 and PP1 phosphatase. Both the downregulation of peIF2a and up-regulation of GADD34 suggest a long-lasting operation of the feedback loop in ADRP retinas deficient in ATF4.

Activation of the ATF6 arm results in the cleavage of pATF6 which, together with the PERK pathway, contributes to CHOP overexpression. Our analysis of the cleaved pATF6 protein revealed that T17M mice had an almost 2-fold elevation of pATF6. In contrast, activation of the ATF6 UPR arm in P30 T17M ATF4^{+/-} retinas was significantly reduced (Fig. 4C), whereas the level of cleaved pATF6 50 kD protein was comparable to that found in C57BL/6 retinas. These data on pATF6, together with the observed reductions in peIFa and ATF4 in T17M ATF4^{+/-} retinas, can explain the observed downregulation of CHOP in T17M ATF4^{+/-} retinas.

ATF4 knockdown in T17M retinas resulted in a large decrease in executioner caspase activity as compared to all other groups (Fig. 4E). Notably, no differences were detected between T17M ATF4^{+/-} and C57BL/6 retinas. These data suggest that, like in our previous studies with ablation of caspase 7 and 12 in T17M mice [1,24], reduction of the level of apoptosis achieved by ATF4 knockdown could benefit degenerating retinas. Next we found that downregulation of apoptotic markers in T17M ATF4^{+/-} retinas coincided with a reduction in phosphorylated tumor suppressor p53 (pp53) (Fig. 4E), which is known to induce apoptosis [25].

Our results demonstrated that the UPR is activated in both ADRP retinas as early as P15. However, limited ATF4 expression dramatically reduced overall ER stress by lessening the activation of the PERK and ATF6 arms and essentially abolished caspase activation and p53 over-expression, indicating resolution of apoptosis at P30.

Figure 4

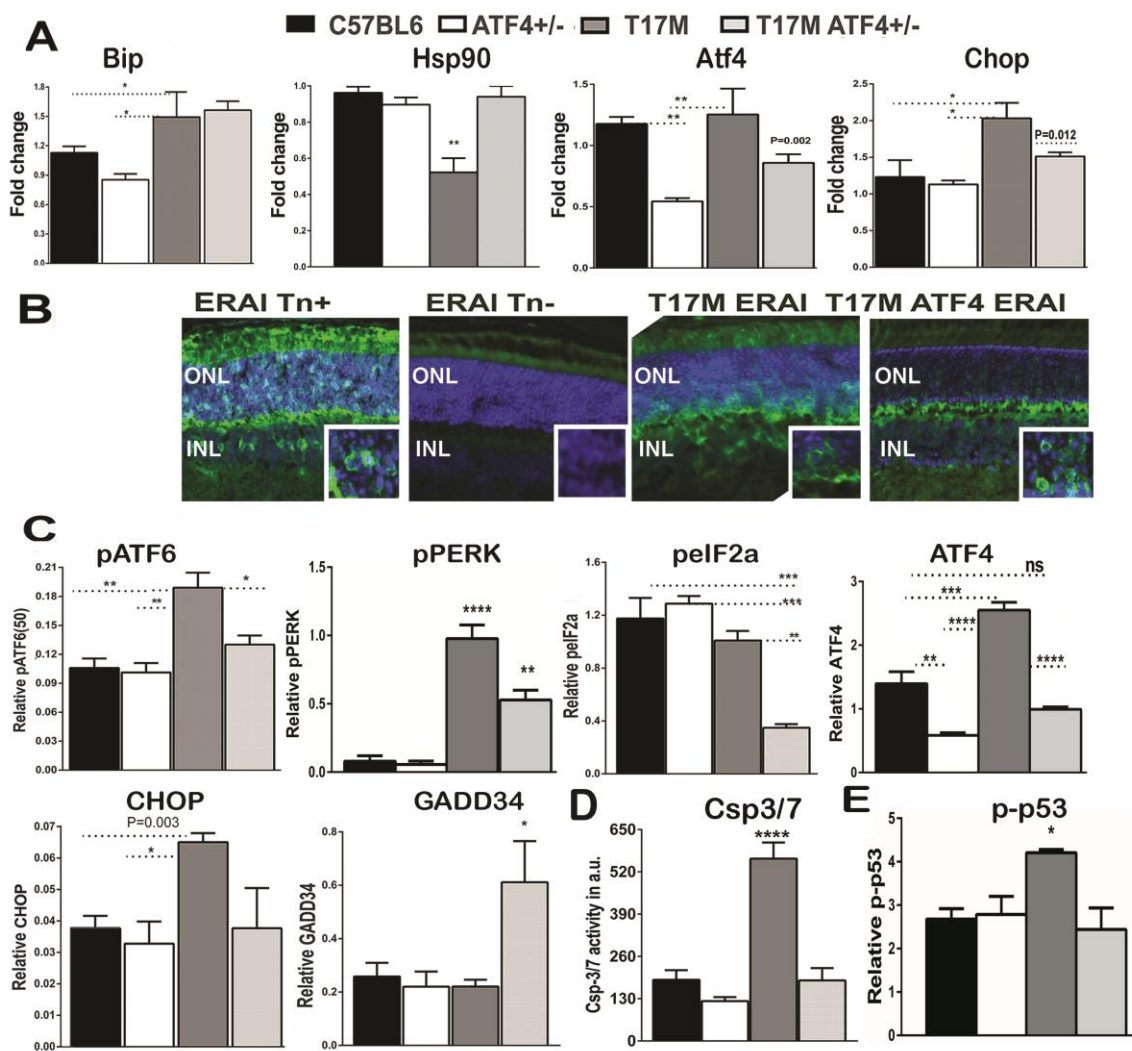


Figure 4. ATF4 knockdown in the ADRP retinas reduces overall ER stress (N=4). (A) The qRT-PCR data were analyzed by one-way ANOVA. *Bip*, *ATF4* and *CHOP* mRNA expressions were elevated in T17M retinas as compared to C57BL/6 and ATF4 mice ($P < 0.05$ for both). The ATF4-deficient ADRP retinas, in general, expressed less *Chop* mRNA as compared to T17M retinas (t -test, $p = 0.012$). *Hsp90* mRNA expression was significantly downregulated in T17M retinas ($P < 0.05$ as compared to all groups). (B) The splicing of *XBP1* mRNA resulted in immunohistochemical detection of GFP expression in the ONL of both ERA1 T17M and ERA1 T17M ATF4^{+/-} retinas at P15 and suggested activation of IRE1 UPR signaling in both ADRP groups. (C) Western blot analysis revealed while T17M retinas demonstrated upregulation of pATF6 (50), pPERK, ATF4, and CHOP as compared to C57BL/6 ($P < 0.01$; $P < 0.0001$; $P < 0.0001$ and $p = 0.003$ t -test, respectively), the ATF4 deficiency in these retinas led to downregulation of these UPR markers as compared to T17M mice ($P < 0.05$; $P < 0.01$; and $P < 0.001$ respectively) and a trend toward downregulation for the CHOP protein. The T17M ATF4^{+/-} retinas

were the only group with a significant decrease in peIF2a ($P < 0.01$ as compared to T17M retinas) and increased GADD34 protein levels ($P < 0.05$ for all groups). The T17M ATF4^{+/-} retinas showed increased peIF4E protein levels as compared to T17M retinas ($P < 0.05$). Representative images of western blots treated with antibodies against cleaved pATF6, pPERK, peIF2a, peIF4E, ATF4, CHOP, GADD34, and β -actin proteins are shown in Fig. S2. **(D)** Knockdown of ATF4 in ADRP retinas led to downregulation of caspase-3/7 activity. The T17M retinas demonstrated an almost 3-fold activation of caspase-3/7 ($P < 0.0001$ as compared all four groups), whereas the T17M ATF4^{+/-} retinas were characterized by a level of caspase-3/7 activity comparable with wild type at P30. **(E)** Phosphorylated p53 was overexpressed in T17M retinas, as determined from protein extracts ($P < 0.05$ as compared to all groups). The data are presented as mean \pm SEM.

The T17M ATF4^{+/-} mice demonstrate increases in NRF2 and diminished oxidative stress.

The elevation of pPERK in both P30 ADRP retinas predicted an activation of the NRF2-induced antioxidant signaling in both ADRP retinas. However, analysis of the NRF2 levels by western blotting revealed an elevation of NRF2 in T17M ATF4^{+/-} retinas at P30 ($P < 0.01$ as compared to both the C57BL/6 and T17M retinas) (Fig. 5A). The *Nrf2* mRNA level was significantly increased in the T17M retina, but the NRF2 protein level matched that found in the C57BL/6 retinas. Recent lines of evidence have suggested that the NRF2-dependent elevation of ATF4 can occur in the cell concomitantly with enhanced translation of ATF4 mRNA due to the PERK-dependent phosphorylation of eIF2a [26, 14]. Therefore, NRF2 elevation could be responsible for a slight up-regulation of ATF4 in T17M ATF4^{+/-} retinas with reduced peIF2a level during ADRP progression. In contrast to T17M mice, the T17M ATF4^{+/-} retinas showed 1.5- and 3-fold up-regulation of the HO-1 mRNA and protein, respectively, which is known to be regulated by NRF2 ($P < 0.01$ as compared to all groups). This finding was not surprising, since NRF2 is known to carry out transcriptional activation of *Hmox1* [27]. Therefore, the elevation of

both the NRF2 and HO-1 proteins indicated the launching of an antioxidant program in the T17M ATF4^{+/-} retinas. This program was perhaps impeded in the T17M retinas.

The NRF2 level in T17M mice did not differ from that of the wild type retinas suggesting that no antioxidant battle was ongoing in these retinas. The activation of the UPR at P15 (Fig. 4B) and PERK upregulation in ADRP retinas at P30 suggested a possible obstruction of the antioxidant program in T17M retinas at later time points. Analysis of the T17M retinal protein extract at P15 revealed that the NRF2 level was indeed increased in P15 T17M retinas when compared to C56BL6 mice ($P < 0.01$) (Fig. S1). This would suggest an existence of inhibitory signal that prevents the elevation of NRF2 expression between P15 and P30. Our search for this signal revealed a dramatic reduction of p62 in T17M retinas (Fig. 5 A and B). The silencing of p62 attenuates NRF2 activation [28], while its phosphorylation promotes activity of KEAP1-CUL3 E3 ligase [29]. Therefore, posttranslational regulatory events, such as KEAP1-ubiquitination and enhanced degradation of NRF2, most likely occurred in T17M retinas.

We confirmed the results of oxidative stress-associated gene expression by performing immunohistochemical analysis and detection of reactive oxygen species (ROS) in retinal cryostat sections using a chloromethyl derivative of H2DCFDA as a general oxidative stress indicator (Fig. 5D). The T17M mice exhibited oxidative stress during ADRP, whereas the T17M ATF4^{+/-} retinas showed a resistance to oxidative stress, as indicated by the lack of ROS-positive cells. These observations agreed with our protein analysis that demonstrated no signs of oxidative stress in T17M ATF4^{+/-} retinas. Thus, an anti-oxidant defense and diminished ER stress occur concomitantly in the T17M ATF4^{+/-} retinas.

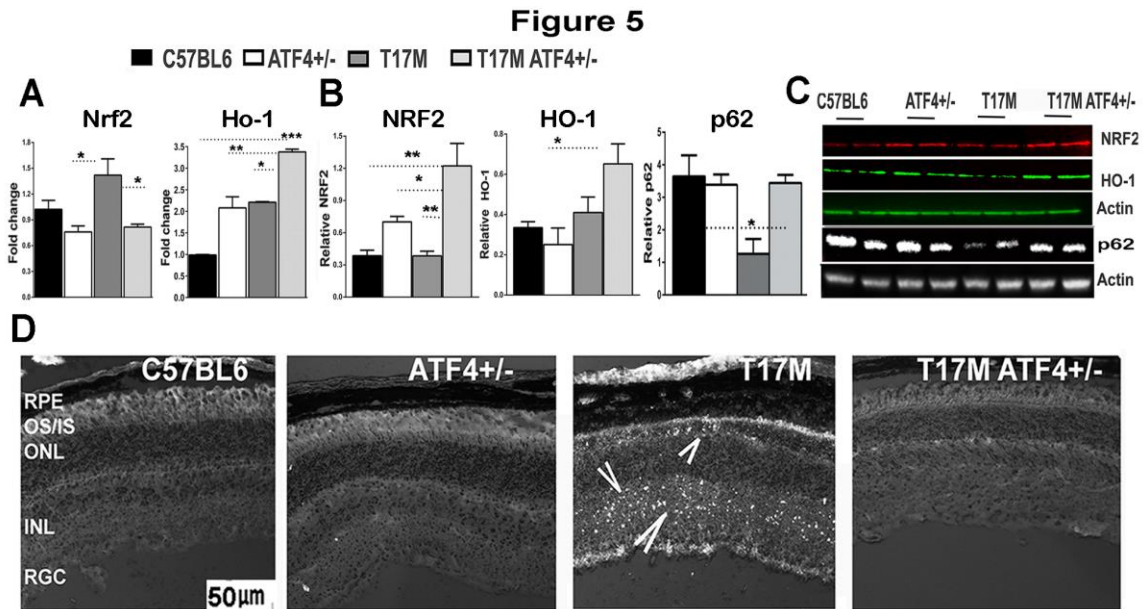


Figure 5. ATF4 knockdown launches the antioxidant cellular defense mechanism in T17M and protects the ADRP retina against oxidative stress (N=4). (A) *Nrf2* mRNA expressions were elevated in T17M retinas ($P < 0.05$ as compared to all groups). But, *Ho-1* mRNA was only upregulated in T17M ATF4^{+/-} retinas ($P < 0.05$; $P < 0.01$ and $P < 0.001$ when compared to T17M, ATF4^{+/-} and C57BL/6 respectively). (B) Results of western blotting, analyzed by one way ANOVA, demonstrated that the antioxidant NRF2 and HO-1 expression was significantly up-regulated in T17M ATF4^{+/-} retinas as compared to C57BL/6 retinas ($P < 0.01$ and $P < 0.05$, respectively) and T17M retinas ($P < 0.01$ and t -test=0.04 respectively). In addition, p62 was significantly lower in T17M retinas as compared to all other groups ($P < 0.05$). (C) Representative images of western blots treated with antibodies against p62, NRF2, HO-1, and β -actin proteins. (D) Oxidative stress was significantly diminished in the T17M ATF4^{+/-} retinas compared to T17M retinas with ongoing oxidative stress. Representative images of retinal cryostat sections stained with H2DCFDA. ROS positive cells are evident in the ONL and INL of the T17M retina and are indicated with arrows. The data are presented as mean \pm SEM.

Retinal degeneration in T17M mice is associated with an impaired autophagy signaling.

Expression of p62 is required for the formation of autophagosome through interaction with LC3 protein (MAP1LC3A in human) [31]. Our western blot analysis of LC3 cleavage revealed a tremendous reduction in T17M retinas as compared to all other groups, including the T17M ATF4^{+/-} mice ($P < 0.01$). Expression of the LC3 gene is

controlled by ATF4, and ATF4 is known to bind to the MAP1LC3A promoter and activate its transcription [32, 33], which raised the question of how up-regulation of the ATF4 in T17M retinas could result in reduction of LC3-I and II, but not vice versa, as occurred in T17M ATF4^{+/-} retinas.

Recent study of selenite-induced UPR activation in Jurkat cells has proposed the p53-p38-MAPK-eIF4E-induced ATF4 target selection between apoptosis and autophagy [32]. The switch from apoptosis to autophagy in cells could occur by up-regulation of phosphorylated eIF4E. Therefore, we checked the peIF4E level in degenerating retinas. In agreement with a previous study [32], up-regulation of ATF4 was correlated with a tremendous decline in the peIF4E in T17M retinas, while the T17M ATF4 retinas demonstrated increases in the peIF4E protein (Fig. 6).

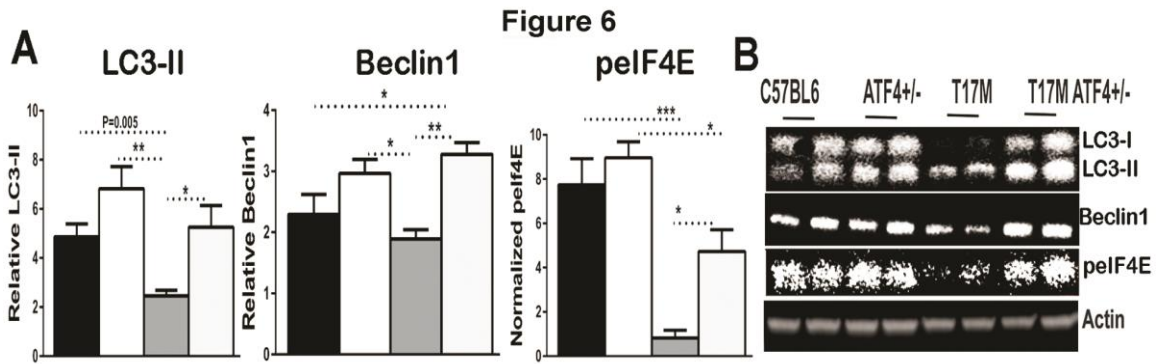


Figure 6. ATF4 deficiency in T17M retinas results in upregulation of autophagosome associated genes. (A) Level of autophagy-related LC3-II (lipidated form) and Beclin-1 proteins was diminished in T17M retinas as compared to controls ($P=0.005$, *t*-test and $P<0.05$ when compared to C57BL/6 and to ATF4, respectively) and significantly up-regulated in T17M ATF4^{+/-} retinas as compared to T17M ($P<0.05$ and $P<0.01$, respectively). The T17M ATF4^{+/-} retinas showed increased peIF4E protein levels as compared to T17M retinas ($P<0.05$). The data are presented as mean \pm SEM.

Delay of the onset of retinal degeneration in T17M ATF4 mice is associated with improved RHO biosynthesis.

ER stress-inducible miRNA-708 expression governs *Rho* mRNA [34]. We found an elevation and a large drop in miRNA-708 expression in T17M and T17M ATF4^{+/-} retinas, respectively. Therefore, we further determined if ATF4 deficiency in ADRP retinas with reduced miRNA-708 level improves RHO expression and perhaps promotes degradation of misfolded or aggregated proteins in the cytosol. We performed a measurement of RHO mRNA and protein expression in all four groups of animals (Fig.7). Previously, we have detected a reduction in transgene and endogenous rhodopsin mRNA in T17M Rho^{+/+} mice associated with a decline in *Nrl* and *Crx* transcriptional factors and an increase in CHOP expression [2]. In the current study, with T17M Rho^{+/-} mice, we also observed a drastic (99%) drop in mouse *Rho* mRNA expression, associated with elevation of CHOP protein. However, unlike the previous findings, we also observed a marked elevation of CHOP-induced miRNA-708, suggesting that mi-RNA-708, in addition to transcriptional NRL and CRX factors, could control expression of RHO in both ADRP groups.

The drop in miRNA708 levels in T17M ATF4^{+/-} mice was associated with an enormous (16-fold) increase in expression of human and mouse mRNAs (Fig. 7A) and in total protein levels (Fig. 7B) when compared to T17M retinas. The total RHO level was a half that detected in the wild type retinas. Enhancement of RHO production also correlated with the correct RHO localization within the rod photoreceptor (Fig. 7D). Immunohistochemical analyses revealed that while T17M retinas experienced a mislocalization of a fraction of the RHO stained with the 1D4 antibody, no accumulation of RHO was detected within the ONL in T17M ATF4^{+/-} retinas. Clearance of trapped RHO was in agreement with results indicating activation of autophagy (Fig. 6).

Therefore, taken together, the present findings support a link between retinal degeneration and the status of ER stress, anti-oxidative defense, activated autophagy, and enhanced rhodopsin biosynthesis.

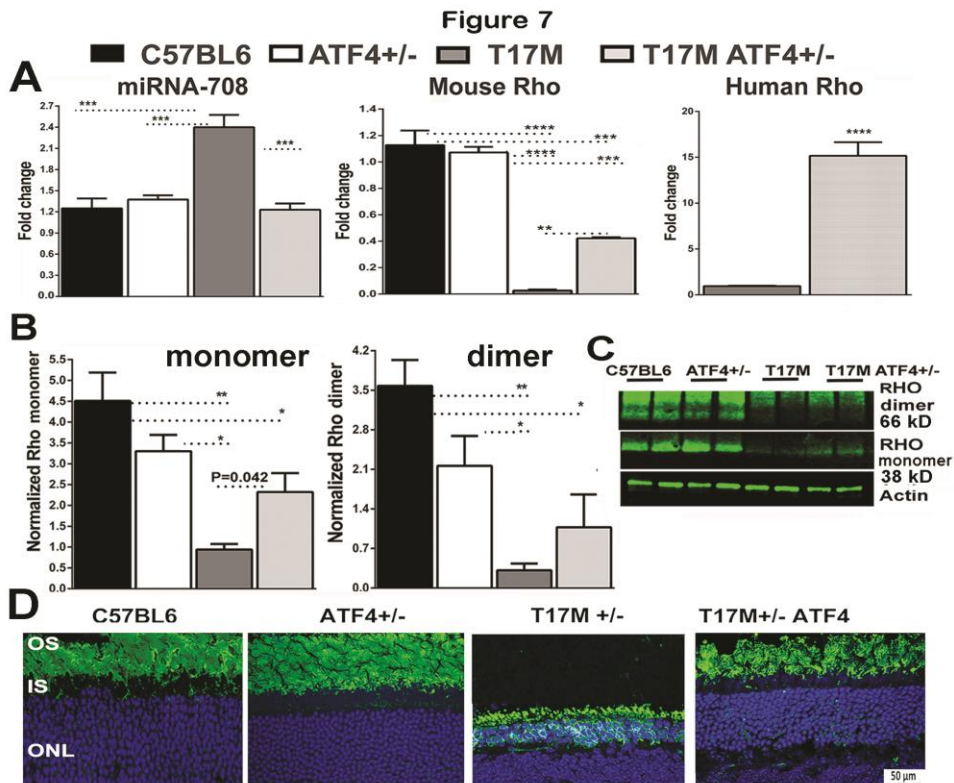


Figure 7. ATF4 knockdown in T17M photoreceptors has a positive influence on the RHO expression machinery (N=4 for all groups). (A) A significant decrease in the mouse RHO mRNA, analyzed by one way ANOVA, was found in the T17M retina as compared to C57BL/6 and ATF4^{+/-} mice ($P < 0.001$ for both). However, deficiency of ATF4 in these retinas led to a dramatic increase (16-fold) of mouse and human RHO mRNA expression as compared to T17M mice ($P < 0.01$ and $P < 0.0001$, respectively). The increase in RHO mRNA corresponded with an attenuation of the ER stress-induced miRNA-708 ($P < 0.001$ as compared to T17M mice). (B) Increase in RHO mRNA led to elevated production of the RHO monomer and dimer in T17M ATF4^{+/-} retinas, whereas T17M mice experienced a dramatic (99% and 98%) loss of RHO production in photoreceptors, as measured by detection of dimer and monomer bands ($P < 0.01$ for both bands as compared to C57BL/6). (C) Representative images of western blots treated with antibodies against RHO. (D) Immunohistological analyses of P30 retinas with anti-RHO antibody (1D4, in green) revealed normal localization of rhodopsin in the T17M ATF4^{+/-} OS, compared with T17M mice with partially mislocalized RHO, suggesting improved clearance of RHO in the ADPR ATF4 deficient retina. ONL, outer nuclear layer; IS,

Inner segments; OS, outer segments. Scale bar indicates 50 μ m. The data are presented as mean \pm SEM.

Discussion

Elevation of ATF4, a mediator of PERK UPR signaling, accompanies progressive retinal degeneration [20]. However, the role of ATF4 in photoreceptor cellular pathology has not been previously explored. Our study demonstrates that ATF4 plays a proapoptotic role during the ADRP progression associated with ER stress. Sustained overexpression of ATF4 is lethal because it leads to over-expression of CHOP and activation of executioner caspases resulting in photoreceptor cell death. Conversely, ATF4-deficiency in ADRP retinas results in a significant delay in the onset of retinal degeneration and increases photoreceptor survival. The mechanism underlying the cytoprotection provided by the ATF4 deficiency in degenerating retinas is most likely linked to the key players' p62, NRF2 and autophagy genes, which together orchestrate a reduction in ER stress, launch antioxidant defenses, activate autophagy, and enhance rhodopsin biosynthesis. A proposed mechanism to explain the neuroprotection associated with ATF4 deficiency in ADRP retinas is presented in Fig. 8.

Figure 8

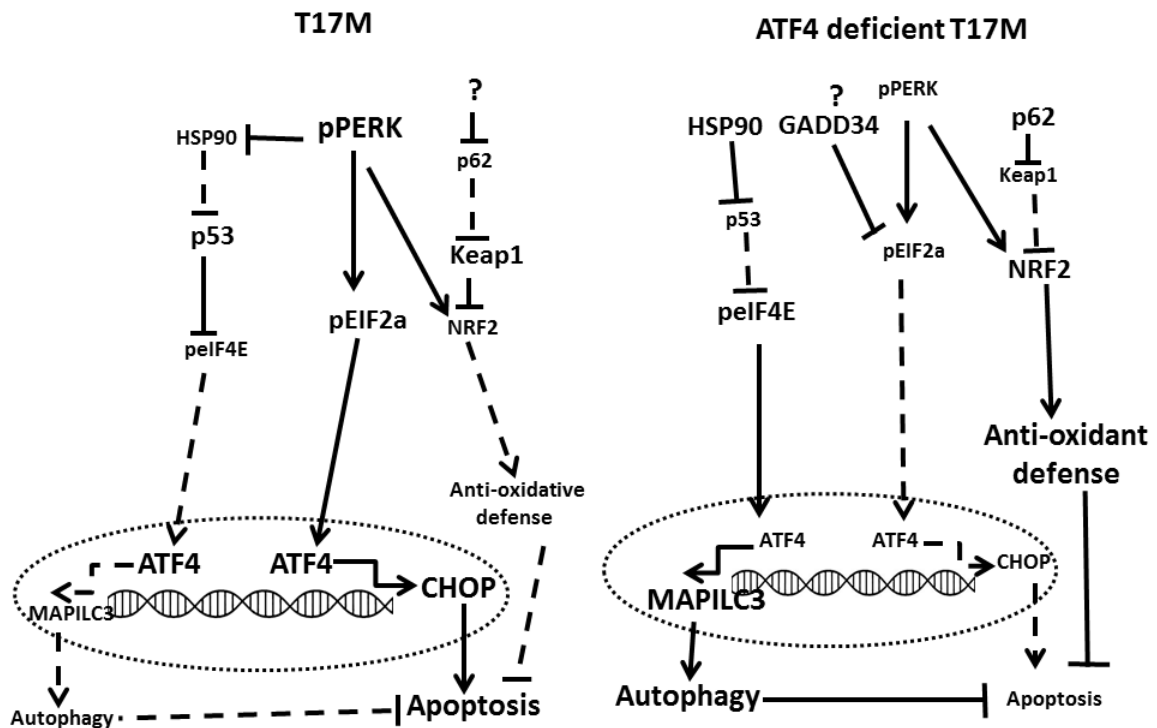


Figure 8. Proposed mechanism of retinal degeneration in T17M and T17M ATF4^{+/-} mice. In T17M retinas, we observed up-regulation of pPERK, ATF4, CHOP, p53 proteins resulting in activation of apoptosis. In T17M retinas deficient in ATF4 we detected up-regulation of Hsp90, peIF4E, NRF2, GADD34 and autophagy genes resulting in delay of retinal degeneration. Increased and decreased levels of proteins in the retina are present as small and large fonts, correspondingly. Increased and decreased effects in solid and dashed lines correspondingly are shown as well.

Molecular mechanism of T17M photoreceptor degeneration

A persistently activated UPR in T17M mice is accompanied by severe retinal degeneration. Although no photoreceptor cell death is detected at P15, the T17M ERAI retinas expressing GFP as a result of *Xbp1* splicing, indicate activation of the IRE1 arm at P15, pointing to continued UPR activation

The activation of PERK signaling in T17M retinas, detected in this study at P30 and in the previously conducted study at P15 [3], is associated with Nrf2 up-regulation and

perhaps the launching of an antioxidant defense at P15 (Fig. 8). Later, at P30, p62 is downregulated in these retinas, which may result in elevated KEAP1 activity and degradation of excess NRF2 [29]. The p62 has been previously shown to govern oxidant stress in cultured RPE and in the retinas of mice exposed to cigarette smoke [35]. This previous study revealed that p62 silencing exacerbated the cigarette smoke-induced accumulation of damaged proteins, both by suppressing autophagy and by inhibiting the Nrf2 antioxidant response, which, in turn, increased protein oxidation. Therefore, the observed reduction of p62 in T17M retinas may impede the PERK-NRF2-anti-oxidant defense. Consequently, over the subsequent 2 weeks, the T17M retinas lose a great number of photoreceptors and experience rapid onset of retinal degeneration, resulting in a severe decline in both scotopic ERG amplitudes and photopic recordings. This implies that during the interval from P15 and P30, the T17M retinas experience rod cell death as well as the loss of cone cell function.

Activation of PERK signaling promotes ATF4 over-expression in T17M at P30. We showed, in a separate experiment, that this was cytotoxic for photoreceptors and induced severe retinal degeneration. Accelerated and induced photoreceptor cell death occurs respectively in T17M and the wild type mice with AAV-mediated ATF4 over-expression at two weeks after AAV2/5- ATF4 delivery. The advanced decline in ERG amplitudes in naive T17M mice is due to a dramatic loss of photoreceptors and is associated with elevations of CHOP and pp53 proteins. As was observed in degenerating and wild type retinas following viral ATF4 delivery, naïve P30 T17M retinas underwent activation of apoptosis. We also found in these mice that a portion of total RHO was trapped in the ONL suggesting prevention of RHO clearance due to malfunctioned autophagosome-lysosome system.

Therefore, persistent UPR, failure to launch antioxidant defenses, and autophagy occurring during stress may all contribute to pathogenesis of retinal degeneration in T17M mice. During ADRP progression, T17M mice experience a progressive loss of a- and b-wave scotopic ERG, which culminates in only 5 rows of photoreceptors remaining by 3 months of age.

Molecular mechanism of T17M ATF4^{+/-} photoreceptor degeneration

The major contribution of ATF4 knockdown to the mechanism of retinal degeneration is likely through a reduction of overall ER stress, induction of an antioxidant program, and activation of autophagy, which together result in a delay of apoptotic photoreceptor cell death. The dramatic reduction in pPERK, pATF6, peIF2a, and CHOP proteins indicates a significantly lower degree of UPR activation in T17M ATF4^{+/-} retinas. The ATF4 level, as expected, is reduced in these animals and is undistinguishable from the level in C57BL/6 mice. However, this level might be sufficient to overcome oxidative stress in degenerating retinas when NRF2 levels are also elevated. The rise in NRF2 is most likely mediated by the PERK, which, despite its dramatic decrease in T17M ATF4^{+/-} as compared to T17M mice, may contribute into an NRF2-induced antioxidant defense. The NRF2 elevation, in turn, correlates with the rise in p62 level, which perhaps reduces KEAP1-mediated targeting of NRF2.

Targeting of HSP90 during retinal degeneration has been proposed as a valid therapeutic strategy [36, 37]; however, the retinal degeneration in T17M retinas is associated with downregulation of *Hsp90* at P30 when compared to the wild type. This reduction could perhaps be responsible for the p53 overexpression observed in T17M retinas since inhibition of HSP90 expression induces p53 over-expression [38]. Therefore, not surprisingly, the T17M ATF4^{+/-} mice show increases in *Hsp90* that are also associated

with restoration of p53 to normal levels. This observation could perhaps relate to the proposed switch of ATF4-mediated apoptosis and autophagy during stress, since p53 appears to hold a core position in transducing the p38-promoted signal to either eIF2a or eIF4E [32]. Consequently, an increase in peIF4E and a decrease in peIF2a, as observed in T17M ATF4^{+/-} retinas with limited ATF4 expression, are perhaps associated with binding of ATF4 to the LC3 promoter and activation of autophagy. Conversely, the T17M retinas experience impairment of autophagy activation associated with downregulation of *Hsp90* and p62, elevation of p53, a strong knockdown of peIF4E, and elevation of CHOP protein. Taken together, these findings support the preferential activation of apoptosis vs. autophagy in T17M retinas, and alternatively, autophagy vs. apoptosis in T17M ATF4^{+/-} mice. In support of this hypothesis, the ER stress reduction in these retinas correlates with normal levels of activated caspase-3/7 at P30.

Reduction in apoptosis-related CHOP is associated with a paradoxical increase in GADD34, which, in turn, correlates with downregulation of peIF2a protein in T17M ATF4^{+/-} retinas. The latest findings would support a feedback loop provided by GADD34, canonical UPR signaling, and the enhancement of autophagy [39-41], but the GADD34 increase during CHOP downregulation in retinas needs to be studied in further detail. In particular, these data indicate that signaling molecules or pathways other than ATF4-CHOP can regulate expression of GADD34 or stabilize/degrade its level in the retina. This finding also points to a therapeutic approach that could be taken to treat ADRP retinas, based on modulation of GADD34 levels.

Analyzing the T17M ATF4 retinas, we found that both scotopic and photopic ERG amplitudes were preserved, and that cone photoreceptor function was well maintained in 1-month-old animals. This most likely occurs due to the presence of normally functioning

rod photoreceptors in which the reduction in ATF4 reprograms the ER stress signaling network. This result, in itself, is of great importance as it supports the idea that inherited retinal degeneration can be delayed. To our knowledge, this is the first report to demonstrate rescue of rapidly degenerating ADRP retinas at P30 and a significant delay in retinal degeneration afterwards. The SD-OCT imaging shows a difference in average superior and inferior ONL thicknesses in the T17M ATF4^{+/-} mice, but this difference would appear to be due to altered photoreceptor morphology rather than a change in the number of photoreceptors. The H&E staining confirmed this hypothesis as it revealed no observable difference between C57BL/6 and T17M ATF4^{+/-} mice, suggesting that no photoreceptor cell death occurred at P30.

Rhodopsin expression machinery in ADRP retinas

The enhancement of the RHO expression machinery in T17M ATF4^{+/-} retinas is most likely associated with a reduction in the ER-stress regulated miRNA-708. Its downregulation in T17M ATF4^{+/-} retinas resulted in elevated expression of both the mouse and human RHO mRNAs and increased RHO protein production. Our previous study with T17M CHOP^{-/-} [2] was conducted with mice expressing the T17M transgene in addition to two endogenous copies of rhodopsin. These mice might possibly have a different rate of retinal degeneration as well as different kinetics of activation of UPR. Therefore, although we did not detect the difference in miRNA-708 found in the T17M RHO^{+/+} retinas in the previous study. We proposed that the T17M CHOP^{-/-} mice exhibit a reduction of RHO through impeded transcriptional regulation detected by downregulation of CRX and NRL. Furthermore, in these mice we found 8-fold upregulation in pEIF2a resulting in ablation of general protein synthesis including rhodopsin protein leading to aggravated photoreceptor cell death. In the current study, downregulation of miRNA-708

and peIF2a in T17M ATF4^{+/-} most likely contribute together in rhodopsin expression and elevation of total RHO protein.

Total RHO is elevated in T17M ATF4^{+/-} retinas to a level about half that of RHO measured in C57BL/6 mice (monomer). Moreover, this level corresponds to that found in RHO^{+/-} mice with normal vision that express 50% of the wild type RHO. Unlikely the RHO^{+/-} mice, the T17M ATF4^{+/-} mice have both human and mouse RHO in the outer segments of photoreceptors and the level of wild type rhodopsin may then be sufficient to maintain the function of photoreceptors through activation of activated antioxidant signaling and autophagy during the first month of life. However, later on, the mutant rhodopsin transported to the outer segment could cause problems by reducing the ability to regenerate pigment after light exposure [42], thereby initiating the progression of retinal degeneration.

Activated autophagy in ATF4-deficient ADRP mice could be responsible for the clearance of partially accumulated RHO in the ONL of P30 retinas (Fig. 7D). Our findings correlate with previously published data indicating that autophagy-dependent rhodopsin degradation prevents retinal degeneration [43] and that autophagy is essential to the long-term health of rod photoreceptors [44-46]. An increase in autophagy genes could therefore temporally protect the T17M ATF4^{+/-} mice and maintain photoreceptor health. However, this support is evidently not sufficient to maintain cellular homeostasis at later time points.

Therefore, the diminishing of cellular stress that result in reduction of apoptosis and enhancement of autophagy and total rhodopsin in T17M retinas deficient in ATF4 at P30 delay the onset of retinal degeneration. However, the therapeutic effect of ATF4

deficiency in animal models of other dominant rhodopsin mutations requires additional investigation.

Conclusions

Our results indicate an essential role for ATF4 in the induction of photoreceptor cell death. We can however conclude that increased ATF4 expression during retina degeneration contributes to T17M photoreceptor cell death. Reduced ATF4 expression in degenerating retinas experiencing UPR activation, conversely, plays a pro-survival role, suggesting a therapeutic strategy for intervention in ADRP progression. ATF4 deficiency in the T17M retina under conditions of UPR activation, on the other hand, satisfies a photoreceptor cellular demand by adapting the UPR, overall reducing cellular stress in ADRP photoreceptors and activating autophagy that may clear a trapped rhodopsin in the ONL of ADRP retinas resulting in its delivery to the OS. Therefore, this signaling provides functional and morphological benefits to ADRP photoreceptors. This scenario is perhaps, sufficient to rescue the one-month-old ADRP retina and significantly delay further ADRP progression. Overall this indicates that PERK signaling in general and ATF4 in particular, is a target for delaying retinal degeneration in ADRP patients.

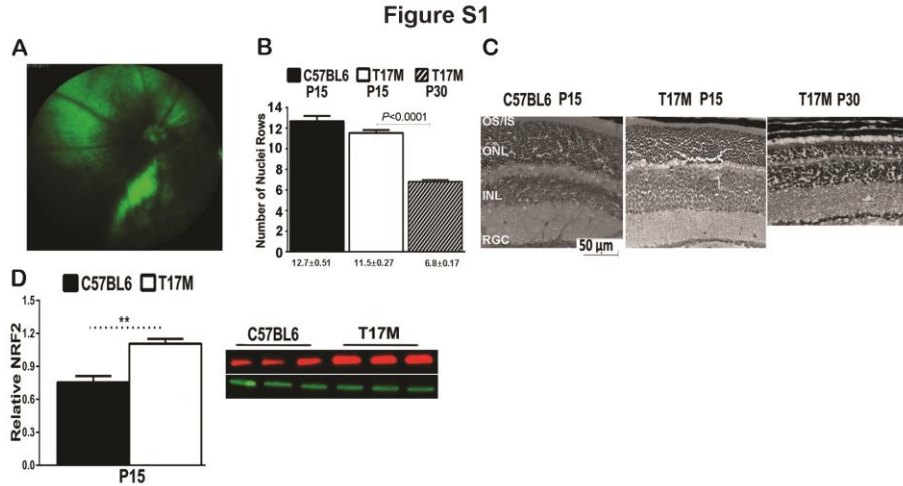


Figure S1. Expression of T17M RHO in ADRP rod photoreceptors results in photoreceptor cell death and leads to severe retinal degeneration. (A) Micron IV fluorescence image obtained from T17M retinas injected with AAV2/5-GFP. (B) Analysis of H&E stained T17M retinal sections demonstrated dramatic photoreceptor cell loss that occurs between P15 and P30 (N=4 for both, (*P*<0.0001). (C) Representative images of P15 C57BL/6 and P15 and P30 T17M cryostat-sectioned retinas stained with H&E are shown on the side. (D) Expression of NRF2 in P15 T17M retinas. A western blot image is shown on a side. The data are presented as mean ± SEM.

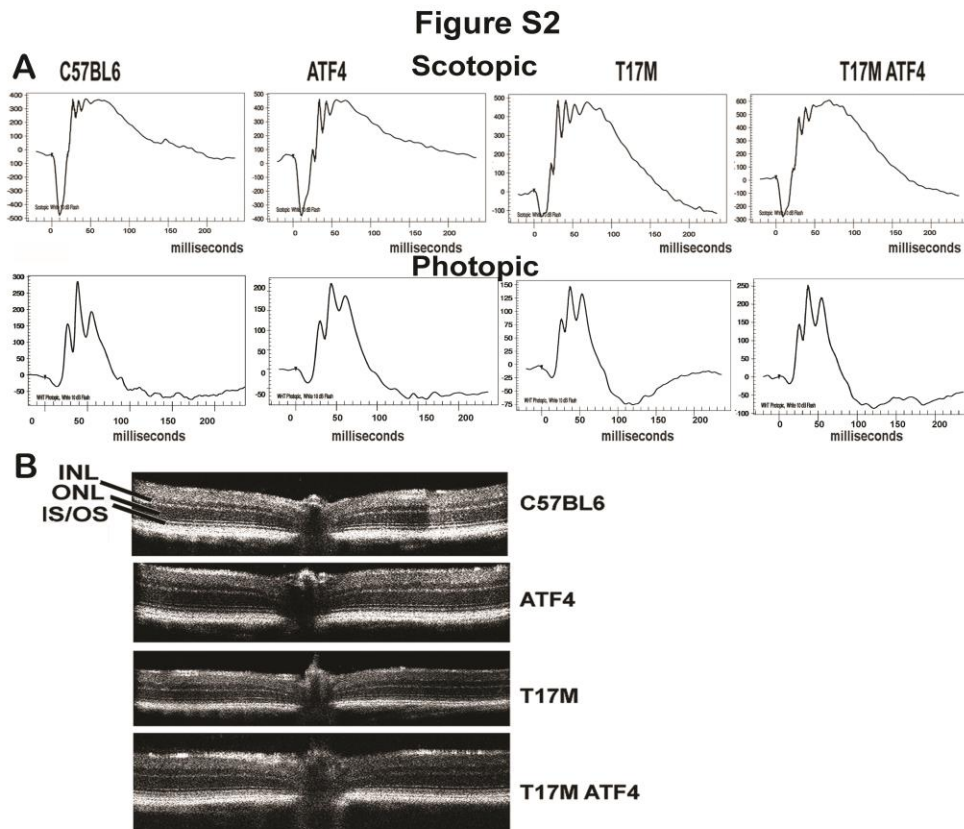


Figure S2. Knockdown of ATF4 prevents loss of function and photoreceptor cell death in the one-, two-, or three-month-old T17M retinas. (A) Representative images of the scotopic and photopic ERG amplitudes registered at 25 cd*s/m² for all four groups of animals. Please take in account that the scales (μ V) for photopic ERG amplitudes are varied in all four groups of animals. For C57BL/6 and ATF4 mice, the max amplitude is 300 and 200 μ V respectively; for T17M is 150 μ V, for T17M ATF4^{+/-} are 250 μ V. (B) Representative SD-OCT images of retinas for all four groups of animals.

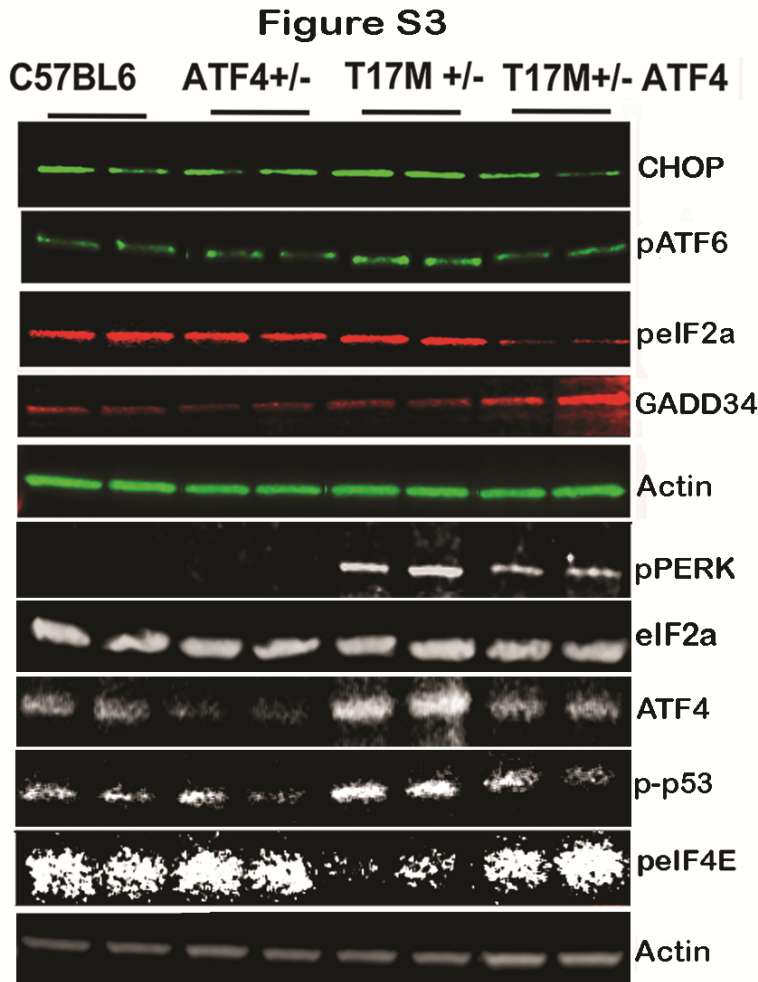


Figure S3. Representative images of western blots. Images were obtained by running retinal protein extracts from all four animal groups on polyacrylamide gels and probed with antibodies against the indicated proteins.

Acknowledgments

The authors acknowledge Pravallika Kotla for assistance with genotyping. This work was supported by the National Eye Institute at the National Institutes of Health Grant R01EY020905 and VSRC core grant P30 EY003039.

References

1. Choudhury S, Bhootada Y, Gorbatyuk O, & Gorbatyuk M (2013) Caspase-7 ablation modulates UPR, reprograms TRAF2-JNK apoptosis and protects T17M rhodopsin mice from severe retinal degeneration. *Cell death & disease* 4:e528.
2. Nashine S, Bhootada Y, Lewin AS, & Gorbatyuk M (2013) Ablation of C/EBP homologous protein does not protect T17M RHO mice from retinal degeneration. *PloS one* 8(4):e63205.
3. Kunte MM, *et al.* (2012) ER stress is involved in T17M rhodopsin-induced retinal degeneration. *Investigative ophthalmology & visual science* 53(7):3792-3800.
4. Krebs MP, *et al.* (2010) Molecular mechanisms of rhodopsin retinitis pigmentosa and the efficacy of pharmacological rescue. *Journal of molecular biology* 395(5):1063-1078.
5. Gorbatyuk MS, *et al.* (2010) Restoration of visual function in P23H rhodopsin transgenic rats by gene delivery of BiP/Grp78. *Proceedings of the National Academy of Sciences of the United States of America* 107(13):5961-5966.
6. Mendes HF, van der Spuy J, Chapple JP, & Cheetham ME (2005) Mechanisms of cell death in rhodopsin retinitis pigmentosa: implications for therapy. *Trends in molecular medicine* 11(4):177-185.
7. Rutkowski DT, *et al.* (2006) Adaptation to ER stress is mediated by differential stabilities of pro-survival and pro-apoptotic mRNAs and proteins. *PLoS biology* 4(11):e374.
8. Malabanan KP & Khachigian LM (2010) Activation transcription factor-4 and the acute vascular response to injury. *Journal of molecular medicine* 88(6):545-552.
9. Wang C & Guo F (2012) Effects of activating transcription factor 4 deficiency on carbohydrate and lipid metabolism in mammals. *IUBMB life* 64(3):226-230.
10. Singleton DC & Harris AL (2012) Targeting the ATF4 pathway in cancer therapy. *Expert opinion on therapeutic targets* 16(12):1189-1202.
11. Sun X, *et al.* (2013) ATF4 protects against neuronal death in cellular Parkinson's disease models by maintaining levels of parkin. *The Journal of neuroscience : the official journal of the Society for Neuroscience* 33(6):2398-2407.
12. Lange PS, *et al.* (2008) ATF4 is an oxidative stress-inducible, prodeath transcription factor in neurons in vitro and in vivo. *The Journal of experimental medicine* 205(5):1227-1242.
13. Baird TD & Wek RC (2012) Eukaryotic initiation factor 2 phosphorylation and translational control in metabolism. *Advances in nutrition* 3(3):307-321.
14. Harding HP, *et al.* (2003) An integrated stress response regulates amino acid metabolism and resistance to oxidative stress. *Molecular cell* 11(3):619-633.
15. Miyamoto N, *et al.* (2011) Transcriptional regulation of activating transcription factor 4 under oxidative stress in retinal pigment epithelial ARPE-19/HPV-16 cells. *Investigative ophthalmology & visual science* 52(3):1226-1234.

16. Gorbatyuk M & Gorbatyuk O (2013) Review: retinal degeneration: focus on the unfolded protein response. *Molecular vision* 19:1985-1998.
17. Zhong Y, *et al.* (2012) Activation of endoplasmic reticulum stress by hyperglycemia is essential for Muller cell-derived inflammatory cytokine production in diabetes. *Diabetes* 61(2):492-504.
18. Li J, Wang JJ, Yu Q, Wang M, & Zhang SX (2009) Endoplasmic reticulum stress is implicated in retinal inflammation and diabetic retinopathy. *FEBS letters* 583(9):1521-1527.
19. Wang X, Wang G, Kunte M, Shinde V, & Gorbatyuk M (2013) Modulation of angiogenesis by genetic manipulation of ATF4 in a mouse modulation of angiogenesis by genetic manipulation. *Investigative ophthalmology & visual science* 54(9):5995-6002.
20. Shinde VM, Sizova OS, Lin JH, LaVail MM, & Gorbatyuk MS (2012) ER stress in retinal degeneration in S334ter Rho rats. *PLoS one* 7(3):e33266.
21. Komaromy AM, *et al.* (2008) Targeting gene expression to cones with human cone opsin promoters in recombinant AAV. *Gene therapy* 15(14):1049-1055.
22. Janssen A, *et al.* (2008) Effect of late-stage therapy on disease progression in AAV-mediated rescue of photoreceptor cells in the retinoschisin-deficient mouse. *Molecular therapy : the journal of the American Society of Gene Therapy* 16(6):1010-1017.
23. Fawcett TW, Martindale JL, Guyton KZ, Hai T, & Holbrook NJ (1999) Complexes containing activating transcription factor (ATF)/cAMP-responsive-element-binding protein (CREB) interact with the CCAAT/enhancer-binding protein (C/EBP)-ATF composite site to regulate Gadd153 expression during the stress response. *The Biochemical journal* 339 (Pt 1):135-141.
24. Iwawaki T, Akai R, Kohno K, & Miura M (2004) A transgenic mouse model for monitoring endoplasmic reticulum stress. *Nature medicine* 10(1):98-102.
25. Teske BF, *et al.* (2013) CHOP induces activating transcription factor 5 (ATF5) to trigger apoptosis in response to perturbations in protein homeostasis. *Molecular biology of the cell* 24(15):2477-2490.
26. Bhootada Y, Choudhury S, Gully C, & Gorbatyuk M (2015) Targeting Caspase-12 to Preserve Vision in Mice With Inherited Retinal Degeneration. *Investigative ophthalmology & visual science* 56(8):4725-4733.
27. Amaral JD, Xavier JM, Steer CJ, & Rodrigues CM (2010) The role of p53 in apoptosis. *Discovery medicine* 9(45):145-152.
28. Satoh T, *et al.* (2006) Activation of the Keap1/Nrf2 pathway for neuroprotection by electrophilic [correction of electrophilic] phase II inducers. *Proceedings of the National Academy of Sciences of the United States of America* 103(3):768-773.
29. Ryoo IG, Choi BH, & Kwak MK (2015) Activation of NRF2 by p62 and proteasome reduction in sphere-forming breast carcinoma cells. *Oncotarget* 6(10):8167-8184.

30. Ichimura Y, *et al.* (2013) Phosphorylation of p62 activates the Keap1-Nrf2 pathway during selective autophagy. *Molecular cell* 51(5):618-631.
31. Pankiv S, *et al.* (2007) p62/SQSTM1 binds directly to Atg8/LC3 to facilitate degradation of ubiquitinated protein aggregates by autophagy. *The Journal of biological chemistry* 282(33):24131-24145.
32. Jiang Q, *et al.* (2013) ATF4 activation by the p38MAPK-eIF4E axis mediates apoptosis and autophagy induced by selenite in Jurkat cells. *FEBS letters* 587(15):2420-2429.
33. B'Chir W, *et al.* (2013) The eIF2alpha/ATF4 pathway is essential for stress-induced autophagy gene expression. *Nucleic acids research* 41(16):7683-7699.
34. Behrman S, Acosta-Alvear D, & Walter P (2011) A CHOP-regulated microRNA controls rhodopsin expression. *The Journal of cell biology* 192(6):919-927.
35. Wang L, Cano M, & Handa JT (2014) p62 provides dual cytoprotection against oxidative stress in the retinal pigment epithelium. *Biochimica et biophysica acta* 1843(7):1248-1258.
36. Tam LC, *et al.* (2010) Prevention of autosomal dominant retinitis pigmentosa by systemic drug therapy targeting heat shock protein 90 (Hsp90). *Human molecular genetics* 19(22):4421-4436.
37. Aguila M, *et al.* (2014) Hsp90 inhibition protects against inherited retinal degeneration. *Human molecular genetics* 23(8):2164-2175.
38. Regan PL, *et al.* (2011) Hsp90 inhibition increases p53 expression and destabilizes MYCN and MYC in neuroblastoma. *International journal of oncology* 38(1):105-112.
39. Hyrskyluoto A, Reijonen S, Kivinen J, Lindholm D, & Korhonen L (2012) GADD34 mediates cytoprotective autophagy in mutant huntingtin expressing cells via the mTOR pathway. *Experimental cell research* 318(1):33-42.
40. Ito S, *et al.* (2015) GADD34 inhibits activation-induced apoptosis of macrophages through enhancement of autophagy. *Scientific reports* 5:8327.
41. Uddin MN, Ito S, Nishio N, Suganya T, & Isobe K (2011) Gadd34 induces autophagy through the suppression of the mTOR pathway during starvation. *Biochemical and biophysical research communications* 407(4):692-698.
42. Tam BM, Noorwez SM, Kaushal S, Kono M, & Moritz OL (2014) Photoactivation-induced instability of rhodopsin mutants T4K and T17M in rod outer segments underlies retinal degeneration in *X. laevis* transgenic models of retinitis pigmentosa. *The Journal of neuroscience : the official journal of the Society for Neuroscience* 34(40):13336-13348.
43. Midorikawa R, *et al.* (2010) Autophagy-dependent rhodopsin degradation prevents retinal degeneration in *Drosophila*. *The Journal of neuroscience : the official journal of the Society for Neuroscience* 30(32):10703-10719.
44. Chen Y, *et al.* (2013) Autophagy protects the retina from light-induced degeneration. *The Journal of biological chemistry* 288(11):7506-7518.

45. Frost LS, Mitchell CH, & Boesze-Battaglia K (2014) Autophagy in the eye: implications for ocular cell health. *Experimental eye research* 124:56-66.
45. Zhou Z, Doggett TA, Sene A, Apte RS, & Ferguson TA (2015) Autophagy supports survival and phototransduction protein levels in rod photoreceptors. *Cell death and differentiation* 22(3):488-498.

CHAPTER 3

CONTROLLING PERK-ATF4-CHOP BRANCH OF THE UPR IS THE KEY TO REVERSE RETINAL DEGENERATION OF T17M RETINA

by

YOGESH BHOOTADA, CLARK GULLY, AND MARINA GORBATYUK.

In preparation for *Investigative Ophthalmology and Visual Science*

Format adapted for dissertation

Controlling PERK-ATF4-CHOP branch of the UPR is the key to reverse retinal degeneration of T17M Retina

Abstract

The T17M *RHO* transgenic mice carrying a mutated human rhodopsin transgene, expression of which in the retina leads to protein misfolding, demonstrate an activation of the Unfolded Protein Response (UPR) and rod photoreceptor cell death. Activating transcription factor 4 (ATF4) is a key transcription factor of the UPR and a major mediator of RNA-activated protein kinase-like ER kinase (PERK) signaling that plays a crucial role in both adaptations to stress and activation of pro-apoptotic C/EBP homologous protein (CHOP). Recently, we have shown that down regulation of ATF4 completely rescues one-month-old degenerating retinas expressing the T17M rhodopsin protein and delayed cell death at later time points. We hypothesized that simultaneous down regulation of two PERK mediators, ATF4 and CHOP, would give long term preservation to in these mice as compared to a single ATF4 knockdown. Double knockdown of the PERK mediators resulted in a higher therapeutic effect than was provided by a single knockdown. At P90, these mice had an even greater increase in amplitudes of scotopic a- and b- waves (359% and 151%, respectively) as compared to T17M transgenic mice. This effect was sustained and lasted at least 6 months and leads to a dramatic reduction in the rate of retinal degeneration. We also show that pharmacological knockdown of ATF4 cause downregulation of CHOP protein and were able to restore cone physiological function of one month old T17M animals.

Introduction

The T17M mutation within the Rhodopsin (*RHO*) gene substituting a threonine with a methionine at position 17 affects the assembly of the opsin protein with 11-cis-retinal and presumably impairs protein stability, folding and trafficking (1). This leads to a severe form of retinal degeneration (2) mimicking autosomal dominant retinitis pigmentosa (ADRP) in humans. A significant loss of scotopic a- and b-wave ERG amplitudes together with a compromised retinal integrity and a photoreceptor cell death characterize the ADRP progression in one-month-old T17M *RHO* retinas. In these mice we have shown that the RNA-activated protein kinase-like ER kinase (PERK) signaling is up regulated, leading to an increase in *ATF4* mRNA and CHOP starting at postnatal day (P) 18 (3). Recent studies also have shown that prolonged activation of PERK-ATF4-CHOP branch in various animal models of neurodegeneration (4), diabetes (5), oxygen induced retinopathy, and retinitis pigmentosa (6) leads to cell death due to persistent endoplasmic stress (ER) stress.

ATF4 is a bZIP transcription factor belonging to the activating transcription factor/cAMP response element binding (ATF/CREB) protein family. It binds to cAMP response elements (CRE), binds CCAAT/enhancer binding protein (C/EBP)/ATF response elements (CARE), and regulates genes involved in cellular stress response, hematopoiesis, lens and skeletal development, inflammation, angiogenesis, oxidative stress, and apoptosis (7-9). The most well-studied target gene of ATF4 during persistent ER stress is C/EBP homologous protein-10 (CHOP), also known as growth-arrest and DNA-damage-inducible gene 153 (GADD153) (10). Although each of the three branches of the UPR is capable of activating CHOP, ATF4 is considered to be the major

transcription factor inducing *CHOP* transcription (11). *CHOP* also signals apoptosis through binding directly to the promoter of the *TRB3* gene and inhibiting *AKT* activation, as well as through increasing calcium influx from the ER to the mitochondria, resulting in the activation of mitochondria-dependent apoptotic pathway (12).

Previous study from our lab has shown that complete ablation of *CHOP* does not rescue T17M photoreceptors and, in fact, worsens the pathophysiology (13). Recently, we investigated the role of *ATF4* in retinal degeneration. Deficiency of *ATF4* completely rescued physiology and morphology of one month old T17M retinas. In current studies, we downregulated two *PERK* mediators (*ATF4* and *CHOP*) simultaneously and validated both as therapeutic targets that control the rate of retinal degeneration in T17M *ADRP* photoreceptors. We also inhibited their expression by pharmacological action and were able to restore photopic physiological response in T17M mice.

Materials and Methods

Animals

Transgenic mice expressing human T17M *RHO*^{+/+}, C57BL/6J, *RHO*^{-/-}, *ATF4*^{+/-} and *CHOP*^{-/-} knockout mice were used in this study to generate T17M *RHO*^{+/-} *ATF4*^{+/+} *CHOP*^{+/+} (further referred to T17M), T17M *RHO*^{+/-} *ATF4*^{+/-} *CHOP*^{+/-} (further referred to T17M *ATF4*^{+/-} *CHOP*^{+/-}). C57BL/6J, *ATF4*^{+/-} and *CHOP*^{-/-} mice was purchased from Jackson (Bar Harbor, ME; <http://www.jax.org>). The genotyping of *ATF4*^{+/-} mice was performed using forward primers: ATATTGCTGAAGAGCTTGGCGGC for Neo allele and AGCAAACAAGACAGCAGCCACTA for wild type allele and a common reverse primer GTTCTACAGCTTCCTCCACTCTT for both alleles. The T17M genotyping

was performed as previously described (14). All mice were raised under a 12-h dim light/12-h dark cycle.

Drug Treatment

Integrated stress response inhibitor (ISRIB) was purchased from Calbiochem (Cat#509584). The drug was administered at 0.25 mg/kg once daily by intraperitoneal injection or vehicle alone (45% saline, 50% PEG 400, 5% DMSO) from post-natal day (P) 15 to P30.

Electroretinography

Mice were dark-adapted overnight, then anesthetized with ketamine (100 mg/kg) and xylazine (10 mg/kg), and their pupils were dilated in dim red light with 2.5% phenylephrine hydrochloride ophthalmic solution (Akorn, Inc.). Scotopic ERGs were recorded using a wire contacting the corneal surface with 2.5% hypromellose ophthalmic demulcent solution (Akorn, Inc.). ERG was performed at different light intensities (0 db (2.5 cd*s/m²), 5 db (7.91 cd*s/m²), 10 db (25 cd*s/m²), and 15 db (79.1 cd*s/m²). Five scans were performed and averaged at different light intensities. Photopic, cone-mediated responses were performed following 10 min light adaptation on the background light intensity of 30 cd*s/m². Recordings were obtained at the light intensity of 25 cd*s/m². Fifteen waveforms from each animal were recorded and the values were averaged. The a-wave amplitudes were measured from the baseline to the peak in the cornea-negative direction, and the b-wave amplitudes were determined from the cornea-negative peak to the major cornea-positive peak. The signal was amplified, digitized, and stored using the LKC UTAS-3000 Diagnostic System (Gaithersburg, MD).

Histology

Mouse eyes were enucleated at 1 and 6 months of age and were fixed overnight in 4% paraformaldehyde freshly made in phosphate-buffered saline (PBS) as previously described [1]. Hematoxylin and eosin staining of 12-micron retinal cryosections as well as counting of retinal nuclei were performed as previously described [2]. Digital images of right and left retinas of individual mice were analyzed in the central superior and inferior equally located from the optic nerve head. A masked investigator analyzed the images.

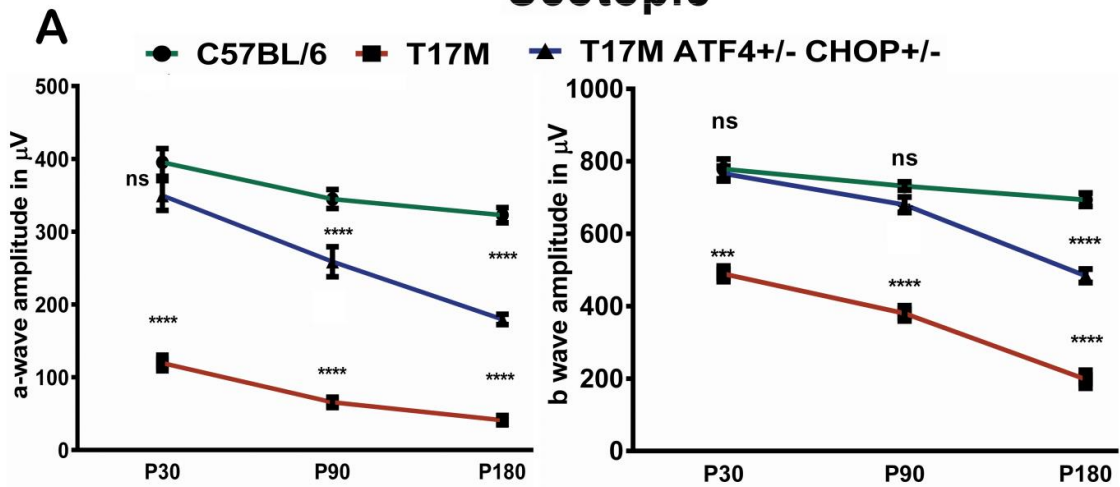
Results

Coupled downregulation of ATF4 and CHOP preserves ADRP mice from vision loss

Analysis of the scotopic ERG responses (Fig. 1A) demonstrated that while T17M mice already demonstrated profound loss of a- and b-wave amplitudes by 56% and 36%, respectively, at 1 month of age; the age-matched T17M ATF4^{+/-} CHOP^{+/-} animals demonstrated full functional rescue of ADRP photoreceptors as measured by a- and b-wave amplitudes. No difference was observed between T17M ATF4^{+/-} CHOP^{+/-} and C57BL/6 animals. However, by 3 months of age when T17M mice exhibited significant decreases in their ERG responses, T17M ATF4^{+/-} CHOP^{+/-} mice did begin to demonstrate a slight drop in a-wave amplitudes, with b-wave amplitudes remaining unchanged relative to C57BL/6 controls. At 6 months of age the drop in ERG amplitudes for T17M ATF4^{+/-} CHOP^{+/-} mice became more noticeable. Nevertheless, despite the initial degeneration, the scotopic a- and b-wave ERG amplitudes were greater in T17M ATF4^{+/-} CHOP^{+/-} mice by 4.4- and 2.4-fold, respectively when compared to T17M animals.

Photopic ERG measurements at 1 month of age also exhibited complete preservation of a- and b-wave amplitudes in T17M ATF4^{+/-} CHOP^{+/-} mice as compared to C57BL/6, while T17M animals showed 41% and 22% decline in a- and b-wave amplitudes (Fig. 1B). By 6 months of age, a- and b-wave amplitudes showed decline (56% and 12%, respectively) in double knock down T17M animals compared to C57BL/6 mice, but were still higher (145% and 173% respectively) when compared to T17M animals.

Figure 1
Scotopic



Photopic

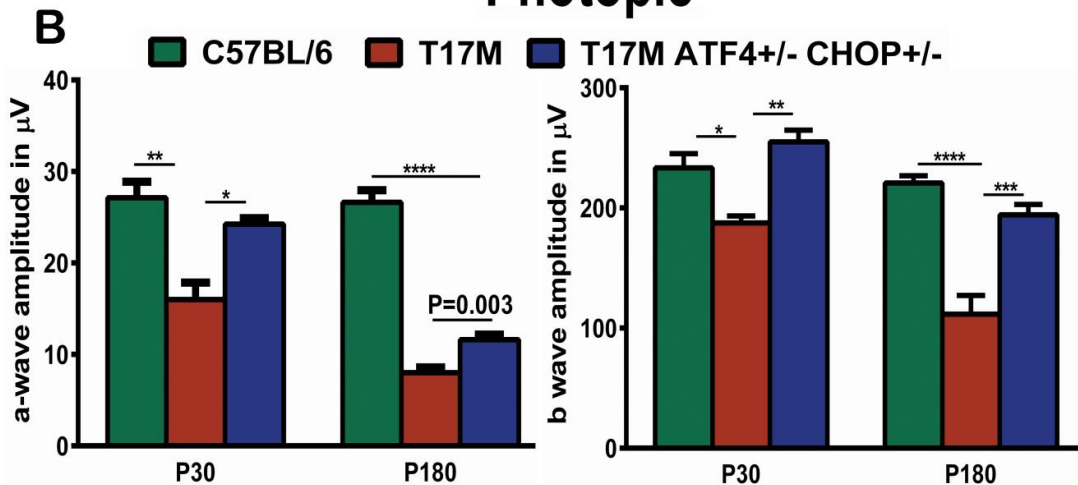


Fig.1: ATF4 and CHOP deficiency prevents functional loss of T17M retina as measure by scotopic and photopic ERG. (N=8) (A) The a-wave of the scotopic ERG amplitude was diminished in 1-month-old T17M mice by over 56% ($P<0.0001$). At one month of age T17M ATF4^{+/-} CHOP^{+/-} retina demonstrated no difference in the a-wave amplitude compared to C57BL/6 mice suggesting a functional rescue of T17M photoreceptors. However, a decline in the a-wave amplitudes began at 3 months in the T17M ATF4^{+/-} CHOP^{+/-} retina, with a subsequent decline at 6 months of age, when compared to C57BL/6 retinas ($P<0.0001$ for both time points); but the T17M ATF4^{+/-} CHOP^{+/-} amplitudes were higher than those of 3- and 6-month-old T17M mice, ($P<0.0001$ for both time points). The b-wave of the scotopic ERG amplitude was better preserved in the T17M ATF4^{+/-} CHOP^{+/-} retinas. No difference between T17M ATF4^{+/-} CHOP^{+/-} and C57BL/6 mice (n.s.) was detected during the first 3 months. By 6 months of age, the T17M ATF4^{+/-} CHOP^{+/-} started to exhibit a 30% decline in b-wave amplitudes as compared to C57BL/6 retinas ($P<0.0001$). (B) Using one-way ANOVA the photopic ERG analysis demonstrated that by 1 month the a- and b-wave amplitudes in T17M retinas were dramatically declined (40% and 20%, respectively) and by 6 month (70% and 50%, respectively) compared to C57BL/6 mice suggesting impaired cone function in these retinas. Knockdown of ATF4 and CHOP in the T17M retina however, rescued cone photoreceptors from functional loss at one month. By 6 month of age a- and b-wave amplitudes showed decline (56% and 12%, respectively) in T17M ATF4^{+/-} CHOP^{+/-} animals compared to C57BL/6 mice, but were still higher (145% and 173% respectively) when compared to T17M animals.

Coupled downregulation of ATF4 and CHOP in ADRP mice prevents photoreceptor cell death

We performed histological analysis and counted the number of photoreceptor nuclei rows in the retinas of C57BL/6, T17M, and T17M ATF4^{+/-} CHOP^{+/-} retinas (Fig. 2). Cryostat-sectioned retinas were stained with hematoxylin and eosin (H&E). One-month-old T17M retinas showed loss of photoreceptor cell nuclei, shortening of the outer segments, and general disorganization. No difference in nuclei rows was detected between C57BL/6 and T17M ATF4^{+/-} CHOP^{+/-} retinas at 1 month. However, by 6 months the T17M ATF4^{+/-} CHOP^{+/-} mice experienced a loss of photoreceptor cells. Despite this fact, the difference between T17M and T17M ATF4^{+/-} CHOP^{+/-} mice was still dramatic and was measured as a 343% increase in the number of photoreceptors ONL nuclei rows.

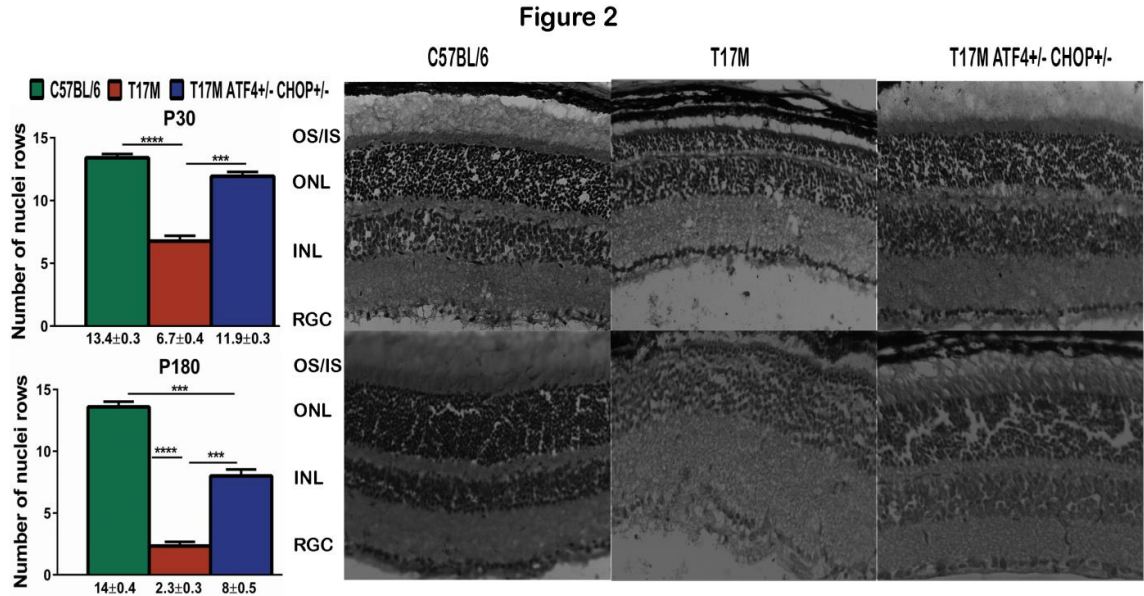


Fig.2: ATF4 and CHOP knockdown protects T17M mice from loss of photoreceptors. Histological analyses of C57BL/6, T17M and T17M ATF4^{+/-} CHOP^{+/-} retinas (N=4). Cryostat-sectioned retinas were stained with hematoxylin and eosin (H&E). The number of rows of photoreceptor nuclei between T17M ATF4^{+/-} CHOP^{+/-} and C57BL/6 retinas was similar at P30, whereas the T17M mice lost 43% of their photoreceptor cells ($P < 0.0001$ as compared to both groups). However, by 6 months the T17M ATF4 CHOP mice experienced a loss of photoreceptor cells. Despite this fact, the difference between T17M and T17M ATF4 CHOP^{+/-} mice was still dramatic and was measured as a 343% increase in the number of photoreceptors ONL nuclei rows. One-way Anova with multiple comparison analysis demonstrated differences in all 3 groups of animals (***) $P < 0.001$, **** $P < 0.0001$) at 6 months of age. Representative images of one and six month-old retinas are on the right.

ISRIB reduces ATF4 and CHOP levels rescues photopic ERG function in one month old T17M Mice.

T17M mice show PERK/eIF2 α -mediated translational repression and activation of ATF4-CHOP translation starting at P15 resulting in photoreceptor loss that progresses to vision loss and death at one month. T17M mice were treated daily with 0.25 mg/kg of ISRIB or vehicle alone from P15. Mice were analyzed for vision loss and biochemically at P30 (Fig. XX), when T17M mice demonstrated significantly loss of scotopic and photopic physiological function. ISRIB treatments reduced levels of ATF4 and CHOP markedly

($P < 0.001$ as compared to vehicle treated T17M mice) and is consistent with its point of action downstream of eIF2 α -P, as previously described (15). ISRIB treatment was not able to rescue scotopic vision loss, although photopic ERG function was improved in the treatment group. Photopic ERG measurements at 1 month of age exhibited complete preservation of a- and b-wave amplitudes in T17M treated mice. No difference was observed between 1-month-old T17M treated mice and C57BL/6 animals, while T17M vehicle treated animals showed 41% and 22% decline in a- and b-wave amplitudes similar to naïve T17M animals. Treatment of C57BL/6 mice shows no changes in scotopic and photopic physiological response.

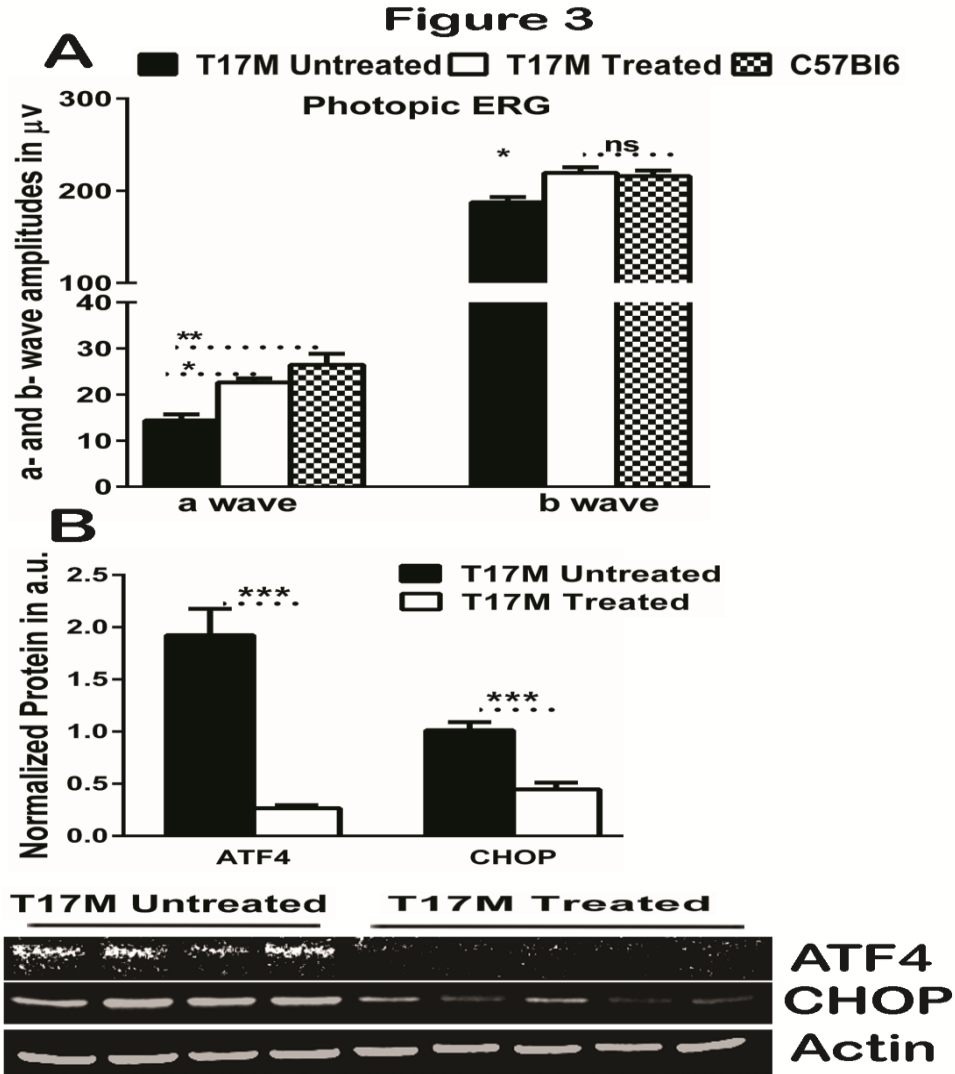


Fig.3: ISRIB reduces ATF4 and CHOP expression rescues photopic ERG function in one month old T17M Mice. Data analysis demonstrated that ISRIB treatment led to a preservation of cone photoreceptor function in the T17M animals compared to the vehicle treated T17M animals (N=5, $P < 0.05$ for both a- and b-wave amplitudes). **(B)** ISRIB treatment abolishes ATF4 expression in T17M retinas was measured by western blotting, whereas vehicle treated T17M retina showed 7.2-fold (N=5, t -test $p < 0.001$) increase in ATF4 protein level. ISRIB treatment resulted in downregulation of CHOP protein (N=5, t -test $p < 0.001$) as compared to vehicle treated T17M retinas. Representative images of western blots probed with antibody against ATF4, CHOP, and β -actin are shown on the side.

Discussion

Previously, we have shown that the activated PERK signaling could be a common hallmark of progressive ADRP (6). In chapter 2 we showed that ATF4 haploinsufficiency provides functional rescue of one-month-old T17M ATF4^{+/-} retinas that, to our knowledge, is the first report to demonstrate a reversed rapid degeneration of ADRP retinas at P30. The major contribution of ATF4 knockdown to the mechanism of retinal degeneration is likely through a reduction of overall ER stress, induction of an antioxidant program, and restoring of autophagy, which together result in a delay of apoptotic photoreceptor cell death. The dramatic reduction in pPERK, pATF6, peIF2a, and CHOP proteins indicates a significantly lower degree of UPR activation in T17M ATF4^{+/-} retinas. In this study, we determined by potentially targeting two mediators of the PERK-ATF4-CHOP axis in UPR signaling provides longer functional and morphological rescue of the profoundly degenerating transgenic retina expressing the T17M rhodopsin mutant; this rescue lasted 6 months.

Here we also demonstrated that pharmacological modulation of ATF4-CHOP inhibition can be achieved to produce neuroprotection. We found that treatment with the ISRIB drug, which successfully reduced ATF4 and CHOP expression, restored cone physiological response in T17M mice which usually shows diminished light-adapted (photopic) ERG amplitude at P30.

ATF4 and CHOP modulation could be a promising therapeutic target for delaying retinal degeneration in ADRP patients.

Acknowledgments:

This study was supported by NIHR01EY020905 and the VSRC Core Grant P30 EY003039.

References

1. Mendes HF, van der Spuy J, Chapple JP, & Cheetham ME (2005) Mechanisms of cell death in rhodopsin retinitis pigmentosa: implications for therapy. *Trends in molecular medicine* 11(4):177-185.
2. White DA, Fritz JJ, Hauswirth WW, Kaushal S, & Lewin AS (2007) Increased sensitivity to light-induced damage in a mouse model of autosomal dominant retinal disease. *Investigative ophthalmology & visual science* 48(5):1942-1951.
3. Kunte MM, *et al.* (2012) ER stress is involved in T17M rhodopsin-induced retinal degeneration. *Invest Ophthalmol Vis Sci* 53(7):3792-3800.
4. Salminen A, Kauppinen A, Hyttinen JM, Toropainen E, & Kaarniranta K (2010) Endoplasmic reticulum stress in age-related macular degeneration: trigger for neovascularization. *Molecular medicine* 16(11-12):535-542.
5. Zhong Y, *et al.* (2012) Activation of endoplasmic reticulum stress by hyperglycemia is essential for Muller cell-derived inflammatory cytokine production in diabetes. *Diabetes* 61(2):492-504.
6. Gorbatyuk M & Gorbatyuk O (2013) Review: retinal degeneration: focus on the unfolded protein response. *Mol Vis* 19:1985-1998.
7. Lange PS, *et al.* (2008) ATF4 is an oxidative stress-inducible, prodeath transcription factor in neurons in vitro and in vivo. *The Journal of experimental medicine* 205(5):1227-1242.
8. Masuoka HC & Townes TM (2002) Targeted disruption of the activating transcription factor 4 gene results in severe fetal anemia in mice. *Blood* 99(3):736-745.
9. Roybal CN, *et al.* (2004) Homocysteine increases the expression of vascular endothelial growth factor by a mechanism involving endoplasmic reticulum stress and transcription factor ATF4. *The Journal of biological chemistry* 279(15):14844-14852.
10. Oyadomari S & Mori M (2004) Roles of CHOP/GADD153 in endoplasmic reticulum stress. *Cell Death Differ* 11(4):381-389.
11. Scheuner D, *et al.* (2001) Translational control is required for the unfolded protein response and in vivo glucose homeostasis. *Mol Cell* 7(6):1165-1176.
12. Giorgi C, De Stefani D, Bononi A, Rizzuto R, & Pinton P (2009) Structural and functional link between the mitochondrial network and the endoplasmic reticulum. *The international journal of biochemistry & cell biology* 41(10):1817-1827.
13. Nashine S, Bhootada Y, Lewin AS, & Gorbatyuk M (2013) Ablation of C/EBP homologous protein does not protect T17M RHO mice from retinal degeneration. *PLoS One* 8(4):e63205.

14. Choudhury S, Bhootada Y, Gorbatyuk O, & Gorbatyuk M (2013) Caspase-7 ablation modulates UPR, reprograms TRAF2-JNK apoptosis and protects T17M rhodopsin mice from severe retinal degeneration. *Cell death & disease* 4:e528.
15. Sidrauski C, *et al.* (2013) Pharmacological brake-release of mRNA translation enhances cognitive memory. *Elife* 2:e00498.

CHAPTER 4

**TARGETING CASPASE-12 TO PRESERVE VISION IN MICE WITH
INHERITED RETINAL DEGENERATION**

by

**YOGESH BHOOTADA, SHREYASI CHOUDHURY, CLARK GULLY AND
MARINA GORBATYUK**

Investigative Ophthalmology and Visual Science

Copyright

2015

By

The Association for Research in Vision and Ophthalmology

Used by permission

Format adapted for dissertation

Targeting caspase-12 to preserve vision in mice with inherited retinal degeneration

Abstract

Purpose: The unfolded protein response is known to contribute to the inherited retinal pathology observed in T17M Rhodopsin (T17M) mice. Recently it has been demonstrated that the endoplasmic reticulum stress-associated caspase-12 is activated during progression of retinal degeneration in different animal models. Therefore, we wanted to explore the role of caspase-12 in the mechanism of retinopathy in T17M mice and determine if thereby inhibiting apoptosis is a viable approach for halting retinal degeneration.

Methods: One, two and three month-old C57BL/6J (wt), Caspase-12^{-/-}, T17M and T17M Caspase12^{-/-} mice were analyzed by scotopic ERG, SD-OCT, histology, qRT-PCR and western blot analyses of retinal RNA and protein extracts. Calpain and caspase-3/7 activity assays were measured in P30 retinal extracts.

Results: Caspase-12 ablation significantly prevented a decline in the a- and b- wave ERG amplitudes in T17M mice at 1, 2 and 3 months of age increasing the amplitudes from 232% to 212% and from 160% to 138%, respectively. SD-OCT results and photoreceptor row counts demonstrated preservation of retinal structural integrity and postponed photoreceptor cell death. The delay in photoreceptor cell death was due to significant decreases in the activity of caspase 3/7 and calpain, which correlated with an increase in calpastatin expression.

Conclusions: We validated caspase-12 as a therapeutic target, ablation of which significantly protects T17M photoreceptors from deterioration. Although the inhibition of apoptotic activity alone was not sufficient to rescue T17M photoreceptors, in

combination with other non-apoptotic targets, caspase-12 could be used to treat inherited retinopathy.

Introduction

Mice expressing a mutant form of human rhodopsin with a threonine to methionine substitution at position 17 (T17M) develop severe retinal degeneration and thus mimic the human autosomal dominant retinitis pigmentosa (ADRP) (1, 2). The study of molecular mechanisms underlying the retinopathy in these mice has demonstrated that the unfolded protein response (UPR), along with inflammatory signaling significantly contribute to the progression of retinal degeneration (3). Thus, the activation of all three UPR branches, including PERK (Protein Kinase R-Like Endoplasmic Reticulum Kinase), ATF6 (Activating Transcriptional Factor 6) and IRE1 (Inositol-Requiring Enzyme 1), have been detected in T17M retinas as early as postnatal (P) day 15. Moreover, we have recently revealed that the rate of retinal degeneration could be significantly altered in these mice by modifying the expression of UPR hallmark proteins. For example, we found that full knockout of the UPR pro-apoptotic CHOP protein in degenerating retinas dramatically accelerated the rate of retinal degeneration (4,5) while full ablation of the UPR downstream marker, the ER (endoplasmic reticulum) stress-associated caspase (Csp)-7 significantly slowed the rate of retinal degeneration (6). In addition to Csp-7, Csp-12 localizes to the Golgi complex and is also activated during ER stress (7). Several studies have suggested that Csp-12 acts as an initiator caspase during ER stress-induced apoptosis, activating an effector caspase-3 or -7 which then cleaves key substrates required for normal cellular functions, thus leading to apoptosis (8). Recently, it has also been reported that Csp-12-deficient mice are resistant to ER

stress-induced apoptosis, but their cells do undergo apoptosis in response to other stimuli. Thus, in experiments with primary cortical neurons the link between ER stress and Csp-12 activation has been proposed by demonstrating the reduced susceptibility of Csp-12^{-/-} neurons to A β -induced UPR activation and subsequent cell death (9). These experiments have clearly demonstrated that activation of Csp-12 during ER stress plays a proapoptotic role and contributes to neuronal death in Alzheimer disease (9).

Recent studies have proposed that there are two mechanisms for ER stress-mediated Csp-12 activation that act in different compartments of the cell. The first involves the interaction of proCsp-12 with the IRE1–TRAF2 complex (IRE1 UPR arm) on the cytosolic side of the ER membrane (10). This interaction occurs as a result of altered complex formation between IRE1 α and TRAF2 (tumor necrosis factor receptor-associated factor 2) in response to ER stress and modified activity of Jun N-terminal inhibitory kinase (JIK) against its binding partner IRE1 α (10). This suggests that Csp-12 activated by TRAF2 plays a crucial role in signal transduction from IRE1 to downstream signaling molecules and thus links the stress sensor molecule IRE1 to the activation of caspase-12. The second mechanism for Csp-12 activation occurs in the cytosol, where an increase in Ca²⁺ concentration results in calpain activation. The μ -calpain activation in turn precedes expression/activation of Csp-12 and is required for activation/cleavage of Csp-12 (11). Given that a cytosolic Ca²⁺ increase could also occur in response to ER stress, this pathway along with the above-mentioned TRAF2-pathway point to Csp-12 as the ER stress-induced caspase promoting apoptosis.

Involvement of Csp-12 in the mechanisms of several different retinopathies has been recently described by a number of studies (12-16). Although a combination of inhibiting Csp-12, upregulating the ER-resident chaperone BiP and inhibiting CAP-dependent

translation have been proposed as the most efficient way to maintain BBS-12 photoreceptors (13), the direct impact of inhibiting Csp-12 on loss of photoreceptor function and cell death has yet to be shown, since Csp-12 has not been previously assigned a direct role in retinal degeneration. The Csp-12 inhibitor INH in this study has been used in combination with other drugs such as guanabenz and valproic acid pointing the necessity of conducting a study demonstrating a direct link between Csp-12 activation and retinal degeneration.

Therefore, in the current study we explored the role of Csp-12 in the mechanism of retinal pathogenesis in T17M mice. Our goal was to determine if ER stress-induced apoptosis played a role in ADRP photoreceptor demise and whether the therapeutic approach of targeting ER stress-promoted apoptosis was sufficient to rescue ADRP photoreceptors. Building on a previous study that looked exclusively at Csp-7 in T17M mice, the current work genetically modulated Csp-12 activity in T17M mice and compared the results to our previous findings. We also attempted to answer the question of whether blocking apoptosis overall proved sufficient to rescue ADRP retinas and prevent further loss of retinal integrity. Our data point to inhibition of Csp-12 as a potential therapeutic approach that significantly slows retinal degeneration and together with other non-apoptotic targets could dramatically delay photoreceptor cell death.

Material and Methods

Animals

All animal groups were maintained in a C57BL/6J (wt) background. The Csp-12^{-/-} mice were created as previously described (17). Cryopreserved sperm from Csp-12^{-/-} mice was

purchased from the Mutant Mouse Regional Resource Center (Chapel Hill, NC, United States) and injected in a surrogate wt female. The litter resuscitated from the cryo-archive was genotyped, and breeding was carried out by monogamous mating. A pair of male and female homozygous *Csp-12^{-/-}* mice was kept in the same cage for mating. Pups were weaned at an age of 3 wk and separated according to gender. Animals were in a 12 h light/dark cycle with unlimited access to food and water. The T17M genotyping was performed as previously described (6).

Electroretinography. Mice were dark-adapted overnight, then anesthetized with ketamine (100 mg/kg) and xylazine (10 mg/kg), followed by their pupils being dilated in dim red light with 2.5% phenylephrine hydrochloride ophthalmic solution (Akorn, Inc.). Scotopic ERGs were recorded using a wire contacting the corneal surface with 2.5% hypromellose ophthalmic demulcent solution (Akorn, Inc.). ERG was performed at different light intensities (0 db (2.5 cd*s/m²), 5 db (7.91 cd*s/m²), 10 db (25 cd*s/m²), and 15 db (79.1 cd*s/m²). Five scans were performed and averaged at different light intensities. The a-wave amplitudes were measured from the baseline to the peak in the cornea-negative direction, and the b-wave amplitudes were determined from the cornea-negative peak to the major cornea-positive peak. The signal was amplified, digitized, and stored using the LKC UTAS-3000 Diagnostic System (Gaithersburg, MD).

Spectra domain-optical coherent tomography. SD-OCT was performed in one, two and three month-old animals using the Spectral Domain Ophthalmic Imaging System (SDOIS) (Bioptigen). The mice were anesthetized as mentioned above. Horizontal volume scans through the area dorso-temporal to the optic nerve (superior retina) and the area ventro-temporal to the optic nerve (inferior retina) were used to evaluate the thickness of the ONL. For measuring the thickness of the ONL, six calibrated calipers

were placed in the superior and inferior hemispheres of retinas within 100, 200, 300 and 400 μm of the optic nerve head. The thickness of the ONL was determined by averaging ten measurements.

Histology. Hematoxylin and eosin staining of 12-micron retinal cryosections retinal nuclei counts were performed as previously described⁶. Digital images of right and left retinas from individual mice were analyzed in the central superior and inferior regions equidistant from the optic nerve head. A masked investigator analyzed the images. For hematoxylin and eosin staining, mouse eyes were enucleated at 1 and 3 months of age and were fixed overnight using freshly-made 4% paraformaldehyde in phosphate-buffered saline (PBS). Afterwards, eye cups were transferred to PBS to remove formaldehyde and submerged sequentially in solutions of 10%, 20% and 30% sucrose for at least 1 h each. Eye cups were then embedded in cryostat compound (Tissue TEK OCT, Sakura Finetek USA, Inc., Torrance, CA, USA) and frozen at -80°C .

Quantitative real-time RT-PCR. For RNA extraction, whole retinas were isolated from 1- month-old mice (wt, *Csp-12^{-/-}*, T17M and T17M *Csp-12^{-/-}*) by surgical excision. Total RNA was extracted using the QIAGEN RNeasy Mini Kit. One μg of purified RNA was reverse transcribed into cDNA using iScript Reverse Transcription Supermix (BioRad). Integrity of the RNA samples and efficiency of the cDNA reaction were verified prior to the qRT-PCR. TaqMan Gene Expression Assay for caspase-12 (Id: Mm00802897_m1) and Bax (Id: Mm00432051_m1) from Applied Biosystems were used to measure gene expression. Quantitative real-time PCR was performed with the Step One PlusTM Real-Time PCR System (Applied Biosystems) based on the relative standard curve method. Reactions were performed at 50°C for 2 minutes and 95°C for 10 minutes, followed by 40 cycles at 95°C for 15 seconds and 60°C for 1 minute. Results

were expressed as cycle threshold time (Ct) and were normalized to Ct times for the housekeeping gene GAPDH. The replicated RQ (Relative Quantity) values for each biological sample were averaged. Four biological samples from each strain were used for qRT-PCR analyses.

Western Blot Analysis For protein extraction. Whole retinas were isolated from 1-month-old mice (wt, Csp-12^{-/-}, T17M and T17M Csp-12^{-/-}) by surgical excision. Total protein was extracted via sonication in a protein extraction buffer containing 25 mM sucrose, 100 mM Tris-HCl, pH = 7.8, and a mixture of protease inhibitors (PMSF, TLCK, aprotinin, leupeptin, and pepstatin). Protein concentrations were determined using BioRad Protein Assays based on the Bradford method of protein quantitation. Proteins (30–40 ug) were separated on 4–20% Criterion Precast gels (BioRad), transferred to a polyvinylidene difluoride (PVDF) membrane using the Trans-Blot Turbo Transfer System (BioRad) and incubated with primary antibodies (Calpastatin #4146, BAX #2772, TRAF2 #4712 from cell signaling and Caspase12 #ab18766 from abcam) overnight at 4oC with agitation. Goat anti-rabbit (1:10,000, #926-68021), and donkey anti-mouse (1:10,000, #926-32210) secondary antibodies were used (LI-COR Odyssey). β -actin was used as a gel loading control and was detected using an anti- β -actin antibody (1:5000, Sigma-Aldrich, #A1978). The developed membrane was imaged using the LI-COR Odyssey Quantitative Fluorescence Imaging System.

Calpain Activation Assay. The detection of calpain activity was performed using the Calpain Activity Assay kit from BioVision in accordance with the manufacturer's recommendations and compared the activation of calpains in wt, Csp-12^{-/-}, T17M and T17M Csp-12^{-/-} retinal tissues. The detection of the cleavage substrate Ac-LLY-AFC was

performed in a fluorometer that was equipped with a 400-nm excitation filter and 505-emission filter.

Caspase 3/7 Activity Assay. The detection of caspase 3/7 activity was performed using the Caspase-Glo 3/7 Luciferase assay (#G8091; Promega, Madison, WI) kit in accordance with the manufacturer's recommendations. Luciferase signal was read by a luminescent plate reader (Infinite m200, Tecan Group Ltd., Meannedorf, Switzerland) and used to compare the activation of caspase 3/7 in wt, Csp12^{-/-}, T17M and T17M Csp12^{-/-} retinal tissues.

Statistics. Two-way ANOVA comparisons were used to calculate differences in a- and b-wave ERG amplitudes and in the average ONL thickness of inferior and superior retinas in 1-, 2- and 3-month-old mice. A one-way ANOVA and t-test were used to calculate a fold change in mRNA expression and the level of normalized proteins in P30 retinas. For all experiments, a P-value <0.05 was considered significant (*P<0.05, **P<0.01, ***P<0.001, ****P<0.0001). Data are represented using mean ± SEM.

Results

T17M mice experience UPR activation in their retinas starting at P15. Thus, being interested in the mechanism of photoreceptor cell death and ER stress-induced apoptosis, we analyzed Csp-12 mRNA expression from P12 to P25.

The T17M mouse retinas demonstrate an increase in the expression and activity of Csp-12.

Fig. 1 presents the results of qRT-PCR analysis demonstrating that Csp-12 mRNA expression increased significantly in T17M retinas and was upregulated 6-fold at P18, prior to declining by 2-fold at P25. At P21 this increase resulted in a 6-fold elevation of

cleaved Csp-12 protein suggesting that ER-stress-induced Csp-12 might play a pivotal role in activation of the apoptotic photoreceptor cell death shown in our earlier experiments^{2,4,6}. Upregulation of Csp-12 activity during ADRP progression prompted us to try to determine a role for Csp-12 in retinal pathogenesis of T17M mice.

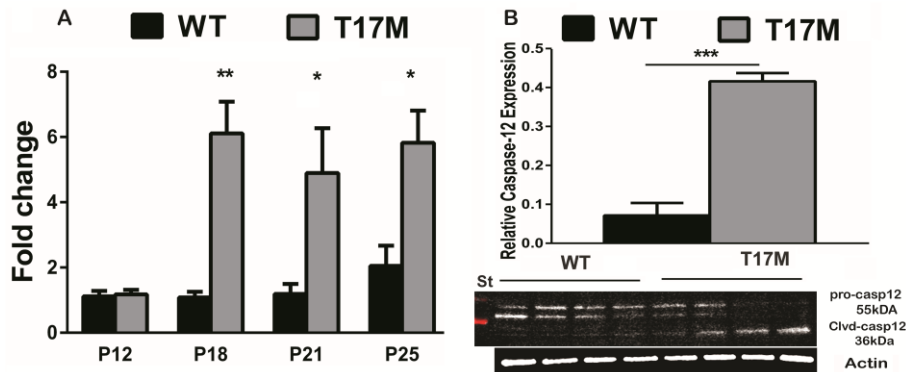


Figure 1. Expression and activation of Csp-12 in the T17M retina during ADRP progression. We used 4 animals per group in this experiment and analyzed retinal protein and RNA extracts at early time points from P12 to P25. (A) Starting at P18, we observed a 6-fold ($P<0.01$) increase in Csp-12 mRNA in T17M mice compared with wt. At P21 and P25, Csp-12 gene expression was upregulated between 4.5 and 1.6-fold. (B) At P21, we detected a 6-fold ($P<0.001$) increase in Csp-12 activation in T17M retinas, suggesting that in addition to the UPR activation detailed in previous studies [4,6], ADRP photoreceptors also experience activation of Csp-12. Data are shown as mean±S.E.M. (* $P<0.05$, ** $P<0.01$, *** $P<0.001$).

Csp-12 ablation significantly delays loss of function for T17M photoreceptors.

We crossed T17M mice with Csp-12^{-/-} mice and followed them by functional and histological analysis, as well as by SD-OCT over a period of three months. Fig. 2 presents the results of the scotopic ERG analysis of one-, two- and three-month-old T17M Csp-12^{-/-} mice. The data demonstrated that the range of photoreceptor specific a-wave amplitude in one-, two- and three-month-old T17M Csp-12^{-/-} mice increased from 2.3- to 2.1-fold, respectively as compared with T17M mice. The b-wave amplitude of the scotopic ERG was also elevated in these animals. The degree of elevation was however less profound as compared to a-wave, thus suggesting that the photoreceptors expressing

the aberrant rhodopsin and experiencing UPR activation were also the retinal cell type most responsive to removal of the UPR downstream player.

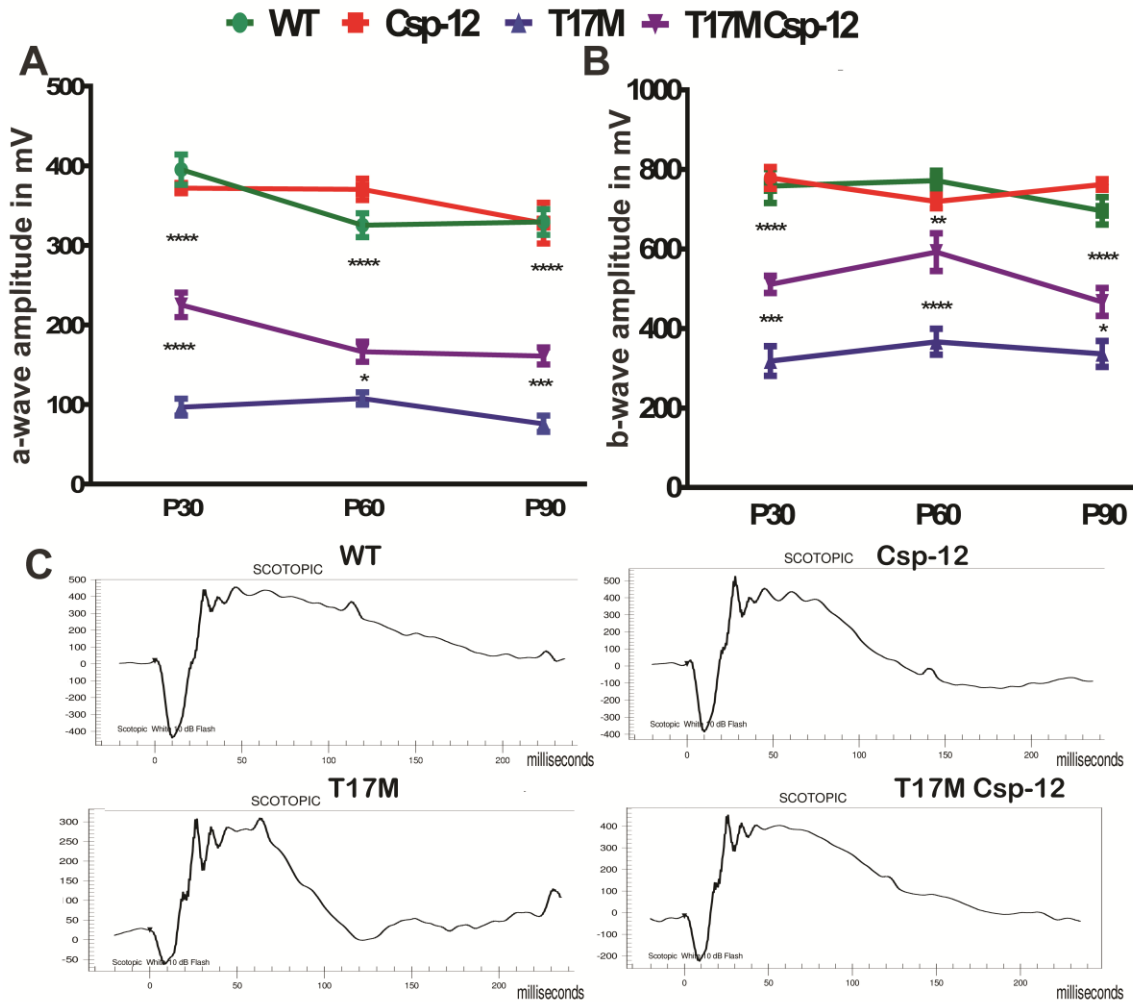


Figure 2. Lack of Csp-12 protects T17M retinas from degeneration, as measured by scotopic ERG responses at 10 dB. We analyzed 4 groups of animals (N = 6). **(A)** Using two-way ANOVA, we demonstrated that a-wave amplitudes of the scotopic ERG were significantly increased in T17M Csp-12^{-/-} mice at 1 month of age and that the value of a-wave amplitudes was 225 $\mu\text{V} \pm 15$ vs 97.0 $\mu\text{V} \pm 11$ in T17M. This data represents a 2.3-fold difference in a-wave amplitudes between T17M and T17M Csp-12^{-/-} mice. At 2 and 3 months, the difference between T17M and T17M Csp-12^{-/-} groups was also dramatic, but somewhat diminished due to a decrease in T17M Csp-12^{-/-} a-wave amplitudes. For example, we registered 166.0 $\mu\text{V} \pm 13$ vs 108.0 $\mu\text{V} \pm 7.8$ and 161.0 $\mu\text{V} \pm 11$ vs. 76.0 $\mu\text{V} \pm 10.0$ in T17M Csp-12^{-/-} vs. T17M at 2 and 3 months, respectively. **(B)** Interestingly, b-wave scotopic ERG amplitudes were also elevated in T17M Csp-12^{-/-} retinas. However, the magnitude of this elevation was less dramatic than for a-wave over the 3 examined months. Thus, one-month-old T17M Csp-12^{-/-} mice demonstrated 511.0 $\mu\text{V} \pm 22.0$ vs 318.0 $\mu\text{V} \pm 37.0$ in T17M. In the 2nd month, the b-wave amplitudes in the T17M Csp-12^{-/-}

^{-/-} mice were also increased by 1.6-fold as compared to T17M. We registered the b-wave amplitude of $592.2 \mu\text{v} \pm 22.0$ in T17M Csp-12 vs. $366.8 \mu\text{v} \pm 32.0$ in T17M. By 3 month of age the stable preservation of b-wave amplitude observed during the first two months changed and the ratio of T17M Csp-12 to T17M amplitudes dropped from 1.6 to 1.38-fold. This would suggest that the bipolar cells are less sensitive to Csp-12 ablation in degenerating retinas. The differences between all groups were statistically significant. (C) Images of the scotopic ERG amplitudes registered at 10 dB or 25 cd*s/m² in four groups of animals. Data are shown as mean±S.E.M. (* $P < 0.05$, ** $P < 0.01$, *** $P < 0.001$, **** $P < 0.0001$).

Csp-12 ablation significantly delays death of T17M photoreceptors and preserves retinal integrity.

Fig. 3 A, B and C demonstrate that Csp-12 ablation prevents the loss of retinal integrity in the superior and inferior hemispheres of T17M retinas. The inferior retina responded to Csp-12 ablation by increased preservation of the ONL thickness. In one, two and three month-old T17M Csp-12^{-/-} mice, we observed a 1.3, 1.6 and 1.8-fold increase in the ONL thickness as compared to T17M mice. Similarly, in the superior retina the average thickness of the ONL measured in one, two, and three month-old T17M Csp-12^{-/-} mice by SD-OCT was increased from 1.2- to 1.5- fold, respectively. We next wanted to compare the data obtained by SD-OCT analysis with results from histological analysis and counted rows of photoreceptor nuclei using images of cryostat sectioned retinas stained with H&E (Fig. D and E). The data revealed that in one-month-old T17M Csp-12^{-/-} mice the prevention of photoreceptor cell death was more noticeable and reached 10 rows vs the 6.7 rows measured in T17M retinas. However, by 3 months of age we observed further decline in the number of photoreceptor rows in T17M Csp-12^{-/-} retinas with an average of 7.9 rows. This would suggest that Csp-12 ablation does not arrest photoreceptor cells death but instead delays it.

Next, looking for the molecular mechanisms responsible for the above-mentioned delay and knowing that two independent pathways may activate Csp-12, we looked for biomarkers of Ca^{2+} -induced cell death and IRE1-TRAF2 activation.

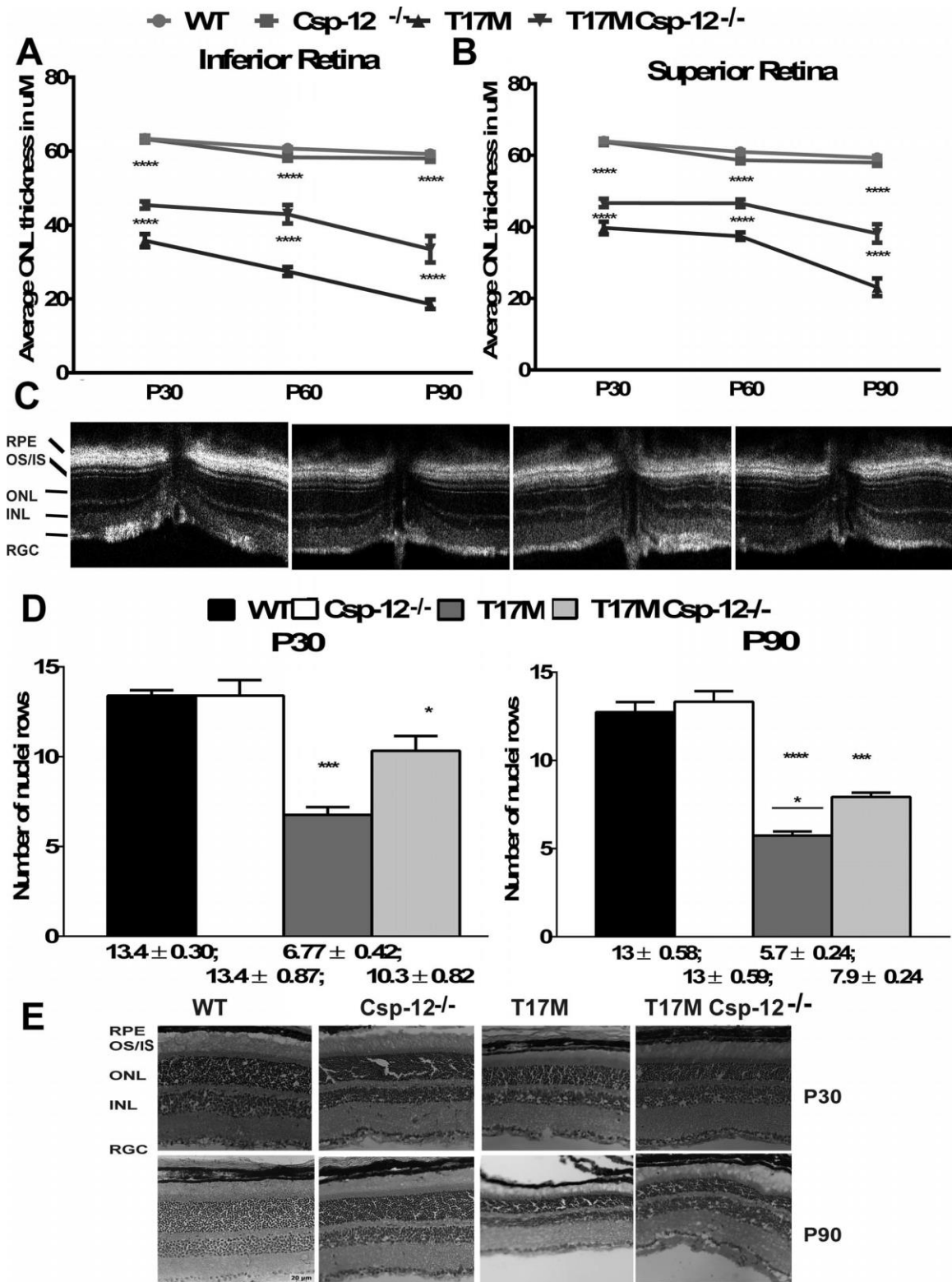


Figure 3. The preservation of retinal structure and prevention of photoreceptor cell death in T17M Csp-12^{-/-} retinas. We analyzed 4 groups of animals (N=6). (A)

Analysis of data from the inferior retina revealed that this region was better preserved than the superior region with increases in the average ONL thicknesses over a period of three months being 1.26-, 1.56- and 1.8-fold. This data also pointed out that despite experiencing the same molecular mechanisms responsible for retinal denegation, activation of pro-death cascades in the inferior and superior regions might occur to different degrees, suggesting that the therapeutic benefit from Csp-12 ablation could also be different. **(B)** Interestingly, the data demonstrated a steady preservation of the average ONL thickness in T17M Csp-12^{-/-} superior retinas from 1.2 to 1.5 over a period of 3 months while T17M mice experienced a continuous decline in the average ONL thickness. **(C)** SD-OCT representative images of wt, Csp-12^{-/-}, T17M, T17M Csp-12^{-/-} retinas. **(D)** Histological analyses of wt, Csp-12^{-/-}, T17M and T17M Csp-12^{-/-} cryostat sectioned retinas stained with hematoxylin and eosin (H&E). Results from photoreceptor row counts in control and experimental mouse retinas at 1 and 3 months of age show preservation of photoreceptor cell death in T17M Csp-12^{-/-} mice. Results from histological analysis of H&E-stained cryostat sections demonstrated partial preservation of T17M retinas from photoreceptor cell death. For example, 1-month-old T17M Csp-12^{-/-} had 10.3 ± 0.82 rows and this number was significantly (1.5-fold) higher when compared to T17M retinas (6.7 ± 0.82). However, by 3 months of age, the number of photoreceptor rows in T17M Csp-12^{-/-} had already declined to 7.9 ± 0.24 rows and preservation was only 1.38-times higher as compared to T17M mice (5.7 ± 0.24). Two-way ANOVA with multiple comparison analysis demonstrated differences in all three groups of animals at 1 and 3 months of age. **(E)** Representative images of one and three month-old wt, csp-12, T17M, and T17M Csp-12^{-/-} retinas stained with H&E. RGC, retinal ganglion cell layer; INL, inner nuclear layer; ONL, outer nuclear layer; IS, inner segments; OS, outer segments. Scale bar indicates 20 μ m. Data are shown as mean \pm S.E.M. (* $P < 0.05$, ** $P < 0.01$, *** $P < 0.001$, **** $P < 0.0001$).

Csp-12 ablation in T17M mice significantly modifies expression of Ca²⁺ sensor genes and reduces apoptosis.

It has been proposed that in the case of retinal degeneration caused by expression of aberrant rhodopsin, an imbalance in Ca²⁺ homeostasis and elevation of intracellular Ca²⁺ may provoke cellular signaling leading to photoreceptor cell death [18-21]. Indeed, an increase in the levels of intracellular Ca²⁺, regardless of whether this is a physiological or pathological event, activates a number of enzymes directly, or indirectly via Ca²⁺-binding proteins. We analyzed the activity of μ -calpain and m-calpain in P30 T17M Csp-12^{-/-} retinas (Fig. 4) since they are the major calpain forms expressed in retinas and because of their well-documented pathological roles in necrotic photoreceptor cell death [21]. Results

from this experiment revealed that while the total μ - and m-calpain activity in T17M retinas increased by 3-fold as compared to wt, T17M Csp-12^{-/-} retinas demonstrated a 2-fold decrease in the level of total calpain activity as compared to T17M retinas. This decrease was not statistically different when compared to wt. Thus, these results indicated that ablation of Csp-12 significantly downregulates calpain activity in degenerating retinas.

Calpastatin (calcium-dependent cysteine protease) is an endogenous calpain-inhibitor protein consisting of an N-terminal domain L and four repetitive calpain-inhibition domains (domains 1-4) (22). We analyzed its levels in degenerating retinas and found it to be elevated 4.5-fold in T17M Csp-12^{-/-} retinas vs T17M, reaching levels found in wt retinas. These data were in agreement with data from a calpain activity assay and indicated calpain inhibition in T17M degenerating retinas by calpastatin as a therapeutic approach leading to retardation of retinal degeneration.

In our previous studies (2,23), we demonstrated increased BAX (Bcl-2-associated X protein) expression and its translocation to the mitochondria. BAX protein is known to be involved in ER Ca²⁺-mediated apoptosis and to antagonize the ER Ca²⁺ modulating activities of Bcl-2 and Bcl-XL (24). Therefore, in the current study we also analyzed BAX expression.

We found that levels of *Bax* mRNA were elevated in both ADRP (T17M and T17M Csp-12^{-/-}) groups as compared to Csp-12^{-/-} mice and did not differ from wt retinas (Fig.4C). However, we detected a 24-fold increase in BAX protein in T17M retina when compared to wt mice. Ablation of Csp-12 in these retinas downregulated BAX levels significantly by 3.8-fold. However, despite the significant decline in BAX protein in T17M Csp-12^{-/-} mice, its level was still over 6-fold upregulated when compared to wt retinas (Fig.4D and

E). These results suggested that despite similar *Bax* mRNA expression levels in the two ADRP groups, there were differences either in the translation efficiency or the degradation of BAX. It is also possible that the examined retinas had different levels of BAX inhibitor protein 1, which is known not only to downregulate BAX protein but to also control the IRE 1-TRAF2 pathway²⁵. Keeping this in mind, we then analyzed the level of TRAF2 protein and Csp3/7 activity in degenerating retinas.

As in our previous study of T17M mice with activated IRE1-TRAF2-cJun signaling (6), we found in the current study that TRAF2 protein was significantly elevated in ADRP retinas. Interestingly, Csp-12 ablation in T17M retinas significantly diminished TRAF2 levels, suggesting that the pro-apoptotic IRE1-TRAF2-cJUN pathway was also downregulated in these retinas.

Decrease in TRAF2 protein was associated with a 2-fold decline in total Csp-3/7 activity in T17M Csp-12^{-/-} mice as compared to T17M animals. The latter animals demonstrated significant upregulation of Csp-3/7 activity as compared to wt supporting a previously proposed hypothesis for the involvement of apoptosis in the mechanism of photoreceptor cell death (26,27) in addition to non-apoptotic pathways (21). We found that the levels of active Csp-3/7 in T17M Csp-12^{-/-} retinas was not statistically different from that found in wt and Csp-12^{-/-} retinas using one-way ANOVA. However, a *t*-test demonstrated a 50% increase in cleaved Csp-3/7 in T17M Csp-12^{-/-} retinas as compared to wt (P=0.026).

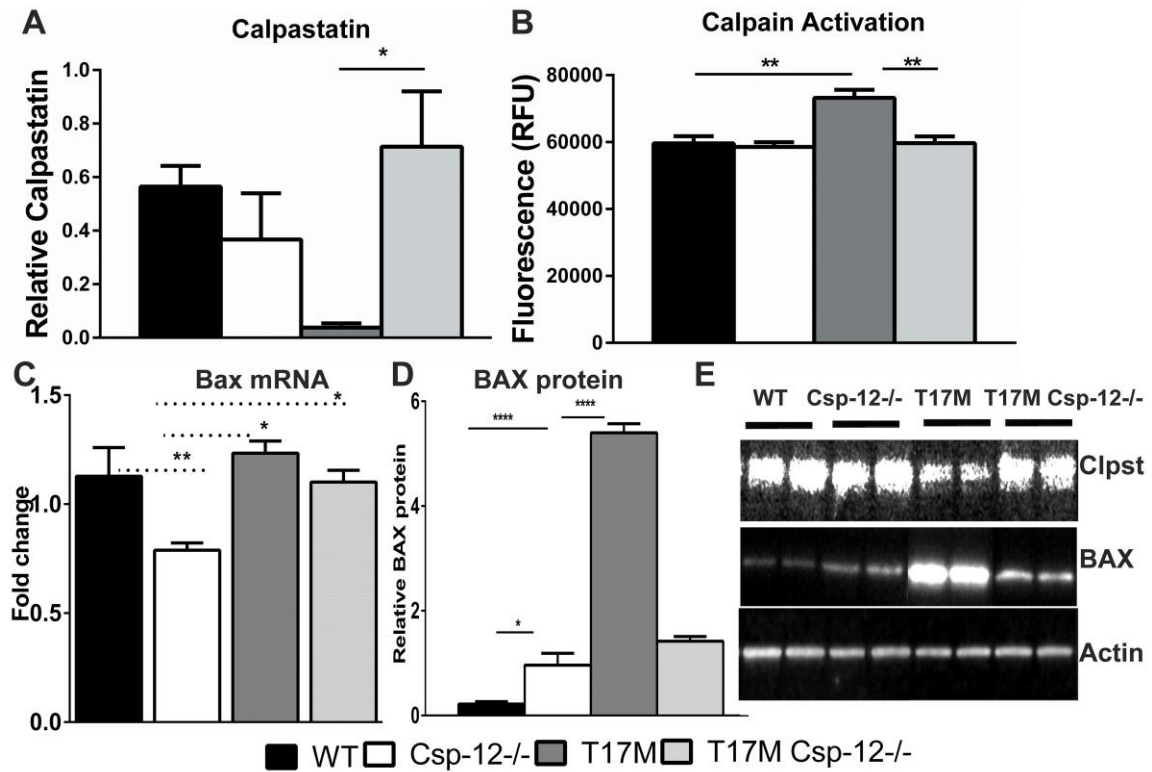


Figure 4. Ca^{2+} sensor protein expression in T17M Csp-12^{-/-} retinas. Western blot analysis of retinal protein extracts isolated from 4 animals in each group at P30. Statistical analysis was performed by using one-way ANOVA. (A) We found that the total calpain activity was increased in T17M retinas by 1.25-fold as compared to wt. Csp-12 ablation however dramatically decreased the levels of active calpains in these retinas and reduced them down to wt levels. (B) In agreement with downregulation of calpain activity in T17M Csp-12^{-/-} mice, we found that the calpain inhibitor, calpastatin was upregulated by 4.5-fold in ADRP retinas that were deficient in the ER stress-associated Csp-12. This points to a link between calpain activation and the calpain inhibitor. Both of these results were in agreement with downregulation of BAX in T17M Csp-12^{-/-} retinas. Although the *Bax* mRNA levels in the two ADRP groups were not significantly different (C), BAX protein production was significantly elevated in T17M retinas and was dramatically decreased (3.8-fold) in T17M Csp-12 mice (D) suggesting less inhibition of the anti-apoptotic BCL-2 protein and consequently, stronger anti-apoptotic activity undermining ADRP progression in T17M Csp-12^{-/-} retinas. (E) Representative images of western blots treated with calpastatin-, BAX- and actin-specific antibodies. Data are shown as mean±S.E.M. (* P <0.05, ** P <0.01, *** P <0.001, **** P <0.0001).

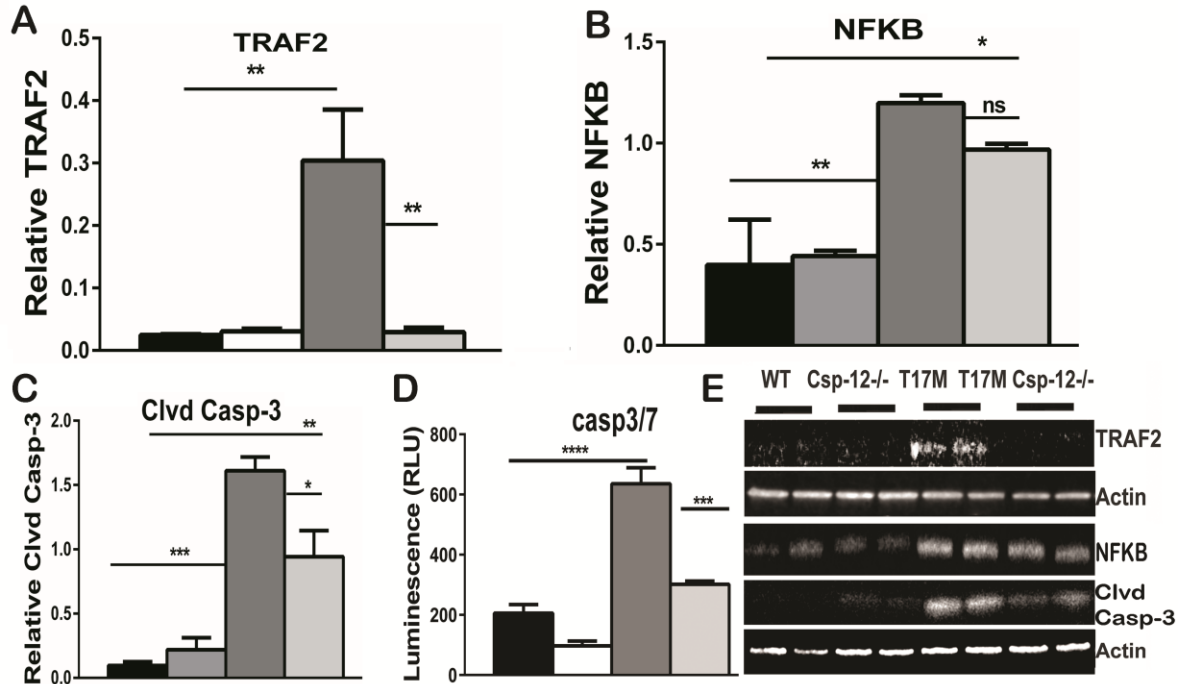


Figure 5. Csp-12 ablation in T17M retinas results in decreased levels of apoptosis. Four animals in each group were used in the experiment. (A) In the current study we confirmed that the level of TRAF2 was 12-fold higher in T17M retinas, implying that the apoptotic IRE1-TRAF2-cJNK pathway could be upregulated in these retinas. Ablation of Csp-12, however, dramatically cut TRAF2 protein expression to levels comparable to wt. (B) Representative images of western blots treated with TRAF2- and actin-specific (internal control) antibodies. (C) Interestingly, downregulation of TRAF2 in T17M Csp-12^{-/-} retinas occurred concomitantly with a decline in Csp-3/7 activity in T17M Csp-12^{-/-} retinas. However, the level of active caspases was still 50% higher as compared to wt retinas. These results along with the observed TRAF2 downregulation indicate that a reduction in apoptotic signaling in ADRP retinas resulted in the partial protection of photoreceptors from functional loss and cell death. Data are shown as mean±S.E.M. (* $P < 0.05$, ** $P < 0.01$, *** $P < 0.001$, **** $P < 0.0001$).

Discussion

Previously, we have reported that the rate of retinal degeneration in ADRP animals could be modified by knockdown or overexpression of UPR mediators [4,6,28]. In T17M RHO mice we have demonstrated that Csp-7 ablation significantly slowed the onset of retinal degeneration. As a logical continuation of that study, we did the work presented here, in which we revealed that ablation of ER stress-associated Csp-12 also partially blocks

deterioration of T17M RHO retinas. However, despite this partial cytoprotective effect, the physiological response and alleviation of photoreceptor cell loss are more striking in animals deficient in Csp-7 than in Csp-12. This observation would confirm that Csp-12 is upstream of the executive Csp-7 and that Csp-7 might activate alternate signaling such as cleavage of auto modified poly (ADP-ribose) polymerase (29) resulting in cell death in T17M retinas. Nevertheless, even though deficiencies in both caspases significantly retard retinal degeneration, our results suggested that blocking apoptotic signaling alone in ADRP photoreceptors is not sufficient to prevent vision loss and the gradual loss of ADRP photoreceptors.

We found that scotopic ERG a- and b-wave amplitudes are preserved in T17M Csp-12^{-/-} mice and these results are in agreement with the delay of onset of photoreceptor cell death in these animals. However, ratios of a- and b-wave amplitudes registered in either T17M Csp-7^{-/-} or T17M Csp-12^{-/-} to corresponding amplitudes found in T17M mice are higher in the first group of animals, suggesting a stronger preservation of ADRP photoreceptors. This was also the case when comparing SD-OCT results and photoreceptor row counts in H&E stained, cryostat sections from both groups. The results demonstrate that the higher preservation of a physiological response corresponds to a more prominent protection and viability of photoreceptor cells.

Ablation of Csp-12 significantly dampened Ca²⁺-promoted calpain activation and dramatically enhanced a cellular defense mechanism activated by increased calpastatin expression. This data also pointed to calpastatin as a potential therapeutic target that was capable of exerting a cytoprotective effect by countering Ca²⁺-induced calpain activation. This data indirectly implies that there could be a decreased concentration of free cytosolic Ca²⁺ in T17M Csp-12^{-/-} retinas. In support of this hypothesis, we observed a dramatic

reduction of BAX protein, which is known to regulate calcium efflux from the ER, thus potentially influencing Ca²⁺-mediated apoptosis (30).

Both Csp-7 and Csp-12 ablation in T17M retinas results in reduction of TRAF2 protein. In our previous study we hypothesized that reduction of Csp-12 may affect TRAF2 protein expression in T17M mice (6). In the current study we provide evidence supporting the fact that there is a feedback loop between TRAF2 and Csp-12 proteins in the retina. Interestingly, both the ER stress-IRE1-TRAF2-Csp12-Csp3/7 and the calcium-induced active calpain-Csp-12-Csp3/7 pathways contribute to retinal pathogenesis in T17M mice through activation of Csp-12. However, in both cases the inhibition of Csp-12 leads to partial preservation of ADRP photoreceptors. Together with results obtained in T17M mice deficient in Csp-7 we have demonstrated that reducing the level of apoptosis alone is not sufficient to rescue ADRP photoreceptors.

That said, we have validated Csp-12 as a potential therapeutic target, which in combination with non-apoptotic molecular targets might be efficiently used to arrest retinal degeneration in ADRP patients.

Acknowledgments

This work was supported by the National Eye Institute at the National Institutes of Health Grant R01EY020905 and VSRC core grant P30 EY003039.

References

- 1 Li T, Sandberg M A, Pawlyk B S, Rosner B, Hayes K C, Dryja T P *et al.* Effect of vitamin A supplementation on rhodopsin mutants threonine-17 --> methionine and proline-347 --> serine in transgenic mice and in cell cultures. *Proceedings of the National Academy of Sciences of the United States of America.* 1998: **95**; 11933-11938.
- 2 Kunte M M, Choudhury S, Manheim J F, Shinde V M, Miura M, Chiodo V A *et al.* ER stress is involved in T17M rhodopsin-induced retinal degeneration. *Investigative ophthalmology & visual science.* 2012: **53**; 3792-3800.
- 3 Rana T, Shinde V M, Starr C R, Kruglov A A, Boitet E R, Kotla P *et al.* An activated unfolded protein response promotes retinal degeneration and triggers an inflammatory response in the mouse retina. *Cell death & disease.* 2014: **5**; e1578.
- 4 Nashine S, Bhootada Y, Lewin A S & Gorbatyuk M. Ablation of C/EBP homologous protein does not protect T17M RHO mice from retinal degeneration. *PloS one.* 2013: **8**; e63205.
- 5 Choudhury S, Nashine S, Bhootada Y, Kunte M M, Gorbatyuk O, Lewin A S *et al.* Modulation of the rate of retinal degeneration in T17M RHO mice by reprogramming the unfolded protein response. *Advances in experimental medicine and biology.* 2014: **801**; 455-462.
- 6 Choudhury S, Bhootada Y, Gorbatyuk O & Gorbatyuk M. Caspase-7 ablation modulates UPR, reprograms TRAF2-JNK apoptosis and protects T17M rhodopsin mice from severe retinal degeneration. *Cell death & disease.* 2013: **4**; e528.
- 7 Viana R J, Nunes A F & Rodrigues C M. Endoplasmic reticulum enrollment in Alzheimer's disease. *Molecular neurobiology.* 2012: **46**; 522-534.
- 8 Gupta S, Cuffe L, Szegezdi E, Logue S E, Neary C, Healy S *et al.* Mechanisms of ER Stress-Mediated Mitochondrial Membrane Permeabilization. *International journal of cell biology.* 2010: **2010**; 170215.
- 9 Nakagawa T, Zhu H, Morishima N, Li E, Xu J, Yankner B A *et al.* Caspase-12 mediates endoplasmic-reticulum-specific apoptosis and cytotoxicity by amyloid-beta. *Nature.* 2000: **403**; 98-103.
- 10 Yoneda T, Imaizumi K, Oono K, Yui D, Gomi F, Katayama T *et al.* Activation of caspase-12, an endoplasmic reticulum (ER) resident caspase, through tumor necrosis factor receptor-associated factor 2-dependent mechanism in response to the ER stress. *The Journal of biological chemistry.* 2001: **276**; 13935-13940.
- 11 Sergeev I N. Calcium signaling in cancer and vitamin D. *The Journal of steroid biochemistry and molecular biology.* 2005: **97**; 145-151.
- 12 Marsili S, Genini S, Sudharsan R, Gingrich J, Aguirre G D & Beltran W A. Exclusion of the Unfolded Protein Response in Light-Induced Retinal Degeneration in the Canine T4R RHO Model of Autosomal Dominant Retinitis Pigmentosa. *PloS one.* 2015: **10**; e0115723.

- 13 Mockel A, Obringer C, Hakvoort T B, Seeliger M, Lamers W H, Stoetzel C *et al.* Pharmacological modulation of the retinal unfolded protein response in Bardet-Biedl syndrome reduces apoptosis and preserves light detection ability. *The Journal of biological chemistry*. 2012: **287**; 37483-37494.
- 14 Mohlin C, Taylor L, Ghosh F & Johansson K. Autophagy and ER-stress contribute to photoreceptor degeneration in cultured adult porcine retina. *Brain research*. 2014: **1585**; 167-183.
- 15 Thapa A, Morris L, Xu J, Ma H, Michalakis S, Biel M *et al.* Endoplasmic reticulum stress-associated cone photoreceptor degeneration in cyclic nucleotide-gated channel deficiency. *The Journal of biological chemistry*. 2012: **287**; 18018-18029.
- 16 Chen C, Cano M, Wang J J, Li J, Huang C, Yu Q *et al.* Role of unfolded protein response dysregulation in oxidative injury of retinal pigment epithelial cells. *Antioxidants & redox signaling*. 2014: **20**; 2091-2106.
- 17 Saleh M, Mathison J C, Wolinski M K, Bensinger S J, Fitzgerald P, Droin N *et al.* Enhanced bacterial clearance and sepsis resistance in caspase-12-deficient mice. *Nature*. 2006: **440**; 1064-1068.
- 18 Shinde V M, Sizova O S, Lin J H, LaVail M M & Gorbatyuk M S. ER stress in retinal degeneration in S334ter Rho rats. *PloS one*. 2012: **7**; e33266.
- 19 Ozaki T, Ishiguro S, Hirano S, Baba A, Yamashita T, Tomita H *et al.* Inhibitory peptide of mitochondrial mu-calpain protects against photoreceptor degeneration in rhodopsin transgenic S334ter and P23H rats. *PloS one*. 2013: **8**; e71650.
- 20 Kaur J, Mencl S, Sahaboglu A, Farinelli P, van Veen T, Zrenner E *et al.* Calpain and PARP activation during photoreceptor cell death in P23H and S334ter rhodopsin mutant rats. *PloS one*. 2011: **6**; e22181.
- 21 Arango-Gonzalez B, Trifunovic D, Sahaboglu A, Kranz K, Michalakis S, Farinelli P *et al.* Identification of a common non-apoptotic cell death mechanism in hereditary retinal degeneration. *PloS one*. 2014: **9**; e112142.
- 22 Sato K, Minegishi S, Takano J, Plattner F, Saito T, Asada A *et al.* Calpastatin, an endogenous calpain-inhibitor protein, regulates the cleavage of the Cdk5 activator p35 to p25. *Journal of neurochemistry*. 2011: **117**; 504-515.
- 23 Sizova O S, Shinde V M, Lenox A R & Gorbatyuk M S. Modulation of cellular signaling pathways in P23H rhodopsin photoreceptors. *Cellular signalling*. 2014: **26**; 665-672.
- 24 Sano R and Reed J C. ER stress-induced cell death mechanisms. *Biochimica et biophysica acta*. 2013: **1833**; 3460-3470.
- 25 Castillo K, Rojas-Rivera D, Lisbona F, Caballero B, Nassif M, Court F A *et al.* BAX inhibitor-1 regulates autophagy by controlling the IRE1 alpha branch of the unfolded protein response. *Embo Journal*. 2011: **30**; 4465-4478.

- 26 Chang G Q, Hao Y & Wong F. Apoptosis: final common pathway of photoreceptor death in rd, rds, and rhodopsin mutant mice. *Neuron*. 1993: **11**; 595-605.
- 27 Marigo V. Programmed cell death in retinal degeneration: targeting apoptosis in photoreceptors as potential therapy for retinal degeneration. *Cell cycle*. 2007: **6**; 652-655.
- 28 Gorbatyuk M S, Knox T, LaVail M M, Gorbatyuk O S, Noorwez S M, Hauswirth W W *et al*. Restoration of visual function in P23H rhodopsin transgenic rats by gene delivery of BiP/Grp78. *Proceedings of the National Academy of Sciences of the United States of America*. 2010: **107**; 5961-5966.
- 29 Oliver F J, de la Rubia G, Rolli V, Ruiz-Ruiz M C, de Murcia G & Murcia J M. Importance of poly(ADP-ribose) polymerase and its cleavage in apoptosis. Lesson from an uncleavable mutant. *The Journal of biological chemistry*. 1998: **273**; 33533-33539.
- 30 Scorrano L, Oakes S A, Opferman J T, Cheng E H, Sorcinelli M D, Pozzan T *et al*. BAX and BAK regulation of endoplasmic reticulum Ca²⁺: a control point for apoptosis. *Science*. 2003: **300**; 135-139.

DISCUSSION AND CONCLUSION

Mice expressing the T17M RHO transgene

A persistently activated UPR in T17M mice is accompanied by severe retinal degeneration. Our histological analysis showed photoreceptor cell loss in H&E stained P15 and P30 T17M RHO retinal sections. Despite a non-significant difference in the number of photoreceptor rows between P15 C57BL/6 and P15 T17M retinas, the P30 T17M mice demonstrated a dramatic (~40%) loss of photoreceptor cells that occurred between P15 and P30 (Chapter 2 Fig. S1). The T17M ERAI retinas expressing GFP as a result of *Xbp1* splicing, indicate activation of the IRE1 arm at P15 (Chapter 2, Fig. 4B), thus, pointing to continued UPR activation. Our previous work has demonstrated that levels of UPR PERK pathway mediator's p-eIF2a, ATF4, and CHOP proteins are elevated in P15 and P30 T17M retinas, indicating that the UPR is involved in retinal degeneration in these mice (1, 2). We therefore became interested in determining how the activated UPR at P15 correlates with the mechanism responsible for the observed retinal degeneration at P30. The UPR could be modulated by targeting the three UPR arms – IRE1, PERK, and ATF6 - which drive apoptotic signaling upon activation. Out of three branches of the UPR, the PERK-ATF4-CHOP branch holds a key position switching cell survival pathways to cell death mechanisms (3-5).

Targeting ATF4 and CHOP to block apoptosis in faster degenerating T17M photoreceptors

Analyzing the ATF4-deficient T17M retinas in Chapter 2, we found that both scotopic and photopic ERG amplitudes were preserved and that cone photoreceptor function was well maintained in 1-month-old animals. This most likely occurs due to the presence of

normally functioning rod photoreceptors in which the reduction in ATF4 reprograms the ER stress signaling network. This result in itself is of great importance because it supports the idea that inherited retinal degeneration can be delayed. To our knowledge, this is the first report to demonstrate both rescue of rapidly degenerating ADRP retinas at P30 and a significant delay in retinal degeneration afterwards. The H&E staining confirmed this hypothesis as it revealed no observable difference between C57BL/6 and T17M ATF4^{+/-} mice, suggesting that no photoreceptor cell death occurred at P30.

The major contribution of ATF4 knockdown to the mechanism of retinal degeneration is likely through a reduction of overall ER stress, induction of an antioxidant program, and activation of autophagy, which together result in a delay of apoptotic photoreceptor cell death. The dramatic reduction in pPERK, pATF6, peIF2a, and CHOP proteins indicates a significantly lower degree of UPR activation in T17M ATF4^{+/-} retinas.

ATF4 deficiency led to a dramatic preservation of photoreceptors and significant reduction in pro-apoptotic CHOP protein. However, ATF4 deficiency was not sufficient to block apoptosis after one month. Therefore, in the next set of experiments we targeted two mediators of the PERK branch simultaneously. In Chapter 3 we demonstrated that by potentially targeting two mediators of the PERK-ATF4-CHOP axis in UPR signaling provides longer functional and morphological rescue of the profoundly degenerating transgenic retina expressing the T17M rhodopsin mutant; this rescue lasted 6 months. Here we also demonstrated that pharmacological modulation of ATF4-CHOP inhibition can be achieved to produce neuroprotection. We found that treatment with the ISRIB drug, which successfully reduced ATF4 and CHOP expression, restored cone physiological response in T17M mice. The T17M mouse usually shows diminished light-adapted (photopic) ERG amplitude at P30 (Chapter 3, Fig.3).

Targeting Caspase-12 to delay cell death in T17M photoreceptors

It has been shown that caspase-12 plays an important role in the mechanism of retinal degeneration. For example, photoreceptor apoptosis in *rd1* mice is accompanied by up-regulation of the protein levels of BiP, caspase-12, phospho-eIF2a, and phospho-PERK in a time-dependent manner (6). This up-regulation coincides with or precedes photoreceptor apoptosis. Recent studies have proposed that there are two mechanisms for ER stress-mediated Csp-12 activation that act in different compartments of the cell. The first involves the interaction of proCsp-12 with the IRE1–TRAF2 complex (IRE1 UPR arm) on the cytosolic side of the ER membrane (10). This interaction occurs as a result of altered complex formation between IRE1 α and TRAF2 in response to ER stress and modified activity of Jun N-terminal inhibitory kinase (JIK) against its binding partner IRE1a (7). This suggests that Csp-12 activated by TRAF2 plays a crucial role in signal transduction from IRE1 to downstream signaling molecules and, thus, links the stress sensor molecule IRE1 to the activation of caspase-12. The second mechanism for Csp-12 activation occurs in the cytosol; an increase in Ca²⁺ concentration results in calpain activation. The μ -calpain activation precedes expression/activation of Csp-12 and is required for activation/cleavage of Csp-12 (8). Given that a cytosolic Ca²⁺ increase could also occur in response to ER stress, this pathway along with the above-mentioned TRAF2 pathway point to Csp-12 as the ER stress-induced caspase promoting apoptosis. Our goal was to determine if ER stress-induced apoptosis played a role in ADRP photoreceptor demise and whether the therapeutic approach of targeting ER stress-promoted apoptosis was sufficient to rescue ADRP photoreceptors. In Chapter 4 we genetically modulated Csp-12 activity in T17M mice and our data point to inhibition of Csp-12 as a potential

therapeutic approach that significantly slows retinal degeneration and together with other non-apoptotic targets could dramatically delay photoreceptor cell death.

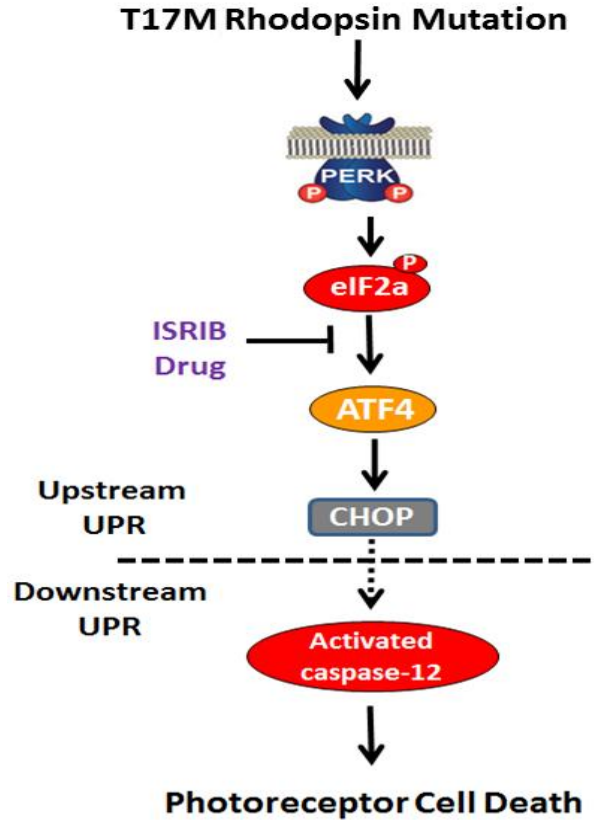


Figure 1: Targeting PERK branch of the UPR could be therapeutic target to prevent Retinal Degeneration. Protein accumulation inside endoplasmic reticulum leads to auto phosphorylation of PERK (protein kinase RNA (PKR)-like ER kinase) branch of the Unfolded Protein Response. PERK phosphorylates alpha subunit of eukaryotic translation initiation factor 2 (eIF2) and makes a stable complex peIF2 α -induced stress granule, resulting in attenuation of general translational program. However, translation of ATF4 mRNA is favored by limited peIF2 and mediated stress signaling. Integrated Stress Response Inhibitor (ISRIB) molecule disintegrates stress granule and rendered cells insensitive towards peIF2. This disintegration of stress granule resumes general translation with no stress signaling (15).

References

1. Choudhury S, Bhootada Y, Gorbatyuk O, & Gorbatyuk M (2013) Caspase-7 ablation modulates UPR, reprograms TRAF2-JNK apoptosis and protects T17M rhodopsin mice from severe retinal degeneration. *Cell death & disease* 4:e528.
2. Kunte MM, *et al.* (2012) ER stress is involved in T17M rhodopsin-induced retinal degeneration. *Investigative ophthalmology & visual science* 53(7):3792-3800.
3. Matsumoto H, *et al.* (2013) Selection of autophagy or apoptosis in cells exposed to ER-stress depends on ATF4 expression pattern with or without CHOP expression. *Biol Open* 2(10):1084-1090.
4. Shen Y, *et al.* (2015) The switch from ER stress-induced apoptosis to autophagy via ROS-mediated JNK/p62 signals: A survival mechanism in methotrexate-resistant choriocarcinoma cells. *Exp Cell Res* 334(2):207-218.
5. B'Chir W, *et al.* (2013) The eIF2alpha/ATF4 pathway is essential for stress-induced autophagy gene expression. *Nucleic Acids Res* 41(16):7683-7699.
6. Yang LP, Wu LM, Guo XJ, & Tso MO (2007) Activation of endoplasmic reticulum stress in degenerating photoreceptors of the rd1 mouse. *Investigative ophthalmology & visual science* 48(11):5191-5198.
7. Yoneda T, *et al.* (2001) Activation of caspase-12, an endoplasmic reticulum (ER) resident caspase, through tumor necrosis factor receptor-associated factor 2-dependent mechanism in response to the ER stress. *J Biol Chem* 276(17):13935-13940.
8. Sergeev IN (2005) Calcium signaling in cancer and vitamin D. *J Steroid Biochem Mol Biol* 97(1-2):145-151.
1. Mendes HF, van der Spuy J, Chapple JP, & Cheetham ME (2005) Mechanisms of cell death in rhodopsin retinitis pigmentosa: implications for therapy. *Trends in molecular medicine* 11(4):177-185.
2. White DA, Fritz JJ, Hauswirth WW, Kaushal S, & Lewin AS (2007) Increased sensitivity to light-induced damage in a mouse model of autosomal dominant retinal disease. *Investigative ophthalmology & visual science* 48(5):1942-1951.
3. Kunte MM, *et al.* (2012) ER stress is involved in T17M rhodopsin-induced retinal degeneration. *Invest Ophthalmol Vis Sci* 53(7):3792-3800.
4. Salminen A, Kauppinen A, Hyttinen JM, Toropainen E, & Kaarniranta K (2010) Endoplasmic reticulum stress in age-related macular degeneration: trigger for neovascularization. *Molecular medicine* 16(11-12):535-542.
5. Zhong Y, *et al.* (2012) Activation of endoplasmic reticulum stress by hyperglycemia is essential for Muller cell-derived inflammatory cytokine production in diabetes. *Diabetes* 61(2):492-504.
6. Gorbatyuk M & Gorbatyuk O (2013) Review: retinal degeneration: focus on the unfolded protein response. *Mol Vis* 19:1985-1998.

7. Lange PS, *et al.* (2008) ATF4 is an oxidative stress-inducible, prodeath transcription factor in neurons in vitro and in vivo. *The Journal of experimental medicine* 205(5):1227-1242.
8. Masuoka HC & Townes TM (2002) Targeted disruption of the activating transcription factor 4 gene results in severe fetal anemia in mice. *Blood* 99(3):736-745.
9. Roybal CN, *et al.* (2004) Homocysteine increases the expression of vascular endothelial growth factor by a mechanism involving endoplasmic reticulum stress and transcription factor ATF4. *The Journal of biological chemistry* 279(15):14844-14852.
10. Oyadomari S & Mori M (2004) Roles of CHOP/GADD153 in endoplasmic reticulum stress. *Cell Death Differ* 11(4):381-389.
11. Scheuner D, *et al.* (2001) Translational control is required for the unfolded protein response and in vivo glucose homeostasis. *Mol Cell* 7(6):1165-1176.
12. Giorgi C, De Stefani D, Bononi A, Rizzuto R, & Pinton P (2009) Structural and functional link between the mitochondrial network and the endoplasmic reticulum. *The international journal of biochemistry & cell biology* 41(10):1817-1827.
13. Nashine S, Bhootada Y, Lewin AS, & Gorbatyuk M (2013) Ablation of C/EBP homologous protein does not protect T17M RHO mice from retinal degeneration. *PLoS One* 8(4):e63205.
14. Choudhury S, Bhootada Y, Gorbatyuk O, & Gorbatyuk M (2013) Caspase-7 ablation modulates UPR, reprograms TRAF2-JNK apoptosis and protects T17M rhodopsin mice from severe retinal degeneration. *Cell death & disease* 4:e528.
15. Sidrauski C, *et al.* (2013) Pharmacological brake-release of mRNA translation enhances cognitive memory. *Elife* 2:e00498.

APPENDIX
INSTITUTIONAL ANIMAL CARE AND USE COMMITTEE APPROVAL




THE UNIVERSITY OF ALABAMA AT BIRMINGHAM

Institutional Animal Care and Use Committee (IACUC)

Notice of Approval for Protocol Modification

DATE: February 25, 2014

TO: MARINA GORBATYUK, Ph.D.
VH -443
(205) 934-6762

FROM: 
Robert A. Kesterson, Ph.D., Chair
Institutional Animal Care and Use Committee (IACUC)

SUBJECT: Title: Unfolded Protein Response as a Therapeutic Target for ADRP Animal Models
Sponsor: NIH
Animal Project_Number: 131109793

On February 25, 2014, the University of Alabama at Birmingham Institutional Animal Care and Use Committee (IACUC) reviewed the animal use proposed in the above referenced application. It approved the modification as described: Personnel: Christopher R. Starr The sponsor for this project may require notification of modification(s) approved by the IACUC but not included in the original grant proposal/experimental plan; please inform the sponsor if necessary.

The following species and numbers of animals reflect this modification.

Species	Use Category	Number In Category
Mice	A	Zero - Procedural modification only
Mice	B	Zero - Procedural modification only

The IACUC is required to conduct continuing review of approved studies. This study is scheduled for annual review on or before November 4, 2014. Approval from the IACUC must be obtained before implementing any changes or modifications in the approved animal use.

Please keep this record for your files.

Refer to Animal Protocol Number (APN) 131109793 when ordering animals or in any correspondence with the IACUC or Animal Resources Program (ARP) offices regarding this study. If you have concerns or questions regarding this notice, please call the IACUC office at (205) 934-7692.

Institutional Animal Care and Use Committee (IACUC) CH19 Suite 403 933 19th Street South (205) 934-7692 FAX (205) 934-1188	Mailing Address: CH19 Suite 403 1530 3rd Ave S Birmingham AL 35294-0019
---	---